AD NUMBER

AD115204

CLASSIFICATION CHANGES

TO: unclassified

FROM: secret

LIMITATION CHANGES

TO:

Approved for public release, distribution unlimited

FROM:

Distribution: Controlled: All requests to Office of Naval Research, Washington, DC.

AUTHORITY

ONR ltr. Ser 93/057, 20 Jan 1998; ONR ltr. Ser 93/057, 20 Jan 1998

SECRET

A SUMMARY OF UNDERWATER ACOUSTIC DATA

PART VII
TRANSMISSION LOSS

R. J. Urick
Ordnance Research Laboratory

and

A. W. Pryce
Office of Naval Research

March 1956

Office of Naval Research
Department of the Navy
Washington, D. C.

SECRET

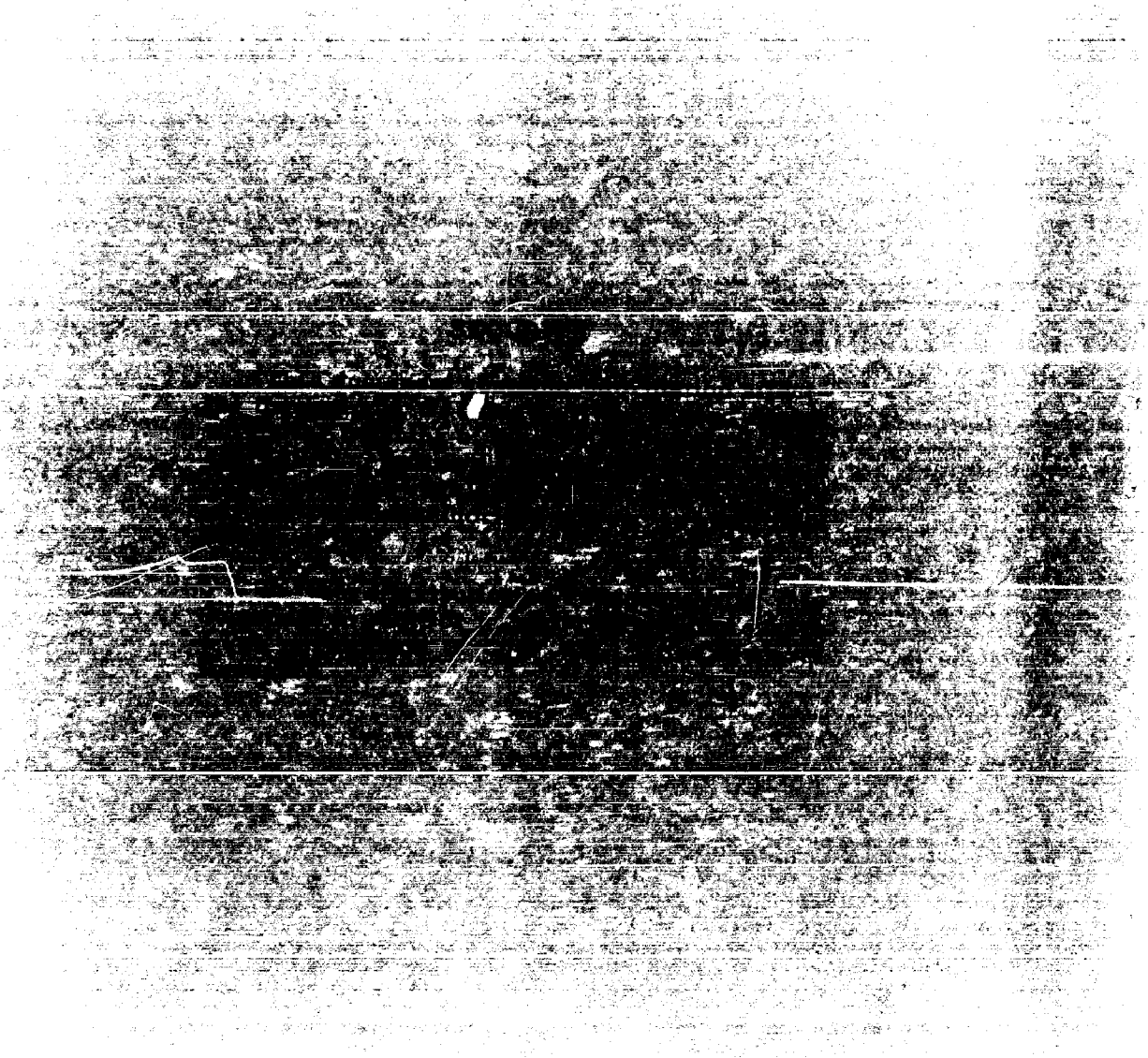

PREFACE

This report is the seventh of a series which attempts to summarize existing knowledge about the parameters which appear in the sonar equations. These relationships which find application in many problems involving underwater sound are stated in Part I of the series. As outlined in Part I, the objective of the Summary is to provide a condensation of some of the basic data in underwater sound for use by practical sonar scientists. The present report, which consists of a series of specially invited contributions, deals with propagation of sound in the sea in terms of the parameter - transmission loss.

The complete series of reports is listed below:

Part I - Introduction (July 1953)

Part II - Target Strength (December 1953)

Part III - Recognition Differential (December 1953)

Part IV - Reverberation (February 1954)

Part V - Background Noise (July 1954)

Part VI - Source Level (Radiated Noise) (May 1955)

Part VII - Transmission Loss (March 1956)

CONTENTS

INTRODUCTION

In the sonar equations, transmission loss is the parameter concerned with the propagation of sound in the sea. It is defined to be the difference in level of a source of sound as measured at the reference distance (one yard in this series) and at the range of interest.

Of all the sonar parameters, transmission loss - as a measure of sound propagation - has been given the longest research attention. The first basic research on the parameters was done on sound propagation in the sea in an attempt to understand the many vagaries of submarine detection ranges observed with early echo-ranging equipment. In 1935, Stephenson at NRL (1) carried out a systematic measurement program with the destroyer SEMMES and the submarine S-20, and obtained numerous plots of signal level at 17 and 23 kc against range from which rough values of absorption coefficient were derived. Later work (2) (3) (4) revealed many of the factors now known to affect the transmission loss. For example, an expression for the absorption coefficient as a function of frequency was deduced that fitted the best data available for many years later.* Shadow zones were observed many times, the "afternoon effect" was correctly accounted for, and the effects of many variables, such as the wind and cloud cover were understood. Even sound-channelling in the surface mixed layer was observed (5) (6), although its significance for long-range detection was not appreciated until later. The extent of this pre-war work in this country is not often realized.

During World War II there were many more investigations of transmission loss, motivated by the needs of kilocycle-frequency submarine detection and acoustic mines. Since then many additional field measurements and theoretical studies have been accomplished, not only in these two fields, but also in connection with the many other applications of underwater sound that have arisen since World War II. At the present time, the subject has been investigated from frequencies of a few cycles up to about one megacycle, and from distances from directly beneath the source out to ranges of hundreds of miles.

But in spite of its long history, transmission loss is still the least satisfactory of the sonar parameters from a quantitative standpoint. No general means for its prediction in quantitative terms exist, even though it may be said to be reasonably well understood theoretically. Much of this uncertainty may be attributed to the large number of variables on which it depends, some of which cannot yet even be specified with any exactness for practical purposes - such as bottom structure, surface roughness, and slight temperature gradients. Another complicating factor is the wide range of distance, frequency, and water depth with which the measurements and theory have been concerned.

To the sonar engineer desiring a numerical db value for use in a given problem, transmission loss will appear as perhaps the least satisfactory of all the sonar parameters. Although much theoretical work has been done, both valid approximation methods and empirical data summaries are lacking on many phases of the subject in which the sonar designer will be concerned. Relatively crude "rules of thumb," of doubtful reliability, are often all that can now be used for practical needs (7). In deep water the most commonly used approximation is that of spherical spreading plus absorption, which often holds surprisingly well within the

*This expression was .064 f^2 [illegible] in units of db per kiloyard when f is in kilocycles.

limits imposed by transmission variations.* For convenience, some curves of spherical spreading plus absorption are given in Fig. 1.

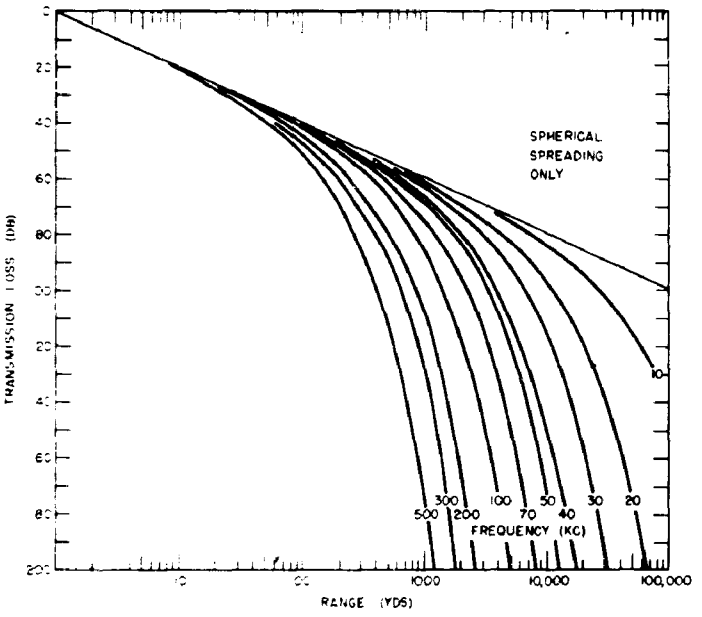

Figure 1 - Transmission loss as a function of range for frequencies of 10 to 500 kcs, assuming spherical spreading and absorption coefficients given in Reference 7 for a temperature of 60°F.

This volume consists of a number of invited contributions, solicited in the spirit of the SAD documents, on separate aspects of transmission loss. The various articles have been arranged according to frequency and water depth as shown in the Table of Contents, with the division very roughly at 1 kc and 100 fathoms, respectively. Except for some minor editorial changes, the separate articles appear as they were submitted.

The articles to follow may be said to provide an up-to-date summary of the subject of transmission loss. Nearly all its important aspects are covered, even though some minor omissions, as well as some duplication of content may be noticed. They represent the effort of many of the present-day authorities on the subject.

To the authors who provided the contributions on the various topics, the gratitude of the writers is gratefully acknowledged.

* When cylindrical spreading exists, boundary losses (leakage, scattering, shear losses) often appear to make the total loss sensibly spherical.

REFERENCES

1. E. B. Stephenson, "Transmission of Sound in Sea Water," NRL Report S-1204, October 16, 1935.

2. E. B. Stephenson, "Absorption Coefficient of Sound in Sea Water," NRL Report S-1466 August 12, 1938.

3. E. B. Stephenson, "Absorption Coefficients of Supersonic Sound in Open Sea Water," NRL Report S-1549, August 2, 1939.

4. E. B. Stephenson, "The Effect of Water Conditions on the Propagation of Supersonic Underwater Sound," NRL Report S-1670, December 3, 1940.

5. R. L. Steinberger, "Underwater Sound Investigation of Water Conditions, GUANTANAMO Bay Area. February 1937," Sound Laboratory, Navy Yard, Washington, D. C., May, 1937.

6. R. L. Steinberger, "Underwater Sound Investigation in Northern Waters, Cruise of USS SEMMES and ATLANTIS, August 1937," Radio Test Shop, Navy Yard, Washington, D. C., January, 1938.

7. R. T. Beyer, "Nomogram for the Sound Absorption Coefficient in Sea Water," Brown Univ., RAG Tech. Report, Contract N7onr 35808, November 20, 1953.

HIGH-FREQUENCY DEEP-WATER TRANSMISSION

HIGH-FREQUENCY DEEP-WATER TRANSMISSION

M. Schulkin and H. W. Marsh, Jr.
USN Underwater Sound Laboratory

INTRODUCTION

The purpose of this chapter is to present a set of formulas and charts which summarize the existing deep-water propagation data for acoustic frequencies above 2 kc.

The major source of data for this purpose comes from Project AMOS (Acoustic, Meteorological, Oceanographic Survey) carried out by the Underwater Sound Laboratory. Project AMOS collected, during the years 1949-1954, large quantities of propagation-loss data and associated environmental data on extensive cruises to all parts of the North Atlantic in all seasons. Measurements were made at frequencies from 2 to 25 kc with projector and receiver depths variable from the surface to 500 feet.

An analysis of AMOS transmission data in the 2- to 25-kc frequency region has been completed (1). Some of the reports and articles consulted during this analysis are listed as references 1a through 1i. It is believed that, for the most part, propagation at these frequencies in deep water is fairly well understood in terms of environmental factors. The final analysis as presented here is considered to be consistent with all known information at the time of exposition. The propagation-loss data obtained from AMOS cruises at discrete frequencies of 2.2, 8, 16, and 25 kc were analyzed and interpreted according to a definite model.

Equations of propagation loss were obtained for the model and fitted with semi-empirical coefficients. The steps used to arrive at this model consisted of:

1. Finding the important acoustic-oceanographic variables.
2. Studying acoustic patterns in situations where one of these variables is dominant.
3. Making the simplest assumptions regarding the acoustic interrelation of these variables and adding complications only when the exigency of incorporating a large body of data into the model required this.

The model was constructed from several modes of propagation, each of which became important under certain conditions of the wide range of geography and season covered by AMOS cruises. While other observed effects could be included readily, it was found that these occurred in an extreme way only in certain localities. It was felt that to introduce other parameters to take these into account would unduly complicate the analysis without improving the prediction capabilities for most of the localities and seasons. The magnitude of the temperature gradient in the thermocline was an important variable of this type. The propagation data for all thermocline gradients were grouped in one class. In addition, the propagation data for all temperature

Note: Paper received June 1955

gradients more positive than -0.3°F per 100 feet were considered in the mixed-layer class. It is realized that these assumptions have to be modified for work in particular localities and at particular times.

Reference to Fig. 1 will show that there are several modes of propagation which determine transmission conditions under any given set of circumstances. Sometimes the different modes are of comparable importance and must be combined in order to estimate the net sound field; at other times the sound field is dominated by a single mode of transmission.

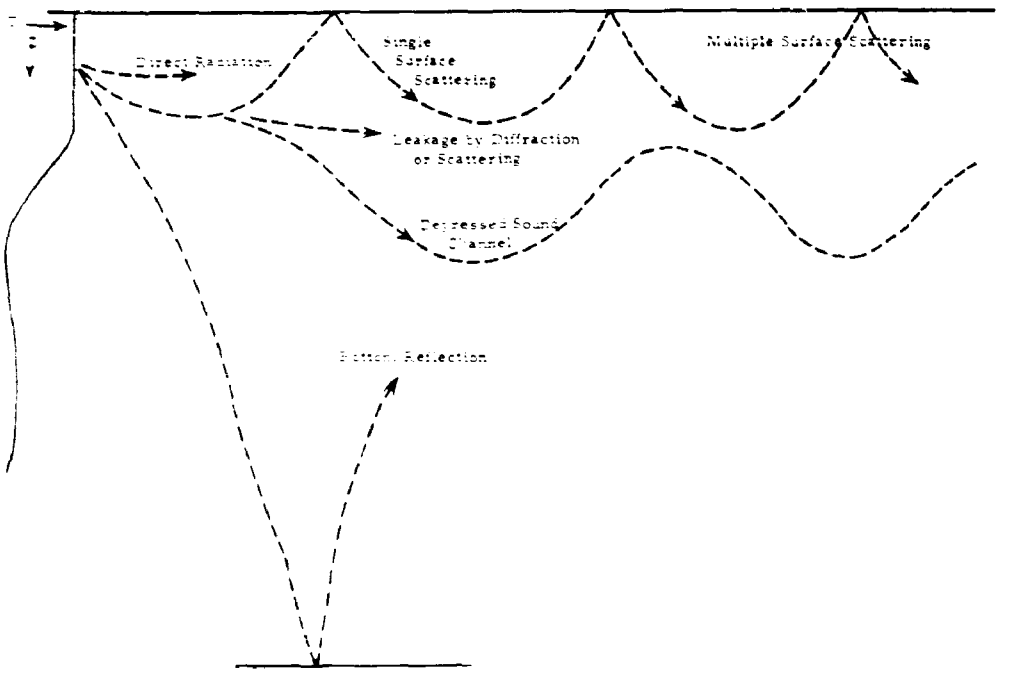

Figure 1 - Modes of sound transmission

In the present analysis an effort has been made to study the various modes separately. This can be done to a great degree by a proper selection of data according to the different oceanographic factors and according to the geometry and acoustic frequency associated with the data. Those factors which have been determined to be of importance are:

1. Depth of isothermal surface layer
2. Sea state (or wind force)
3. Depth of axis of depressed sound channel
4. Depth of ocean bottom
5. Water temperature
6. Range
7. Depth of source
8. Depth of receiver
9. Acoustic frequency

ABSORPTION IN SEA WATER

The important oceanographic-acoustic variables for the frequencies under study were found to be isothermal layer-depth, temperature, and sea state. The temperature effect was best studied in the situation where a constant temperature prevailed to very great depth, of the order of 1000 feet. Under such conditions, it was found that the acoustic field was mostly constant with depth at a fixed range out to ranges of the order of 24 kyds, the limiting range of the experimental measurements. Under such circumstances, the attenuation constants were computed and plotted against temperature for the four frequencies. These data were then considered with respect to existing data of the same kind and other laboratory measurements on absorption. The parameters of a theoretical expression involving the sum of a viscous contribution and a relaxation phenomenon contribution were then determined.

$$a(T, f) = \frac{Af^2 f_T}{f^2 + f_T^2} + \frac{Bf^2}{f_T}.$$

The basis for this theoretical expression is summarized in Ref. 2. The first term is the relaxation phenomenon contribution; the second term is the contribution due to viscosity. These coefficients A, B, and the term f_T were obtained using the data of Pinkerton (3) at very high frequencies, of Leonard and Wilson (4) at middle frequencies, and from AMOS data at lower frequencies. The following results were obtained:

$$A = 0.651 \quad B = 0.0269 \quad f_T = 1.23\times10^{\left(6 - \frac{2100}{T+459.6}\right)}$$

$$= 1.23\times10^6 \times e^{-\frac{4830}{T+459.6}}$$

where f is in kc and T is in °F. Then $A/B = 24.2$ and $f_{50} = 93$ kc. For low frequencies

$$a \approx \frac{0.678\ f^2}{f_T}$$

and

$$a_o \approx 0.0073\ f^2.$$

Figures 2, 3, and 4 are graphs based on this formula. Note that the final value of the relaxation coefficient is less than the 0.76 presented in an earlier work (5). The statement given in this earlier work that the effect of sea state is small, and emphasized by Black (2) as a disagreement with other analyses, applies only to the deep isothermal layers used in that particular study.

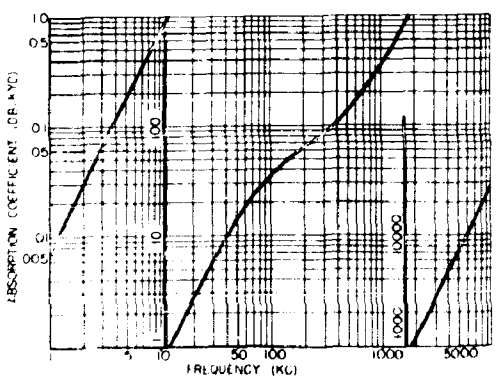

Figure 2 - Attenuation coefficient (in db/kyd) vs frequency (in kc) for T = 50°F

ISOTHERMAL LAYER DEPTH AND LEAKAGE OF ENERGY DUE TO SURFACE SCATTERING

The next variable studied was isothermal-layer depth. In shallower layers than those studied in the previous paragraph, there is a residual attenuation loss which

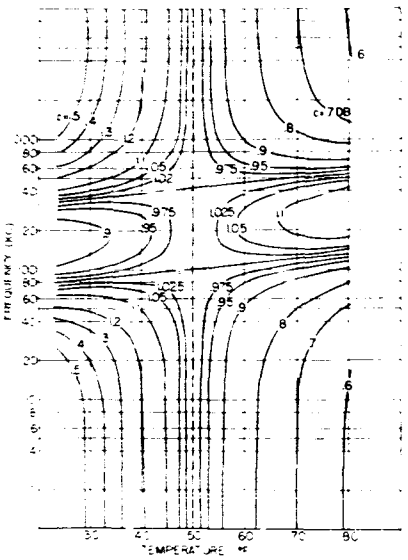

Figure 3 - Temperature dependence of attenuation coefficient ratio ($C = a/a_o$) (a_o = attenuation coefficient at 50°F)

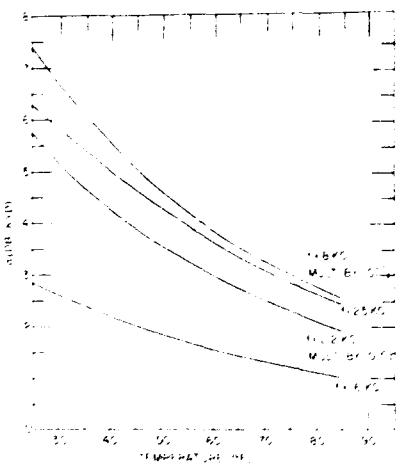

Figure 4 - Absorption coefficient (db/kyd)

depends on layer depth, range, frequency, receiver and projector depth, and sea state. It was quite obvious from the data that at a fixed range and a fixed depth for projector and receiver the residual attenuation increased the higher the sea state and frequency and the shallower the layer depth.

Thus, some kind of scattering phenomenon seemed to be operative which depended directly on sea state, and inversely on volume, since more loss was observed for shallower layers. This could most easily be explained on the basis of a surface-scattering phenomenon. A possible mechanism for volume scattering could be visualized whereby sea state somehow introduced volume-scattering elements so that shallower layers had more intense scattering centers. Assuming that the mechanism is one of surface scattering, the loss can be related to the degree of contact that the acoustic energy has with the sea surface as well as the size and frequency of the surface irregularities. For an omnidirectional source, the fraction of rays which are refracted upwards to meet the surface depends on the layer depth. The range of the limiting ray is a measure of this fraction. This range between successive surface contacts of the limiting ray turns out to be the $\sqrt{L/2}$ in kiloyards if L is expressed in feet. Thus $\sqrt{L}$ is a suitable scaling factor for range if the degree of contact of energy with the surface is a satisfactory measure of the energy loss from a surface channel. By further scaling the projector and receiver depths to layer depth, it would seem possible to normalize the data for all layer depths at any single frequency. This was done, and proved to be a reliable way of condensing a large amount of data into a single propagation class.

Three propagation zones were recognized in connection with propagation in the presence of isothermal layers. The near-zone is defined by a limiting ray leaving a source and returning to the surface after touching the bottom of the surface channel. Energy travels between points by a direct path in this zone and spreads spherically. In the far zone, energy is propagated down the channel after two or more contacts with the surface and the decay of the acoustic field can be represented by a scattering-loss coefficient added to the temperature absorption term at a fixed frequency. Cylindrical spreading holds in this region. The intermediate zone is a zone of transition between the near zone with spherical spreading and the far zone with cylindrical spreading and surface scattering loss. A semi-empirical depth-loss factor was obtained for each zone, depending on the ratio of the scaled range in any zone to the scaled zone width.

PROPAGATION-LOSS FORMULAS

The propagation-loss formulas for the various modes of propagation are the following:

Direct-Radiation Zone of Surface Sound Channel, $0 \leq r \leq r_1$

When both ends of the transmission path lie within or at the bottom of the surface layer, the following formula applies

$$N_w = 20 \log R + a(T,f)R + G(z - z_o)\, r/r_1 + 60 \text{ db} \qquad (1)$$

where, 20 log R is the spherical spreading loss and is given in Fig. 5. $a(T,f)$ is the absorption coefficient and is given in Figs. 2, 3, and 4. $r_1 = 1/4(2 - z - z_o)$ is the scaled range of the limiting ray between z_o and z in the surface channel. $G(z - z_o) = 0.1X10^{2.3(z-z_o)}\ (f/25)^{1/3}$ for $(z - z_o) \leq 1$ and is given in Fig. 6.

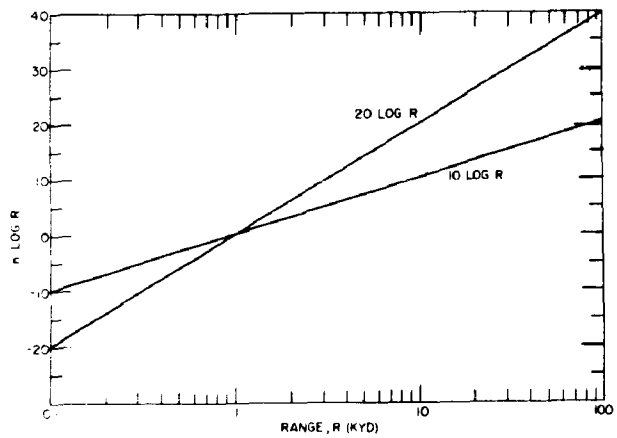

Figure 5 - Spreading loss (db)

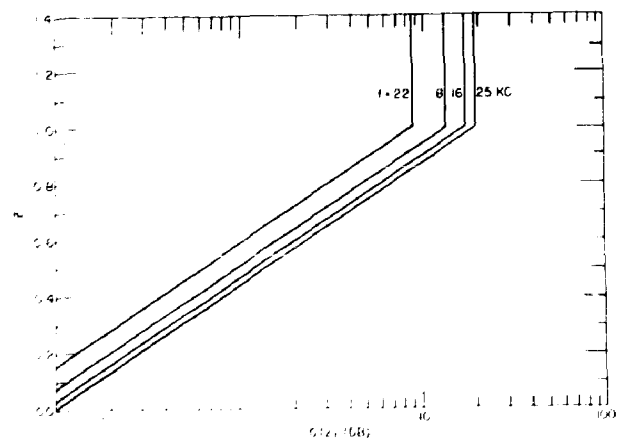

Figure 6 - First depth-loss factor (db)

At all other times take the smaller of the two transmission losses computed by formula (1), using

$$r_1 = \frac{1}{4}(1 - z_o) + \frac{1}{5}\sqrt{z^2 - 1} \; ; \; z \geq 1, \; z_o \leq 1$$

or

$$r_1 = \frac{\sqrt{z_o^2 - 1} + \sqrt{z^2 - 1}}{5} \; ; \; z, z_o \geq 1$$

and

$$G(z - z_o) = 20\left(\frac{f}{25}\right)^{1/3} \text{ if } z - z_o \geq 1$$

and the following formula to be discussed in the next section:

$$N_w = 20 \log R + a(T,f)R + (25 - \sqrt{|Z - L|} - \sqrt{|Z_o - L|} + 5R)\left(\frac{f}{25}\right)^{1/3} + 60 \text{ db.} \qquad (2)$$

Zone of Second-or-Higher-Order Surface Reflection

In the zone of second-or-higher-order surface reflection, energy here has been reflected at least twice at the surface. It covers the region $z_o \leq 1$, $r_1 + 1/2 \leq r$. Then

$$N_w = 10 \log R + (a + a_s)R + H(z, z_o) - a_s\sqrt{L}\left(r_1 + \frac{1}{2}\right) + 10 \log\left[\sqrt{L}\left(r_1 + \frac{1}{2}\right)\right] + 60 \text{ db} \qquad (3)$$

where:

$H(z, z_o)$ = second depth-loss factor (db) and is computed from Figure 7.

$= F(z - z_o) + F(z) + F(z_o)$

$F(z) = 0.4 \times 10^z \left(\frac{f}{8}\right)^{1/3}, \; f \geq 8$

$= 0.4 \times 10^z, \; f \leq 8$

a_s = scattering attenuation coefficient (db/kyd) and is read from Figure 8.

$= 4.5\left(\frac{f}{\sqrt{L}}\right)^{1/2}, \; s < 3$

$= 9\left(\frac{f}{\sqrt{L}}\right)^{1/2}, \; s \geq 3.$

Zone of First-Order Surface Reflection

This is a transition zone between the zone of direct radiation and spherical spreading in a surface channel and the zone of trapping, cylindrical spreading, and surface scattering leakage. Energy has been reflected at least once at the surface. The region covered is $z_o \leq 1$, $r_1 \leq r \leq r_1 + 1/2$. Then

$$N_w = 20 \log R + aR + 2(r - r_1)\,H(z, z_o) + [1 - 2(r - r_1)]G(z - z_o) + 60 \text{ db.} \qquad (4)$$

These formulas provide a propagation loss for any projector-receiver depth pair. When both ends of the propagation path are not in the isothermal layer, energy may penetrate below

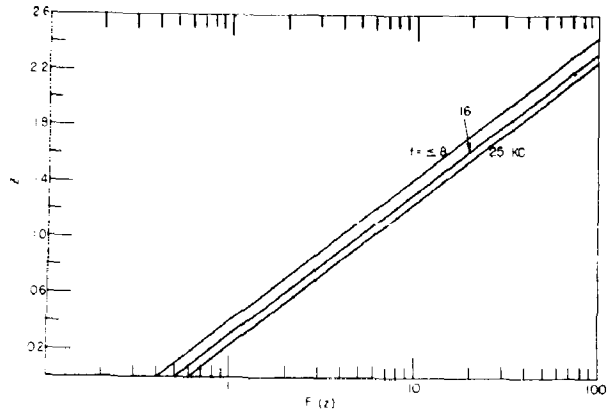

Figure 7 - Chart for computing second depth-loss factor, $H(z, z_o)$

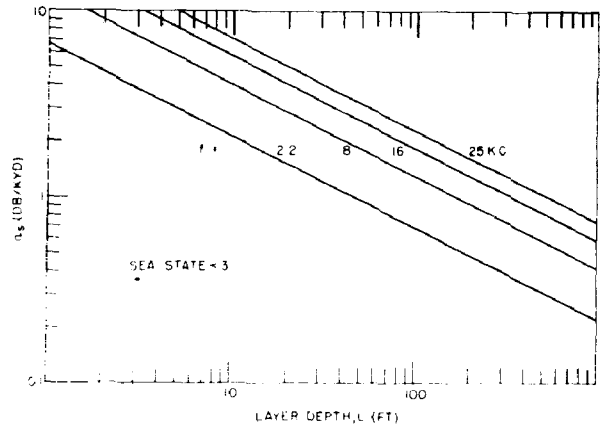

Figure 8 - Scattering attenuation coefficient (db/kyd)

the layer by way of surface scattering, diffractive leakage from the surface channel, or by diffractive leakage from the direct beam. The first two cases are taken care of by the depth-loss factor for each of the propagation zones of the surface-channel mode of propagation.

Shadow Zones and Effect of Negative Temperature Gradients

The case of diffractive leakage from the direct beam must be treated individually when the mode of propagation involving downward refraction prevails. Downward refraction occurs in the presence of a negative velocity gradient directly below the surface when no layer is present, or in the thermocline below an isothermal layer. Thus, when one end of the path is in the surface channel and one end is beneath the surface channel, this mode applies to the portion of the energy which is split at the limiting ray and is refracted downwards. The equations for propagation loss for this mode have been based on a theoretical expression derived previously (6).

As a result of the analysis of AMOS and UCDWR data, it has been found that the propagation loss for the temperature gradients which occur in the ocean is given by

$$N_w = 20 \log R + aR + [25 - \sqrt{|Z - L|} - \sqrt{|Z_o - L|} + 5R] \left(\frac{f}{25}\right)^{1/3} + 60 \text{ db.} \quad (2)$$

The term in the brackets of Eq. (2) has been fitted with empirical coefficients for an average velocity gradient. The equation for the limiting ray under these conditions is

$$R = \frac{1}{5} \sqrt{|Z_o - L|} + \frac{1}{5} \sqrt{|Z - L|} \text{ kyd.} \quad (5)$$

where Z_o, Z, and L are in feet.

Since the acoustic intensity may be dominated either by leakage from the surface channel or diffracted energy from the downward-refracted beam, computations must be made for both these modes when both ends of the propagation path are not in the layer. The mode producing the lesser propagation loss is the one that prevails.

Depressed Channels

An important mode of propagation for variable-depth sonar applications occurs when a depressed or internal sound channel is present. The axis of the channel is the depth of a sound-velocity minimum. This condition usually occurs when the temperature gradient levels off below a steep thermocline and the pressure effect on sound velocity with increasing depth takes over.

The formula for computing propagation loss in depressed channels is based on average measured losses for channel dimensions and temperature gradients as they occurred in the North Atlantic Ocean during the extensive Project AMOS measurements. The model used for the computations, moreover, is consistent with the surface-channel propagation analysis, where the surface channel is considered as a "half-channel" together with surface scattering effects. The model assumes that, on the average, the depressed channel is a wide as the depth of the channel axis. Although depressed channels tend to be more elongated below the channel axis than above, this assumption is felt to be reasonable for projector and receiver depths down to 500 feet. For this mode, depth of source and receiver are referred to the axis of the channel as origin. Thus,

$$N_w = 20 \log R + aR + H\left(\sqrt{\frac{2|Z - D|}{D}}, \sqrt{\frac{2|Z_o - D|}{D}}\right) + 60 \text{ db.} \quad (6)$$

If both an isothermal layer and a depressed channel are present simultaneously, the smaller of the two propagation losses is considered to apply to the situation. The probable errors associated with this model are about the same as those for the negative-gradient mode of propagation. These errors are presented on page 15 in Table 1.

Propagation Via the Bottom

Finally, there are situations for acoustic frequencies above 2 kc, where the dominant energy arrives by way of the ocean bottom. Data from several sources were combined to yield a set of curves of bottom-loss-per-bounce versus bottom-grazing-angle for frequencies from 125 cps to 32 kc/s.

The deep-water bottom-reflection data available as of January 1954 have been assembled in a form which is suitable for use in sonar range predictions. No attempt is made to explain the data; rather, the data are described in terms of a model. The model used is that of propagation by way of the specular path, including an empirical loss at the bottom. At grazing angles approaching 0°, the behavior of the Rayleigh reflection coefficient is assumed. At perpendicular incidence, scattering coefficients deduced from AMOS vertical-sounding measurements at 2, 8, and 34 kc were used.

The most extensive sources of bottom-reflection data in deep water for the 2- to 25-kc frequency range are AMOS Cruises NINE, ELEVEN, and TWELVE. Cruises NINE and ELEVEN were notable for their shallow surface sound channels and low, direct acoustic fields at short ranges. Since continuous wave sources were used on these two cruises, the sound energy could arrive by various paths, and some discretion had to be used in selecting data which arrived by way of the bottom. For this purpose, the depth of the isothermal layer, the decrease of the propagation-loss anomaly with range, the constancy of the field with depth, the magnitude of the propagation loss, and the acoustic frequency were all considered. On Cruise TWELVE, pulses were used, with the result that it was fairly easy to distinguish energy coming via the bottom. Propagation conditions were generally good during this cruise, however, and because only those signals which were less than 40 db below the direct signal could be detected, data were limited to a few stations.

All the AMOS data were assembled into median values, and the bottom loss was plotted against the bottom grazing angle. The geometrical path was used, together with the temperature-dependent absorption coefficients presented earlier, in reducing the propagation-loss values to "bottom loss."

In order to carry the bottom-reflection analysis down in frequency, underwater siren runs from AMOS Cruises ELEVEN and TWELVE were used. Data were considered in frequency bands centered about 1 kc, 2 kc, and 8 kc. Here again judgment had to be exercised in distinguishing bottom reflections, since the source emitted continuously. Bottom-reflection data, obtained by the Naval Electronics Laboratory during 1950 and 1951, were also available for discrete source runs at 500 cps and 1000 cps (7).

Finally, bottom-reflection data (8) obtained by the Woods Hole Oceanographic Institution at frequencies below 1 kc through bomb drops were derived for multiple-hop levels for energy lying between the limiting ray and the critical angle. In working out the data, all possible differences in level were used from the WHOI plots of level versus R/N, where R is the range and N is the order of reflection. Values of N from 1 to 9 were used.

These three sets of data were studied for frequency dependence by plotting median bottom-reflection loss against frequency for the overlapping grazing angle intervals, 10° to 30°, 20° to 40°, and 30° to 50°. Plots of bottom loss versus grazing angle then were made, starting at 125 cps and progressing in octave steps. These are presented in Fig. 9. A plot was also made at 25 kc for convenience. The points at 90° (vertical incidence) were obtained from a previous analysis (9) of the AMOS vertical reverberation and bottom-reflection experiments.

The probable error-versus-frequency curve is shown in Fig. 10. Finally a plot of transmission loss versus horizontal range is presented in Fig. 11 for an average water depth of 2000 fathoms and average water temperature of 38° F for the four frequencies indicated.

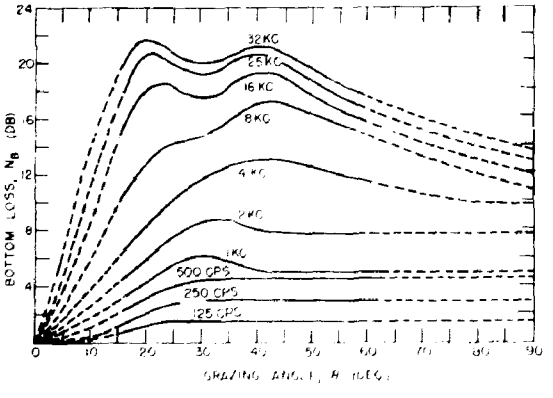

Figure 9 – Bottom loss vs. grazing angle

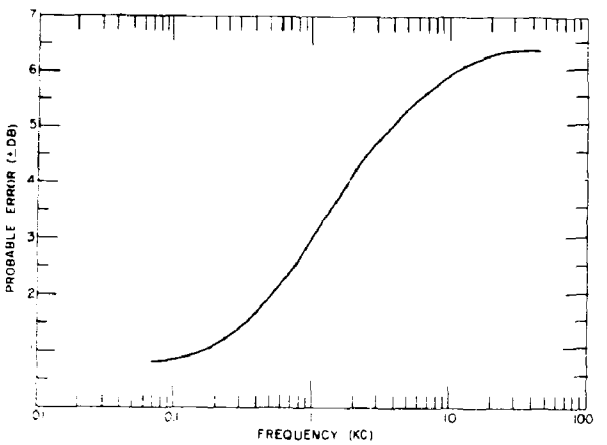

Figure 10 - Probable error in bottom loss vs frequency

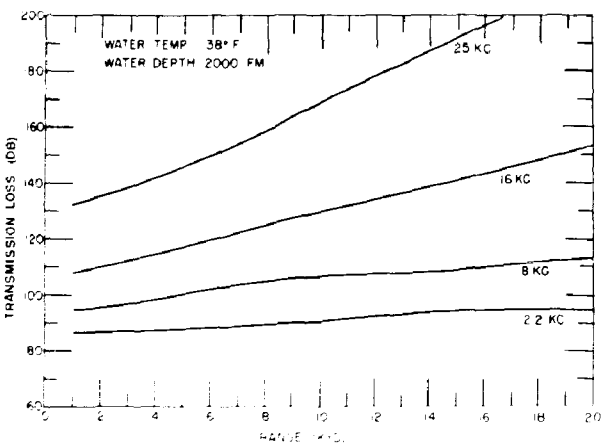

Figure 11 - Transmission loss vs range for bottom-reflected transmission

ERROR STUDY OF AMOS PROPAGATION-LOSS ANALYSIS

An investigation was made of the magnitude of errors to be expected from the use of the semiempirical formulas for computing propagation loss. This was done by working with a representative sample of the entire data file, obtained by selecting, at random, a single IBM card to represent each of the 158 North Atlantic high-frequency deep-water stations which were occupied between 1949 and 1953. Each card so selected contained the measured values of propagation loss for one or more of the four discrete acoustic frequencies (2.2, 8, 16, and 25 kc) for a given range and projector-receiver depth pair.

The mode of propagation which applied to each particular station card was determined from a consideration of the pertinent parameters. The corresponding values of the propagation

loss were then computed from the formulas. It should be noted that more than one propagation mode may apply under the transmission conditions; therefore, calculations using each applicable formula must be made and the result which indicates the least loss must be chosen. This, in effect, increases the numerical effort required by about 50%.

In Table 1 are presented the probable errors of the prediction method obtained by subtracting the computed values of propagation loss from the measured values for the indicated propagation modes.

The magnitude of the probable errors reflects some of the time variability of the ocean itself as a propagation medium. This effect was estimated in this study by considering the reciprocal nature of propagation over the same path with transmitting and receiving positions interchanged within a period of from 15 to 20 minutes. The reciprocal differences referred to in Table 1 are the differences in measured propagation loss over the same path, but with receiver and projector positions interchanged. It may be seen that a sizable part of the probable error of estimation arises from the time variability introduced by the ocean. These errors appear to be independent of range over the ranges of the AMOS experiments (1 to 25 kyd).

It may be seen that the probable errors for the downward-refraction and depressed-channel modes of propagation appear to be larger than those associated with surface-channel propagation. Some reduction in probable error could be achieved perhaps for the downward-refraction mode of propagation. The errors associated with propagation by way of the bottom have been treated separately.

TABLE 1
Probable Errors of Propagation Loss Predictions (AMOS) (±db)

	Frequencies			
	2.2 kc	8 kc	16 kc	25 kc
Mode of Transmission (Formulas 2 and 6)	6.5	5	6.5	9
Mode of Transmission (Formulas 1, 3 and 4)	4	3	4.5	5
Reciprocal Differences	3.5	2.5	1.5	3

PROPAGATION-LOSS CHARTS

It is useful to have a standard reference of transmission loss related to range and frequency. Figures 12 and 13 have been drawn for a 100-foot isothermal layer depth, 50° F water, sea states less than 2 and for a projector and receiver depth of 50 feet. These specific environmental conditions are typical of those occurring naturally, and the curves are recommended for this purpose.

Several internal technical memoranda (10, 11, 12) have been prepared at the Underwater Sound Laboratory presenting propagation-loss contours computed from the foregoing formulas.

CONCLUSION

Available propagation data from 2 to 25 kc have been described by a series of semi-empirical formulas associated with propagation modes occurring in connection with surface isothermal layers, various orders of surface scattering, negative temperature gradients, depressed channels, and bottom reflections. By scaling and by certain laws of combination it is possible to reduce substantially the number of parameters required to characterize any particular mode. Thus it is possible to prepare a limited set of charts or tables which, together with a small amount of computation, can be used to determine transmission loss under any prescribed condition lying within the framework of the analysis.

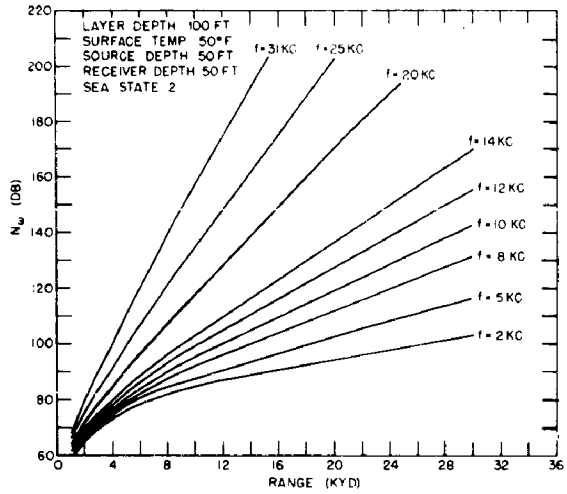

Figure 12 - Transmission loss vs range for standard conditions

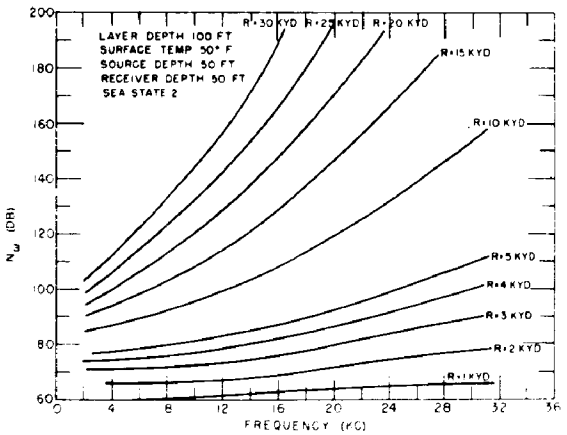

Figure 13 - Transmission loss vs frequency for standard conditions

APPENDIX A - SYMBOLS USED

BASIC VARIABLES

Surface Isothermal Layer Depth (ft)	L
Sea State	S
Depth of Axis of Depressed Sound Channel (ft)	D
Depth of Ocean Bottom (fm)	B
Water Temperature (deg. F)	T
Range (kyd)	R
Depth of Source (ft)	Z_o
Depth of Receiver	Z
Acoustic Frequency (kc)	f
Relaxation Frequency (kc)	f_T
Transmission Loss (db)	N_w
Spreading Loss (db)	10 log R, 20 log R (Fig. 5)
Absorption Coefficient (db/kyd)	a (Figs. 2, 3, 4)
Scattering Coefficient (db/kyd)	a_s (Fig. 8)
First Depth-Loss Factor	G (Fig. 6)
Second Depth-Loss Factor	H (From Fig. 7)
Bottom Loss (db)	N_B (Fig. 9)

SCALED VARIABLES

$$r = R/\sqrt{L}$$

$$z_o = \sqrt{Z_o}/\sqrt{L}$$

$$z = \sqrt{Z}/\sqrt{L}$$

$$r_1 = \frac{1}{4}(2 - z - z_o);\ z < 1,\ z_o \leq 1$$

$$r_1 = \frac{1}{4}(1 - z_o) + \frac{1}{5}\sqrt{z^2 - 1},\ z > 1,\ z_o < 1$$

$$r_1 = \frac{1}{5}\sqrt{z_o^2 - 1} + \frac{1}{5}\sqrt{z^2 - 1};\ z, z_o > 1$$

REFERENCES

1. H. W. Marsh, Jr. and M. Schulkin, "Status of Project AMOS, 1 Jan 1953 - 31 Dec 1954," USL Report 255 (Confidential), March 21, 1955.

1a. "Transmission," Part I, "Physics of Sound in the Sea," S. T. R. Div. 6, NDRC, Vol. 8, 1946.

1b. "Principles and Applications of Underwater Sound," S. T. R. Div. 6, NDRC, Vol. 7 (Confidential), 1946.

1c. G. P. Harwell, U. of Calif., "The Influence of Thermal Conditions on the Transmission of 24-kc Sound," UCDWR U307 (Confidential), March 16, 1945.

1d. R. J. Urick, "Sound Transmission Measurements at 8 and 16 kc in Caribbean Waters, Spring 1949," NRL Report 3556 (Confidential).

1e. R. J. Urick, "Sound Transmission Measurements in the Long Island-Bermuda Region," NRL Report 3630 (Confidential), January 18, 1950.

1f. R. J. Urick, "Sound Transmission to Long Ranges in the Ocean," NRL Report 3729 (Confidential), September 6, 1950.

1g. H. R. Baker, A. G. Pieper, and C. W. Searfoss, "Measurements of Sound Transmission Loss at Low Frequencies 1.5 to 5 kc," NRL Report 4225 (Confidential), September 23, 1953.

1h. W. C. Meecham, W. H. Kelly, and J. R. Frederick, "An Investigation of the Sound Transmission Loss in and Below an Isothermal Layer," Tech. Report, Project M936, Engrg. Res. Inst., Univ. of Mich. (Confidential), July 7, 1953.

1i. J. R. Frederick, J. C. Johnson, and W. H. Kelly, "An Analysis of Underwater Sound Transmission Data," Interim Tech. Report (#1936-1-T) Project M936, Engrg. Res. Inst., Univ. of Mich. (Confidential), April 1954.

2. H. L. Black, "The Absorption of Sound in Sea Water," ORL Tech. Memo TM7.3365-11, Penn. State Univ. (Confidential), March 22, 1954.

3. J. M. M. Pinkerton, "The Absorption of Ultrasonic Waves in Liquids and Its Relation to Molecular Constitution," Proc. Phys. Soc. (London) 62B, 129-41, 1949.

4. O. B. Wilson, "Absorption of Ultrasonic Waves in an Aqueous Solution of Magnesium Sulfate," Univ. of Calif., Dept. of Phys., Tech. Report IV, June 1951.

5. M. Schulkin and H. W. Marsh, Jr., "Report on the Status of Project AMOS "Propagation of Sound in Isothermal Water," (1 Jan - 31 Dec 1952)," USL Report No. 188, Page 55 (Confidential), April 3, 1953.

6. H. W. Marsh, "Theory of the Anomalous Propagation of Acoustic Waves in the Ocean," USL Report 111, p. 35, May 12, 1950.

7. T. P. Condron and R. W. Schillereff, "Long-Range Sound Transmission with a Shallow-Towed Source at 500- and 1000-cps Frequency," NEL Report 323 (Confidential), October 16, 1952.

8. C. B. Officer and J. B. Hersey, "Sound Transmission from Deep to Shallow Water," WHOI Ref. 53-32 (Secret), August 1953.

9. D. L. Cole, J. F. Kelly, and A. W. Dantuono, "Vertical Reverberation and Bottom Strength Measurements - Event SIX - Project AMOS," USL Tech. Memo. 1110-014-53 (Confidential), May 15, 1953.

10. M. R. Powers, K. A. Roche, and P. M. Onyx, "Contours of Transmission Loss for Standard Conditions and Correction Charts," USL Tech. Memo. 1110-101-54 (Confidential) August 17, 1954.

11. T. P. Condron, P. M. Onyx, and K. R. Dickson, "Contours of Propagation Loss and Plots of Propagation Loss vs Range for Standard Conditions at 2, 5 and 8 kc," USL Tech. Memo. 1110-14-55 (Confidential), April 20, 1955.

12. M. Schulkin, K. R. Dickson, and P. M. Onyx, "Propagation Loss Curves for Hull-Mounted and Variable-Depth Sonar Applications at 10 and 25 kc," USL Tech. Memo. 1110-016-55 (Confidential), June 20, 1955.

PRECEDING PAGE BLANK-NOT FILMED

PROPAGATION OF SOUND IN SURFACE-BOUNDED DUCTS

H. L. Saxton
Naval Research Laboratory

INTRODUCTION

The subject of surface-bounded ducts is extremely important in any complete coverage of the propagation of underwater sound. In view of the transition now going on in sonar equipment leading to substantial range increases in these surface-bounded ducts, a review of the mechanism of propagation and loss is particularly timely.

VELOCITY AND VELOCITY GRADIENT OF SOUND IN SEA WATER

Ducts are attributable to sound velocity gradients. The velocity of sound as a function of temperature, salinity, and pressure has been given by several authors. Stephenson and Woodsmall (1) reviewed the subject fifteen years ago. In 1952, DelGrosso (2) determined the velocity of sound in sea water over a temperature range of 32° to 104° F and over a salinity range from 19 to 41 parts per thousand, and arrived at the empirical equation:

$$c = 1474.6 + 4.066T - 0.0218T^2 + 0.000043T^3 + (S - 35)\,10^{-3}\,[1580 - 7.06T + 0.018T^2 - 0.00037T^3 + 0.000003T^4] \qquad (1)$$

in which T is temperature in °F, S is salinity in parts per thousand, and c is velocity in yards per second.* DelGrosso's method was to bring samples of sea water to the Laboratory, where the acoustic interferometer was used at one megacycle to measure wavelength. Theoretically, the deviation from the formula at low frequency should be less than 0.01 yd/sec.

To Eq. (1), there must be added a term to describe the dependence of sound velocity on depth. Unfortunately, this dependence is not well known and no such accuracy as involved in Eq. (1) can be given. We can add to Eq. (1) only the approximate term $0.018y$, in which y is depth (in yards).

For practical calculations of rays, the following relatively crude approximation will suffice:

$$c = 1200\,(1 + 0.2 \log_{[illegible]} T) + (S - 35)\,(2.3 - 0.6 \log_{10} T) + 0.018y. \qquad (2)$$

Note: Paper received January 195[illegible]
*Or usually expressed in meters/[illegible] with temperature in °C.

From (2), the following coefficients of velocity may be obtained:

$$\frac{\partial c}{\partial T} = \frac{100 - 0.26(S - 35)}{T}$$

$$\frac{\partial c}{\partial S} = 2.3 - 0.6 \log_{10} T \qquad (3)$$

$$\frac{\partial c}{\partial y} = 0.018.$$

It should be noted that the change of velocity with temperature for a temperature change of 1° is comparable to the change with depth in a depth variation of several hundred feet. Also $\partial c/\partial T$ is a function of temperature and is greater at lower temperature.

RAY PATHS

Let the velocity of sound as a function of depth in any given layer be expressed by

$$c = c_o (1 + ky) \qquad (4)$$

in which c is velocity of sound at depth y below the top of the layer, c_o is the velocity of sound at the top of the layer, and kc_o is the rate of change of sound velocity with depth, here treated as constant in any given layer. If k is positive, velocity increases with depth and sound is refracted upward. If k is negative, sound is refracted downward. In this form of the expression for sound velocity, k is the curvature of any ray, and $\rho = 1/k$ is the radius of curvature. If y is given in yards, k will be in reciprocal yards. A ray diagram for the two-layer case is given in Fig. 1. For $y < h$, k is positive and refraction is upward. For $y > h$, k is negative and refraction is downward. In Fig. 1, as is customary, the vertical scale is greatly magnified relative to the horizontal to emphasize the behavior of the rays.

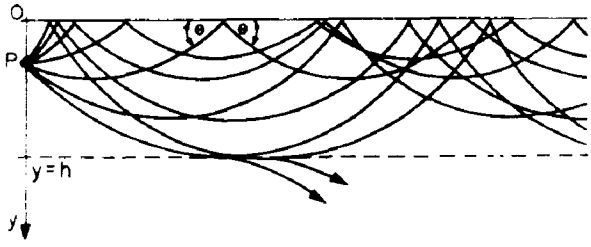

Figure 1 - Ray paths in and below surface-bounded duct
(Reproduced from Ref. 14)

SURFACE-BOUNDED DUCTS

Figure 1 is a typical example of a surface-bounded duct. The rays which do not reach a depth greater than the duct depth, h, in their downward travel, before becoming horizontal, are trapped in the duct so long as they encounter specular reflection from a plane horizontal surface. The rays which do penetrate to a depth greater than h are thereafter bent downward and lost from the duct.

Ray diagrams illustrating ducting were presented in the 30's by Dr. R. L. Steinberger in unpublished Navy Yard work, by Swainson (3) and by Stephenson (4). Considerable work was done during the war on the propagation of sound under various conditions of velocity gradient by

the Woods Hole Oceanographic [illegible] Scripps Institution of Oceanography, and by the University of California, Division of War Research. Theoretical work was carried out by the [illegible] Analysis Group. This latter group [illegible] devotes some slight attention to surface-bounded ducts (hereafter "ducts").

None of the early workers appear to have recognized the great potentiality of ducts for sound propagation to long range. At the frequencies then usually employed (viz. 15 kc and above), attenuation was so great that long ranges appeared impractical. Measurements of attenuation in ducts were confined largely to this higher frequency range.

As a result of a study by an ONR Program Analysis Team, the Naval Research Laboratory, in 1946, undertook research at 10 kilocycles as a first step toward exploiting the potentiality of duct transmission. Reference (6) presents the understanding of the problem on the basis of ray theory as of 1946. Since that time, considerable data have been acquired, particularly at 10 kc, and ray theory has been further developed. In this chapter, some of the salient features of the theory will be brought out.

CHARACTERISTICS OF DUCTS

Before 1948, the occurrence of ducts had been observed but their prevalence seems not to have been appreciated. Actually, the surface layer, which provides upward refraction because of the pressure dependence of sound velocity, usually exists in the North Atlantic. In the 10-kc work carried out by the Naval Research Laboratory, data taken over several years North of Cuba and in the Caribbean Sea indicated that, as a rule, good ducts were encountered.

In 1952, the Hydrographic Office reported on sound channels in the North Atlantic Ocean (westward from Bermuda). Their report (7) indicated that, in the areas covered, surface-bounded ducts usually exist. In Ref. (8), the Naval Research Laboratory has displayed some of the data in a convenient form which is reproduced in Fig. 2. In this figure, the percent of time in which the duct depth exceeded the abscissa is presented for four seasons of the year. Each graph presents data for four different areas. The spacial variation is seen to be rather slight, but the seasonal variation is considerable. The winter and autumn conditions can be seen to be far superior to spring and summer

Other characteristics of ducts which are important are temperature variation within the duct, and uniformity in the horizontal direction. Unfortunately, not very much is known about these important characteristics. The student of ducts must quickly become cognizant of the fact that very slight changes in temperature gradient, of the order of 0.1° F per 100 feet, can make the difference between an excellent duct and no duct. The accuracy of the bathythermograph is inadequate for the measurement required in borderline cases. On the question of uniformity, the results obtainable depend not only on the water conditions in the proximity of the ship but also upon those existing all the way out to a remote target. Horizontal variation is to be anticipated, and deterioration of apparently good ducts can occur at some unknown horizontal range. In echo ranging on a ship which is opening range, echoes frequently come in strong for a time and then abruptly cease. One possible explanation of this is that in the neighborhood of the target the duct has deteriorated.* When the target is a controlled ship, a check on this situation might be obtained by taking a BT from the target ship immediately after abrupt cessation of echoes.

DIVERGENCE LOSS

In a surface-bounded duct, sound from a source, or sound reflected from a target, starts out with spherical divergence. Some of the sound is refracted upward so that it becomes

*[illegible]

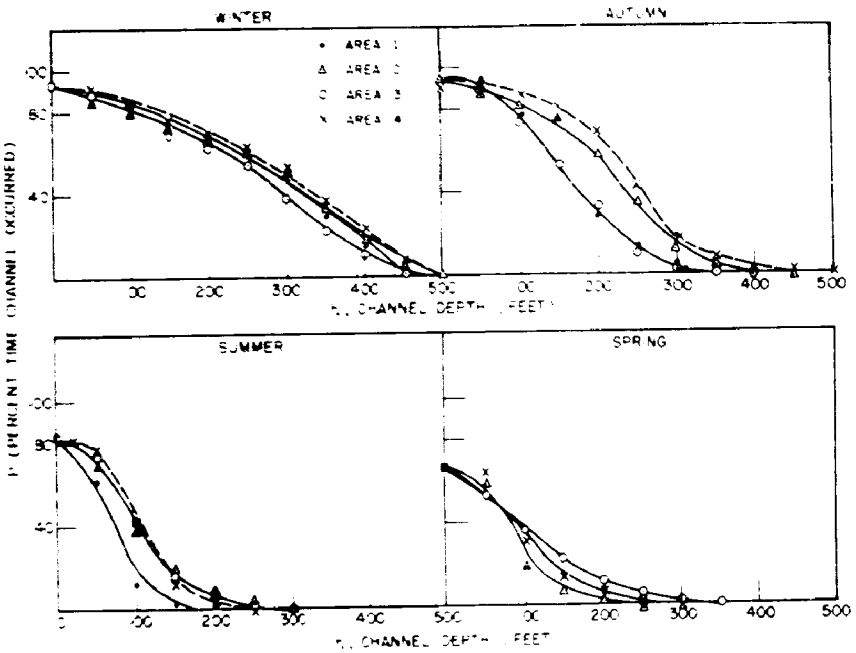

Figure 2 - Distribution of layer depths by season in selected areas

horizontal before reaching a depth equal to the duct thickness. This portion of the sound is effectively trapped between the surface and the bottom of the duct, so that it thereafter experiences only cylindrical divergence. The region between the source and the point of tangency of the limit ray with the bottom of the duct is a zone in which there is a gradual conversion from spherical to cylindrical divergence. Ordinarily, interest is greatest in ranges beyond this zone of transition. At long range, it is enough to consider divergence loss as strictly spherical out to half the distance to the point of tangency and strictly cylindrical thereafter. In Ref. (8), it is shown that the total divergence in the vertical plane, expressed in decibels, is $10 \log x_1/2$ where x_1 is the horizontal distance in yards between the point at which the limit ray impinges on the water surface and the point at which the ray becomes tangent to the lower boundary of the surface-bounded duct. Out to a range x_1 2, the combination of horizontal divergence and vertical divergence yields total divergence loss of $20 \log x_1$ 2. Beyond this, there is only horizontal divergence and the loss is therefore $10 \log r\ x_1$ 2. Combining, the following expression holds

$$\text{Divergence loss} = 20 \log \frac{x_1}{2} + 10 \log \frac{r}{x_1/2} \tag{5}$$

Elementary trigonometry gives

$$\frac{x_1}{2} = \sqrt{\quad} \tag{6}$$

in which r is the radius of curvature of the ray and d is the duct depth. This formula will be used to compute the distance x_1 for an example. For isothermal water (velocity gradient produced only by pressure variation with depth) the radius of curvature is approximately 90,000 yards. Suppose that the isothermal water exists down to a duct depth of 50 yards. Substitution in Eq. (3) gives x_1 = 3,000 yards. The range of spherical divergence, x_1 2, is therefore 1,500 yards for this case. Because of slight local temperature gradients which

partially compensate for the pressure effect a radius of curvature is sometimes obtained which is several times 80,000 yards. Since it is apparent that, for constant duct thickness, the value of r_0 increases with the square root of the radius of curvature, spherical divergence out to several thousand yards may sometimes be expected. While it would appear at this point that the most desirable water condition would be one which would minimize the range of spherical divergence, in practice it works the other way. The increase in divergence loss brought about by increasing the range of spherical divergence is not as great as the decrease of leakage loss out of the duct, because of reduction of incidences of rays on the surface with resulting decrease in scattering. Leakage loss receives further attention later.

ATTENUATION

In the literature, loss in excess of that due to spherical divergence has sometimes been called an anomalous loss. Early measurements revealed that the anomalous loss could be approximately described as an attenuation expressible in decibels per kiloyard. For the case of the surface-bounded duct, attenuation should clearly be the excess loss above the type of divergence loss peculiar to ducts.

Early measurements at the lower sonar frequencies, that is at 10 kc and below, indicated an approximate attenuation coefficient of $0.01\,f^2$ decibels per kiloyard as reported by Urick (9). This value greatly exceeds the results in distilled water and also exceeds values obtained by Leonard (10) and others at UCLA in degassed sea water. Theoretically, Lieberman (11) has shown that a relaxation theory can account for the observed difference in absorption between distilled water and sea water. Small traces of magnesium sulphate were found by Wilson (12) to be involved in the mechanism. The formula for absorption coefficient which Lieberman derives can be approximated as $\alpha_0 = af^2$ at low frequency.

It remains to be explained why the absorption α_0 measured in the Laboratory is less than the attenuation α measured in ducts. It now appears that the attenuation at 10 kc and below in ducts is composed of a temperature-dependent absorption and a leakage loss, usually the larger term, resulting from surface scattering. Moreover, there is at this time considerable doubt as to how much of the difference between attenuation and theoretical absorption may be attributed to leakage and how much should be attributed to increased absorption because of bubble content. It would seem logical to expand the attenuation coefficient, α, into three terms as follows:

$$\alpha = \alpha_0 + \alpha_1 + \alpha_2 \tag{7}$$

in which α_0 is the absorption coefficient as measured in the laboratory as a function of temperature, α_1 is the coefficient of anomalous absorption caused by the presence of bubbles, and α_2 the coefficient of loss due to leakage. However, until such time as experimental techniques permit discriminating between anomalous absorption and leakage loss, the α_1 may as well be omitted and the loss which it represents absorbed in α_2.

Figure 3, the data for which were taken from Kurtze and Tamm (13), shows absorption, α_0, plotted against frequency for a salinity of 35 parts per thousand, with each curve of the family representing a different temperature. At 10 kc, α_0 is approximately given by

$$\alpha_0 = \frac{2F}{T} \tag{8}$$

where T is temperature in °F.

A theory of [illegible] is presented in the Appendix of Ref. (8). There, it is shown that, in ducts, the ratio of energy incident on the surface per unit length of path, W_1, to total energy in the [illegible] is given by

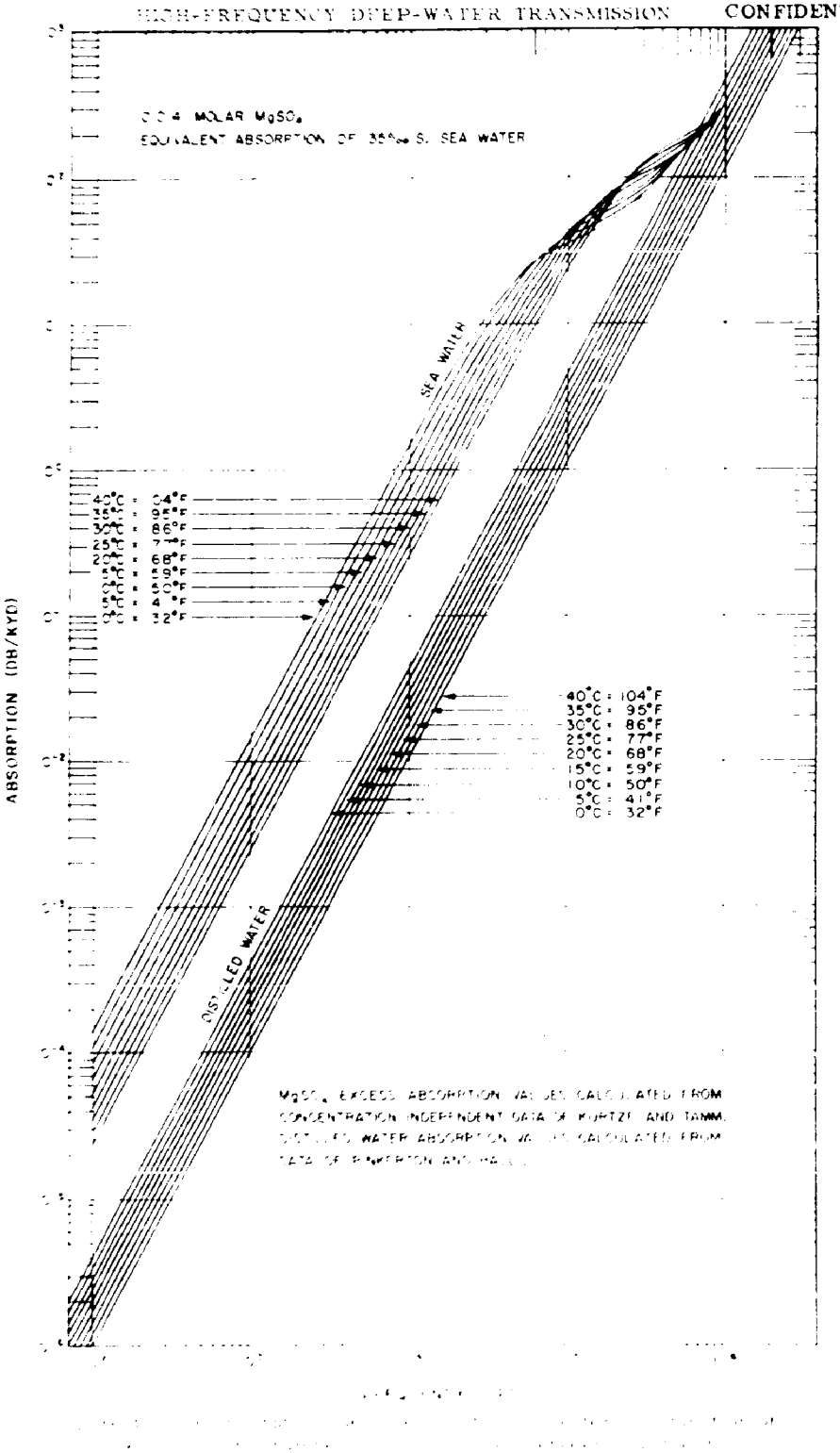
0.04 MOLAR $MgSO_4$
EQUIVALENT ABSORPTION OF 35‰ S. SEA WATER
SEA WATER
DISTILLED WATER
40°C = 104°F
35°C = 95°F
30°C = 86°F
25°C = 77°F
20°C = 68°F
15°C = 59°F
10°C = 50°F
5°C = 41°F
0°C = 32°F
ABSORPTION (DB/KYD)

(9)

[illegible] is the distribution function [illegible] with angle, [illegible] is the angle which the ray [illegible] with the horizontal when it is [illegible] on the surface, [illegible] is radius of curvature, and θ_1 is [illegible] angle at the surface for which [illegible] ray becomes tangent to the bottom of the duct. [illegible] slight liberty has been taken with the symbolism of the referenced report to improve [illegible]. If the integration is performed [illegible] above expression for the case where $w(\theta)$ is [illegible] through the angles contained in the duct, there results an infinite ratio. This result [illegible] be anticipated because mathematically there are an infinite number of angles of incidence of the ray for [illegible] in any finite length of travel. The physical interpretation is that a [illegible] distribution in angle is unstable. [illegible] the referenced report, it was shown that if $w(\theta)$ [illegible] proportional to [illegible] one obtains [illegible] The leakage coefficient, [illegible], is therefore [illegible]

A more sophisticated treatment of leakage out of the duct is presented by Parker and [illegible] (14). The simplifying assumptions which they make lead to a distribution of energy with angle [illegible], which is 0 for [illegible], rises to a maximum and again falls to 0 for $\theta = \theta_1$. The [illegible] recognize a lack of quantitative agreement between their theoretical and experimental [illegible] of channel leakage with layer depth which appears to invalidate the simplifying assumptions. However, this result paves the way for further work in which the assumptions [illegible] adjusted to give a result which agrees with observation. The fundamental equation for the [illegible]-density function as derived by Parker and Bryant is believed to be highly dependable and [illegible] useful. This equation gives the rate of change of $w(\theta)$ as a function of range. Their theory not only leads to a stable distribution at long range but also expresses the transition from the initial distribution and angle to the steady-state distribution. There is predicted an [illegible] which is dependent on range. Some observations appear to confirm this dependence. See, for example, Ref. (8).

[illegible] and Tamarkin (15) have contributed a treatment of the reflection from a sinus[illegible] pressure-release surface which should throw additional light on the subject.

[illegible] SEA STATE ON ATTENUATION

[illegible] attempt has been made at NRL to determine the dependence of leakage loss on sea [illegible]. Data were plotted for different sea states of leakage coefficient versus duct [illegible]. At that time the assumption was made that the tempera[illegible] although it was recognized that there may have been [illegible] of 0.1 or 0.2 [illegible] per hundred feet which could have led to considerable [illegible]. The resulting curves were straight lines with a slope of -1/2 as would be [illegible]. The different curves of the family for sea states 0, 1, 2, 3, and 4 [illegible] separation corresponding to a factor, 1.4. Accordingly, [illegible] a reasonable addition to the expression for [illegible] in terms of [illegible] and h, in order to [illegible] the effect of sea state would be the factor 1.4^n, where n is sea state. More[illegible] proportionality constant, which at that time [illegible] 1200, [illegible]. The complete formula for leakage coef[illegible]

(10)

[illegible]

In order to test further the validity of this formula, range prediction curves for ducts based on Eq. (10) were prepared and sent to SURANTISUBDEVDET with a request that they compare them with experimental data taken with the XHA. This was done in an OPDEVFOR report on the XHA with the following results. Dependence on layer depth agreed reasonably well with theory in a comparison between 75-ft and 150-ft layers; variation with temperature gradient checked reasonably well over an appropriate range of temperature gradients for the water temperature at the surface of 80° F which existed; the proportionality constant appeared to be about 40% higher than that given by NRL. This corresponds to about 1 sea state difference and could possibly be due to a difference in the estimation of sea state. However, we are inclined to believe that the proportionality constant should actually be about 1600.

The whole expression for propagation loss at 10 kc from Eqs. (5), (6), (8), and (10) with a change in the proportionality constant in Eq. (10), is

$$\text{Total loss} = 20 \log \frac{x_1}{2} + 10 \log \frac{r}{x_1/2} + \left[\frac{28}{T} + \frac{1600}{\sqrt{h}} (1.4)^n \right] R \qquad (11)$$

in which r and R are the range in yards and kiloyards respectively and all other quantities have been defined. x_1, [illegible] and h are all expressed in yards, and T in °F.

PROPAGATION LOSS AT LOWER FREQUENCY

As long as the frequency considered is well above that for which diffraction becomes important (i.e., down to 1 kc approximately in a 150-ft-deep isothermal duct), the ray treatment should yield a satisfactory explanation of sound behavior. It is desired to generalize Eq. (11) to cover this range. Divergence loss, expressed by the first two terms on the right of Eq. (11), remains unchanged; a_0, the first term in the coefficient of R, being proportional to the square of the frequency at frequencies below 10 kc, becomes $0.28\, f^2/T$ with f in kilocycles. [illegible] and the second term in the coefficient of R, appears to be approximately generalized in this frequency range when it is multiplied by log f, which reduces to unity at 10 kc. The leakage at 1 kc appears attributable entirely to diffraction, at least in the low sea states which have prevailed when it was measured.

Equation (11) is then converted to Eq. (12) for the frequency range 1 to 10 kc with a mental reservation that diffraction may contribute an additional leakage as discussed later.

$$\text{Total loss} = 20 \log \frac{x_1}{2} + 10 \log \frac{r}{x_1/2} + \left[\frac{0.28\, f^2}{T} + \frac{1600 \log f}{\sqrt{h}} (1.4)^n \right] R. \qquad (12)$$

Further discussion of the mechanism of leakage by scattering and the dependence of leakage on frequency is desirable. Theoretically, there is no mechanism for scattering at a glassy surface. However, when there exist surface waves, there results a distribution of slopes at the surface which causes scattering of incident sound through a statistical distribution of angles of scatter. This distribution holds only when the results of a very large number of scatterings are averaged; the deviations from the average may be very high with a small number of samples.

If one imagines a finite number of plane reflecting facets, each facet having dimensions [illegible] wavelength squared, one would [illegible] reflection to be in the form of a beam

[illegible] if the reflecting facet were moving as a piston. All parts of this facet would probably be excited in phase, and this fact would result in the axis of the beam being steered to the angle of specular reflection. But the different facets would have different angles of specular reflection and different dimensions resulting in different beam sharpness and lobe structure. By averaging many many reflections over many many facets, one would expect some sort of statistical distribution depending upon slope and dimension distributions of the facets. This situation appears to be the mechanism of scattering from the surface.

If, on the other hand, one imagines a multitude of tiny facets, each of dimensions much less than a wavelength, one would expect the contributions of different parts of the whole reflecting area to react approximately as if they were reflected from a single very large horizontal plane surface so placed as to permit the plus and minus position deviations of the actual surface from the hypothetical to average to zero. Scattering is therefore slight.

On the above reasoning one would expect very little scattering except from very rough seas at 1 kc where the wavelength of sound in water is 5 ft, since facets would be of dimensions much less than 5 ft. However, as the frequency rises to about 10 kc, it might be expected that facets would rapidly become comparable in dimensions to a wavelength. One might expect an S-shaped curve with its steepest rise between 1 and 10 kc in low sea states, approximated by a logarithmic curve in this frequency range. One might further expect the curve to shift to lower frequency in higher sea states. It is desired to emphasize the tentative nature of the proposed approximation.

Finally, what can be said about bubbles? Bubbles would be expected to cause absorption. In the UCLA absorption measurements, a pronounced dependence on amount of degassing was observed. The existence of bubbles in shallow water, clear down to the bottom, have been observed by the Woods Hole Oceanographic Institution.

Laird and Kendig (16) derive a theoretical curve of absorption versus frequency in bubbly water and compare this with their experimental work, obtaining good agreement. However, the lack of observations of absorption in sea water of the same magnitude lead to a natural conclusion that their experimental work was done with a much greater concentration of bubbles than would be likely to occur in the ocean except under very special conditions.

NORMAL-MODE THEORY

A number of authors have applied normal-mode solutions to the wave equation of the sonar problem, and in particular to the problem of surface-bounded ducts. One of the first cases in which this solution was used for sonar was by Ide, Post, and Fry (17) in the study of bottom impedance. Marsh's thesis (18) covered cases more closely allied with the problem at hand and Marsh has continued to contribute.

Schweitzer (19) has adapted to the underwater sound problem, part of the work of Booker and Walkinshaw (20), in which the WKB method of solution is used. Schweitzer gives the solution in the form of the absolute value of the ratio of pressure, p, in the duct to the pressure, p_0, that would be there in homovelocity water. His expression is a summation of terms, each of which constitutes a mode. Every term, or mode, contains as a factor a function of transducer depth characteristic of the mode and also as a factor the same function of the depth at which the determination of p/p_0 is made. This form of solution assures us that a reciprocal path exists. Schweitzer also draws curves representing absolute values of this depth function, f_n, plotted against depth for the first, second, third, and fourth modes as in Fig. 4. These curves are characterized respectively by 1, 2, 3, and 4 amplitude loops. The higher modes extend to greater depths.

For a transducer at any given depth, the different modes are excited more or less depending on alignment of transducer depth with the loops of the different depth functions. Reference to Fig. 4 will show that for optimum depth for the excitation of the different modes is different, so that if mode 1 were excited in an optimum manner, modes 2, 3, and 4 might

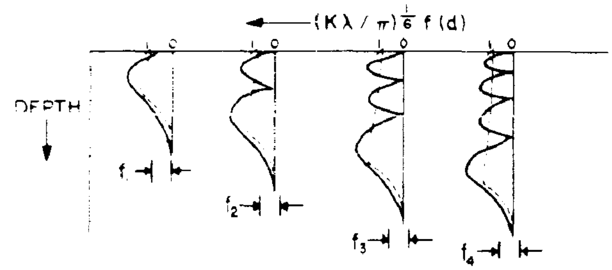

Figure 4 - Approximations for the height functions for the first four modes (Taken from Ref. 19)

receive relatively little excitation. This gives us some choice by control of transducer depth as to which modes we excite.

From Schweitzer's paper a formula may be obtained for the track width of the nth mode in the following form

$$W_n = 0.66\,(n - 1/4)^{2/3}\,\lambda^{2/3}\,\rho^{1/3} \tag{13}$$

in which W_n is the track width, n is the modal number, λ is the wavelength, and ρ is the radius of curvature as in the ray theory. Substituting into this formula λ = 1.67 yds. (for a frequency of 1 kc), n = 1, and ρ = 90,000 yards (correct for isothermal water), one obtains W_n = 112 feet. This is approximately the depth required to contain most of the energy associated with the first mode.

In the utilization of ducts for the transmission of sound, it is quite satisfactory to have only the first mode trapped. Therefore, it would be concluded that 112 feet would be sufficient for good propagation of a 1-kc signal. There is, however, a dependence of leakage out on the condition which exists below the duct, and taking this into account it appears that about a 150-foot depth of duct is desirable at 1 kc. Attenuation has been measured at 1 kc in a particular surface-bounded duct 150 feet deep (16) and has been found to be 0.1 db per kiloyard out to 200 miles range. At the time, this loss was attributed to scattering from the surface but it now appears that it may have been diffraction instead.

At low frequency where higher modes may not be trapped, it is desirable to excite primarily the first mode if propagation to long ranges in ducts is desired. On the other hand, cases may arise where leakage out of a duct is desirable, for example, in order to insonify a target below the duct. For this purpose, it may be desired to place the transducer at an appropriate depth for the excitation of a particular mode or modes which will give the desired leakage. In still other cases, it may prove practical to excite the first mode for propagation in the duct and simultaneously another mode for leakage out, with a transducer at a compromise depth.

The attenuation due to diffraction out of the duct is of great interest. This has been theoretically computed by Voorhis (21) for the case of the duct containing isothermal water and with various negative velocity gradients below the duct. Figure 5, taken from Ref. (21), is for isothermal water in the duct and for a moderate negative gradient below the duct. Generally speaking, attenuation in the duct is increased as the negative temperature gradient below the duct is increased in magnitude.

One feature of leakage from the duct applies in a somewhat similar manner to the cases where (a) leakage is due to scattering from the surface and (b) leakage is due to diffraction. In the first case, it is particularly high near the source because of the greater amount of energy in those rays which strike the surface near to grazing angle. The energy represented by these rays must be rapidly transferred to other angles of incidence or scattered out of the duct, and

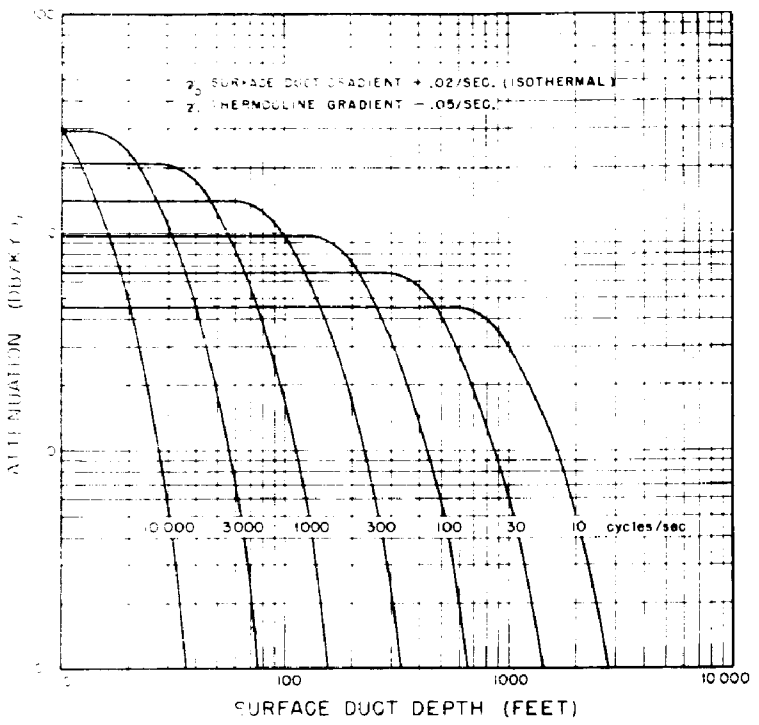

Figure 5 - Attenuation due to diffraction out of a duct. Attenuation of the first mode as a function of surface duct depth for frequencies of 10 to 10,000 cps for a surface duct gradient of +0.02/sec (isothermal) and a thermocline gradient of -0.05/sec (From Ref. 21).

must lead to a high leakage until such transfer has been effected and a stable state set up. Likewise, in the normal-mode theory, the energy associated with the higher modes leaks out much faster than that with the lower modes, thereby resulting in relatively high leakage at short range but, after the percentage of energy associated with these higher modes is dissipated, in relatively low leakage at long range. Much remains to be done experimentally to determine this dependence of z_1 on range.

REFERENCES

1. E. B. Stephenson and F. J. Woodsmall, "The Velocity of Sound in Sea Water," NRL Report R-1722, April 1941

2. V. A. DelGrosso, "The Velocity of Sound in Sea Water at Zero Depth," NRL Report 4002, June 1952

3. G. W. Swenson, "Velocity and Ray Paths of Sound Waves in Sea Water," USC & GS Field Engineer's Bulletin 10, December 1936

4. E. B. Stephenson, "The Effect of Water Conditions on the Propagation of Supersonic Underwater Sound," NRL Report S-1670, December 1940

5. "Physics of Sound in the Sea, Part I: Transmission," STR, Div. 6, NDRC Vol. 8, 1946

6. "Analysis of Long-range Search Sonars for Surface Ships," Prepared by ONR Program Analysis Team (Secret)

7. "Sound Channels in the North Atlantic Ocean (Westward from Bermuda)," Hydrographic Office Report Misc. No. 15678, reprinted as BUSHIPS/NAVSHIPS 900183 (Confidential), 1952

8. H. L. Saxton, H. R. Baker, and N. Shear, "10-Kilocycle Long-range Search Sonar," NRL Report 4515 (Confidential), August 1955

9. R. J. Urick, "Recent Results on Sound Propagation to Long Ranges in the Ocean," USN J. Underwater Acoustics, 1 (No. 2):57-63 (Secret), April 1951

10. R. W. Leonard, "The Attenuation of Sound in Liquids by a Resonator Method," UCLA Dept. Phys. Tech. Report 1, Contract N7onr-27507, 1950

11. L. Liebermann, "Sound Propagation in Chemically Active Media," Phys. Rev. 76:1520-1524, 1949

12. O. B. Wilson, "Absorption of Ultrasonic Waves in Aqueous Solutions of Magnesium Sulphate," UCLA Dept. Phys., Tech. Report IV, Contract N7onr-27507, 1951

13. G. Kurtze and K. Tamm, "Measurements of Sound Absorption in Water and in Aqueous Solutions of Electrolytes," Acustica, 3 (No. 1):33-48, 1953

14. J. G. Parker and R. W. Bryant, "A Statistical Ray Theory of Sound Propagation in Oceanic Isothermal Surface Layers," NRL Report 4196, July 1953

15. E. O. LaCasce, Jr. and P. Tamarkin, "Underwater Sound Scattering from a Corrugated Surface," RAG, Brown Univ. Tech. Report 55-2, August 1955

16. D. T. Laird and P. M. Kendig, "Attenuation of Sound in Water Containing Air Bubbles," J. Acoust. Soc. Amer., 24 (No. 1):29-32, January 1952

17. J. M. Ide, R. F. Post, and W. J. Fry, "The Propagation of Underwater Sound at Low Frequencies as a Function of the Acoustic Properties of the Bottom," NRL Report S-2113, August 1943

18. H. W. Marsh, Jr., "Theory of the Anomalous Propagation of Acoustic Waves in the Ocean," USL Report 111, May 1950

19. B. J. Schweitzer, "An Approximate Method for Determining the Distribution of Intensity in the Mixed Layer Sound Channel," USN J. Underwater Acoustics, 2 (No. 3):66-77 (Confidential), July 1952

20. H. G. Booker and W. Walkinshaw, "The Mode Theory of Tropospheric Refraction and its Relation to Wave Guides and Diffraction," Report of Conference on Meteorological Factors in Radio Wave Propagation at Royal Inst., London, April 1946

21. A. Voorhis, "Sound Transmission in the Surface Isothermal Channel, Part I - An Application of Normal Mode Theory," WHOI Report, Ref. 52-90 (Confidential), November 1952

ABSORPTION*

S. R. Murphy
Applied Physics Laboratory
University of Washington

INTRODUCTION

The recognition of the excess absorption of sound in fresh water, sea water, and other fluids over that predicted by classical theory provided a stimulus to many experimentalists and theoreticians to study this phenomenon. The result has been the accumulation of considerable laboratory data on the variation of the absorption coefficient as a function of frequency and temperature, a general theoretical mechanism to explain these data, and the postulation of several specific liquid models displaying the desired properties. An elementary summary of the theory of sound absorption will be given in the next section, the report of the empirical data being reserved for a later section.

Theory

The propagation of a harmonic plane wave in an absorptive medium can be represented in the form

$$P = P_o e^{-\alpha x} e^{i\omega\left(t - \frac{x}{c}\right)}, \tag{1}$$

where P is the pressure amplitude at a range x from a position where the pressure is P_o, α is the linear absorption coefficient, and c is the phase velocity of sound.

A brief account is presented in (2), chapter 2, page 27, of the classicial theory of absorption as given by Rayleigh (3). In this formulation, the loss of energy from the sound wave as it traverses the medium is attributed to the shear viscosity of the liquid. The absorption coefficient is given to a first approximation by

$$\alpha = \frac{8\pi^2 \mu f^2}{3\rho_o c^3}, \tag{2}$$

where

$$c^2 = \frac{K}{\rho_o}. \tag{3}$$

[illegible] of the absorption coefficient have been added (16).

The notation of (2) is used, with η the coefficient of shear viscosity, f the frequency in cps, ρ_0 the static density, and K the adiabatic bulk modulus.

Thus, the classical theory predicts an absorption coefficient for all fluids that is a function of easily measured parameters and that varies with the square of the frequency. Upon calculating α for Eq. (2) and then examining the experimental determinations for pure water and sea water however, some startling discrepancies were revealed.

Pure water gives a proper frequency-squared dependence, but a value greater by a factor of three than that predicted by viscous absorption. Sea water in the frequency range well below 100 kc also has the proper frequency dependence, but with an attenuation of the order of ten times the classical value. Further, at frequencies well above 100 kc, the attenuation of sea water approaches that of pure water, the transition region occurring between 100 kc and 1 Mc. Obviously, another process for energy absorption of sound is necessary to explain these phenomena.

A second general dissipative process is postulated to be a relaxation phenomenon in which some equilibrium condition in the fluid is disturbed by the passing sound wave. Associated with this perturbation is a relaxation time, which is the time constant of the readjustment toward equilibrium.

The dissipation of sound energy can be thought of as a result of the phase difference between the excess sound pressure and the excess density under harmonic excitation of the relaxation process. When the sound frequency is low, quasi-equilibrium is maintained throughout the pressure cycle, resulting in small absorption; as the frequency increases, the process lags further behind, resulting in increased absorption; and when the frequency is raised well above the reciprocal of the relaxation time, the process is not able to "follow" the rapid variations, resulting in a limiting value of relaxation absorption.

A simple treatment can follow this word description. Suppose we write Eq. (1) as

$$P = P_0 e^{i\omega\left(t - \frac{x}{v}\right)} \tag{4}$$

where v is the complex sound velocity. We now assume a static compressibility β_0 (reciprocal of the bulk modulus) and a compressibility at very high frequency, β_∞. From the previous discussion we would expect β_0 to be greater than β_∞. The compressibility β at a frequency ω is then written as

$$\beta = \beta_\infty + \frac{\beta_0 - \beta_\infty}{1 - i\omega\tau} \tag{5}$$

where τ is the relaxation time.

This expression can be justified (4) on the basis of the assumption of a particular relaxation process. But

$$\frac{1}{v^2} = \rho_0 \beta = \rho_0 \left(\beta_\infty + \frac{\beta_0 - \beta_\infty}{1 + \omega^2 \tau^2} - i\omega\tau \frac{(\beta_0 - \beta_\infty)}{1 + \omega^2 \tau^2} \right) \tag{6}$$

Now, making an identification between Eq. (5) and Eq. (1), we obtain

$$\frac{1}{v} = \alpha \frac{f}{\pi} \tag{7}$$

or

$$\frac{1}{v^2} = \alpha^2 \frac{f^2}{\pi^2} - i \frac{2\alpha f}{\pi} \tag{8}$$

Equating the imaginary parts of Eqs. (6) and (8) we find that

$$\alpha = \left[\frac{\rho_0 c\,(\beta_0 - \beta_\infty)}{2}\right] \frac{\omega^2 \tau}{1 + \omega^2 \tau^2}. \tag{9}$$

Now α and $1/\tau$ have the units of frequency, so we may write

$$\alpha = A \frac{f_r f^2}{f_r^2 + f^2}, \tag{10}$$

where f_r is $1/\tau$, the relaxation frequency; f is the frequency of the sound wave; and A is a parameter depending upon the process involved in the particular fluid.

If we have, in addition, another process that gives another contribution to (e.g., viscous absorption, varying as f^2), then we would expect the total absorption coefficient to be

$$\alpha = A \frac{f_r f^2}{f_r^2 + f^2} + Bf^2. \tag{11}$$

A sketch of this function, along with pure-water absorption, is given in Fig. 1.

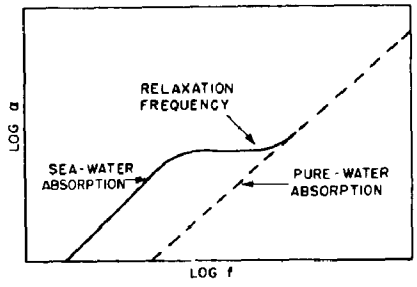

Figure 1 - Sea water absorption curve showing relaxation frequency

Reference ((2), page 105) gives a graph summarizing the absorption measurements made on fresh water and sea water up to 1946. In this graph emphasis was placed on the frequency region from 20 kc to 100 kc, and a few determinations are shown in the megacycle region. The gap between was filled in with a curve strongly resembling that of Fig. 1. Later experimental evidence confirms this general type of dependence.

Equation (10), then, contains the frequency dependence of relaxation absorption but, so far, nothing has been said about the particular physical mechanism in the fluid giving rise to this process. This change in the compressibility with frequency can be obtained from a consideration of thermal relaxation, structural relaxation, and combinations of these; thus, in any given fluid there may be several relaxation processes present in addition to the contribution from viscous absorptions (5).

Hall (6) has considered a possible structural relaxation for pure water to account for the excess absorption over that due to viscous absorption. In this theory the lag between pressure and density results from the rearrangement of molecules during compression between two molecular states of packing. If we use reasonable values for the liquid constants, this theory is sufficient to account for the absorption excess in pure water. Hall obtained a τ of the order of 10^{-12} seconds, agreeing with experimental evidence that the absorption in fresh water is proportional to f^2 up into the hundreds of megacycles, well above the range of interest for sound transmission (7).

The situation for sea water is, of course, much more complicated. In addition to the attenuation present in pure water, we now must add the effects of the many salts that go to make up the natural solution. Direct transmission measurements by Liebermann (8) in 1948, at four frequencies between 100 kc and 1 Mc, substantiated the shape characteristics of Fig. 1 with an experimentally determined relaxation frequency of 130 kc. He was able tentatively to identify this relaxation process with a shift in the ionization equilibrium of sodium chloride. However, later laboratory measurements on sea water, magnesium sulphate solutions, and

sodium chloride solutions by Leonard and Wilson (9) and others indicated that magnesium sulphate, in the same concentration as found in sea water, gave a larger attenuation than sea water alone; further, that the addition of large amounts of sodium chloride essentially eliminated the discrepancy (7). A second theory by Liebermann (4), based upon magnesium sulphate, is sufficient to account for the excess absorption and give a proper order of magnitude.

This discussion may be summarized as follows: viscous absorption alone is not nearly sufficient to account for the observed absorption in pure water or in sea water. A second general mechanism is proposed, called a relaxation process. In pure water, structural relaxation accounts for the excess absorption, giving a frequency dependence of f^2 up into the many-megacycle range. The excess absorption of sea water over that of pure water is attributed to a further relaxation process, having a relaxation frequency in the neighborhood of 130 kc. The total absorption in sea water obeys the relation given by Eq. (11), where the second term is the contribution of pure water and the first includes the sea-water relaxation process. The pragmatic problem now remains as to the values of the constants in Eq. (11). This will be discussed in a later section. For a detailed review of the general problems of sound absorption in liquids, Refs. (5) and (7) are recommended.

EXPERIMENTAL RESULTS

Equation (11) gives a general relation for the expected dependency of absorption on frequency. We may take α in db per kiloyard (where the base 10 rather than e is used), f_r (the relaxation frequency) in kc, f (the sound frequency) in kc, and A and B constants of the particular fluid under constant conditions. Before discussing the evaluation of the three parameters A, B, and f_r for sea water under various conditions of temperature and salinity, we may digress briefly to consider an outline of experimental techniques.

Two general experimental methods are available for studying the absorption of sound in the sea; direct transmission measurements in the medium itself, and laboratory measurements on small samples. Both of these methods are of limited accuracy at the lower frequencies, since, at these frequencies, the loss attributable to absorption becomes small in comparison with losses due to other mechanisms.

To study the mechanisms of sound absorption under controlled conditions, it was essential that reliable laboratory techniques be developed. In the very high frequency ranges (3 Mc to 1000 Mc) optical methods were found reliable because of the large value of attenuation at these frequencies. The degradation of a plane wave determined by these methods verified the prediction of Eq. (1). Fresh water and sea water were found to give essentially the same attenuation at these frequencies (7). For lower frequencies, a laboratory method using the time decay of sound in a resonator was applied with increasing success by many investigators. This method extended the lower frequency limit to the region of 4 kc, well below the relaxation frequency observed in sea water. The technique has been described by several authors (5, 7, and 10). A degassed, filtered sample of the liquid to be investigated is placed in a closed chamber and many modes in the region of the desired frequency are excited. The excitation is shut off and the rate of decay of the energy in the resonator is observed. The overall attenuation is then determined from

$$\alpha = \frac{1}{c_0 t} \ln \frac{I_0}{I_t} , \tag{12}$$

where I_0 is the initial sound intensity, I_t is the intensity after t seconds, and c_0 is the velocity of sound in the liquid. Corrections to this overall attenuation coefficient must be made to allow for the losses at the boundary of the resonator not attributable to volume absorption in the liquid itself. These corrections are discussed by the individual experimenters.

Results obtained for sea water by this method agree with the frequency dependence predicted assuming a relaxation mechanism. Measurements (7, 9, and 10) on pure solutions of the individual components found in sea water demonstrated the excess absorption to be

attributable almost entirely to magnesium sulphate. In fact, a solution of 0.02 mole per liter of $MgSO_4$, the average concentration found in the sea, gave absorption in excess of that of sea water (7, 10). Addition of sodium chloride reduced this to the value of sea water (7). Alternately, sea-water absorption was found to be simulated by a solution of 0.014 mole per liter of magnesium sulphate (7).

Considerable laboratory data are available from Leonard (10), from Wilson (9), and from Kurtze and Tamm (7) on the excess absorption in magnesium sulphate solutions as a function of temperature and concentration. These investigators found the excess absorption to vary linearly with concentration. Further, from the temperature-dependence data, Wilson (9) found the relaxation frequency to be given by a relation of the form

$$f_r = Ce^{-D/T} \tag{13}$$

where T is the absolute temperature (Rankine), f_r is the frequency in kc, and C and D are constants for a magnesium sulphate solution.

From these laboratory measurements, it is thus possible to calculate values for the parameters in the relaxation term, A and f_r, in Eq. (11) for ranges of concentration and temperature of interest. In addition, pure-water measurements by many investigators, summarized in (7), allow a determination of the parameter B under similar conditions.

In making a direct transmission measurement in the sea, the total loss of intensity as a function of range is determined. Then, on the basis of an assumed propagation law, the effect of absorption is separated from the other expected losses. Hence, for this method to yield accurate results for α, care must be taken to assure that the other losses are properly accounted for. Specifically, short pulses can be employed to assure receiving the direct pulse undistorted by reflection from the boundaries. In isothermal water, a spherical-spreading law can then be assumed with confidence. Liebermann (4) used this method for both fresh and salt water, obtaining values in substantial agreement with laboratory measurements in the frequency range of 100 kc to 1 Mc. Garrison (16) in 1955 made a similar series of direct transmission measurements at 60 kc, 142 kc, 272 kc, and 467 kc. Range was accurately determined by the difference in transit time between the acoustic and radio-transmitted pulse. These results are presented in Table 1 together with a comparison between the two summary computations based on laboratory data discussed below. The limits of error quoted are computed on the basis of many measurements made in sea water of 30 parts per thousand salinity and 8 to 9°C temperature.

TABLE 1
A Comparison of the Sound Absorption in Sea Water Between Direct Measurements (16) and the Summary Graphs of Beyer (13) and Del Grosso (15)

Frequency (kc)	Sound Absorption in Sea Water (db/kyd)		
	Experimental (Reference 16) 9°C 30°/oo salinity	Beyer 50°F	Del Grosso 30°/oo salinity 10°C
60	14.4 ±0.2	15	19
142	33.9 ±0.7	33	40
272	51.0 ±1.5	56	64
467	93 ±5	100	110

For lower frequencies, the instrumentation requires longer pulses and, in turn, longer ranges for absorption to be an observable part of the total loss. Two methods of analysis are possible. First, the procedure of Liebermann can be followed, except that now the boundary conditions and the thermal structure of the medium must be considered to determine the law of spreading at the longer ranges. Alternatively, if sufficient data are available under wide ranges of temperature, frequency, and range, Eqs. (11) and (13) may be employed to determine the constants in these equations without resorting to an uncertain spreading law. The AMOS project has made large amounts of transmission data available for analysis. Marsh (11), using the second procedure, analyzed the AMOS data at 8, 16, and 25 kc. He obtained values of 0.76 for A, 2.19×10^7 for C, and 6300 for D. An analysis of the AMOS data by a group at the Michigan Engineering Institute (12) resulted in a value of 0.6 for A. The measurements of Wilson (9) indicate a value of 0.57 for A. In view of the uncertainties in the other possible losses occurring in the medium, and in the properties of the medium themselves, it is not surprising that the direct-transmission data are at some variance with the laboratory measurements.

Two independent extrapolations of the available laboratory data on fresh and sea water have been published recently, extending the results to a wide range of frequency, temperature, and (in one report) salinity.

In 1953, Beyer (13) published a nomogram on the absorption coefficient in sea water. Utilizing the data of Leonard and Wilson (9), Beyer calculated values for A and f_r in the relaxation term of Eq. (11) for temperatures ranging from 32°F to 80°F. The pure-water data of Pinkerton (14) gave values for B over the same temperature range. Neglecting the effect of salinity variations, Beyer presented the results of his calculations in the form of the nomogram reproduced in Fig. 2. He estimates the accuracy of this calculation to be ±10 percent above 30 kc, and possibly greater at 5 to 30 kc considering Marsh's (11) determination from sea water. Linear interpolation between the curves can be made without exceeding the accuracy limits of the figure.

Del Grosso (15) in 1954 published the results of a similar study based on the extensive data of Kurtze and Tamm (7) on magnesium sulphate. In addition to temperature and frequency dependence, his results include the effect of salinity based upon the concentration dependence observed in magnesium sulphate (7). The results of these calculations, presented in an easily accessible form, are available in Del Grosso's report (15).

The comparison presented in Table 1 between the direct transmission measurements in the sea (16) and readings from the summary graphs of Beyer and Del Grosso show agreement within reading and experimental error between Beyer and the sea measurements with Del Grosso consistently in excess of these values. On the basis of this comparison, it appears that Fig. 2 gives the better estimate of the value of the absorption coefficient for sea water as a function of temperature so long as the salinity does not deviate appreciably from 30 to 35 parts per thousand.

SUMMARY AND CONCLUSIONS

In the transmission of sound, absorption processes play an important role in determining, from an engineering point of view, the maximum available range for given equipment. Of the possible mechanisms capable of producing linear attenuation with range, the most outstanding are viscous and relaxation absorption in the volume of the medium. Experimental and theoretical efforts have served to clarify greatly the understanding of the relaxation phenomena and to enable estimates to be made of the temperature, frequency, and salinity dependencies. It would be most desirable if the laboratory measurements were to give lower absolute values of the absorption coefficient than those observed in the medium, and to within a few percent of each other. Then attenuation exceeding these values would be reliably attributable to other loss processes known to operate in the medium. Unfortunately, examination of the laboratory data analyses makes it evident that this ideal has not yet been reached. Although the works quoted in this report give relative information concerning the functional dependence of the

viscous and relaxational absorption coefficient on temperature, frequency, and concentration, much work remains before absolute values of the reliability desired for engineering applications are available. However, the agreement between the direct transmission measurements and Fig. 2 indicate that this graph is reliable to the estimated accuracies of ±10%.

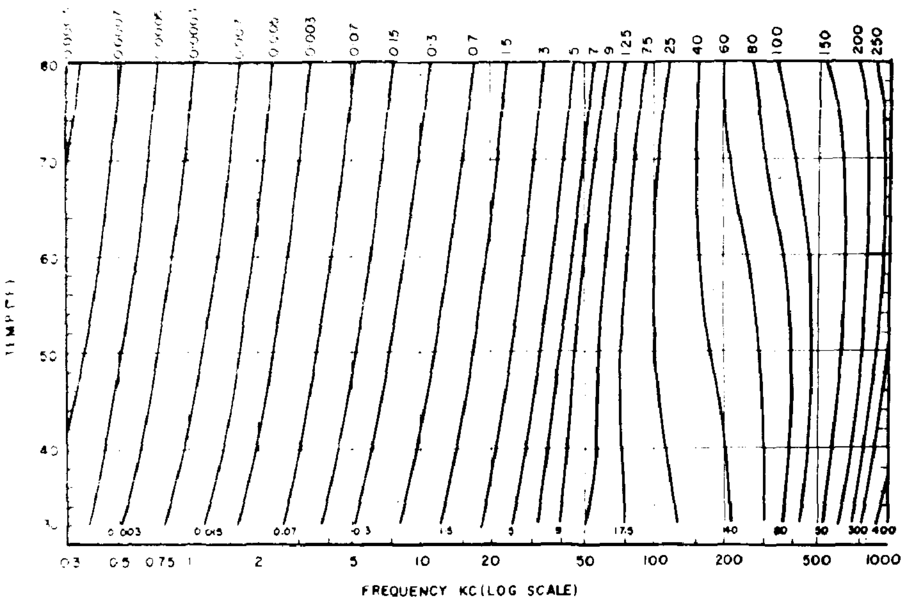

Figure 2 - Sound absorption coefficient in sea water in d/b (from Ref. 13)

REFERENCES

1. S. R. Murphy, L. Beck, Y. Igarashi, and D. C. Whitmarsh, "A Summary of Recent Information on the Acoustics of the Sea with Application to Acoustic Torpedoes," Joint ORL, NOTS and APL, Univ. of Wash. Report, ORL Penn. State Univ., Serial Nord 7958-308 (Confidential), September 1955.

2. "Physics of Sound in the Sea," STR Div. 6, NDRC, Vol. 8, 1946

3. J. W. S. Rayleigh, "The Theory of Sound," 2:315, Dover, 1945

4. L. Liebermann, "Sound Propagation in Chemically Active Media," Phys. Rev., 76:1520-1524, 1949

5. J. J. Markham, R. T. Beyer, and R. B. Lindsay, "Absorption of Sound in Fluids," Rev. Mod. Phys., 23:353-411, 1951

6. L. Hall, "The Origin of Ultrasonic Absorption in Water," Phys. Rev., 73:775-781, 1948

7. G. Kurtze and K. Tamm, "Measurements of Sound Absorption in Water and in Aqueous Solutions of Electrolytes," Acustica, 3:33-48, 1953

8. L. N. Liebermann, "The Origin of Sound Absorption in Water and in Sea Water," J. Acoust. Soc. Amer., 20:868-873, 1948

9. O. B. Wilson, "Absorption of Ultrasonic Waves in Aqueous Solutions of Magnesium Sulfate," Tech. Report IV, Dept. of Phys., Univ. of Calif., Los Angeles, June 1951

10. R. W. Leonard, "The Attenuation of Sound in Liquids by a Resonator Method," Tech. Report I, Dept. of Phys., Univ. of Calif., Los Angeles, June 1950

11. H. W. Marsh and M. Schulkin, "Report on the Status of Project AMOS," USL Report 188 (Confidential), April 3, 1953

12. W. C. Meecham, W. H. Kelly, and J. R. Frederick, "An Investigation of the Sound Transmission Loss In and Below an Isothermal Layer," Univ. of Mich. Engrg. Res. Inst. Tech. Report Project M936 (Confidential), July 7, 1953

13. R. T. Beyer, "Nomogram for the Sound Absorption Coefficient in Sea Water," RAG, Brown Univ. (Confidential), November 20, 1953

14. J. M. M. Pinkerton, "A Pulse Method For the Measurement of Ultrasonic Absorption in Liquids: Results for Water," Nature, 160:128-129, 1947

15. V. A. Del Grosso, "Dependence of Sound Absorption on Concentration, Frequency, and Temperature in $MgSO_4$ Solutions Equivalent to Sea Water - Graphs from Calculations Based on a Review," NRL Report 4279, January 13, 1954

16. "Acoustical Properties of the Medium," APL, Univ. of Wash., 4th Semi-Annual Report, APL UW TE 55-51, April 1, 1955 - September 30, 1955

FLUCTUATIONS*

S. R. Murphy
Applied Physics Laboratory
University of Washington

INTRODUCTION

Whenever sound is transmitted in the ocean, irregular variations in received intensity are observed. Under some conditions the ratio of maximum to minimum intensity is in excess of ten to one. This fluctuation is most important in the detection of echoes or signals. It becomes particularly important in the case of active-acoustic torpedoes. Since the torpedo acoustic homing system depends on the receipt of an echo for steering information, it is quite possible that a target may not be detected or may be lost after detection because of fluctuation in echo intensities. Since, in general, both signal and background levels fluctuate, passive acoustic torpedo systems are also affected. Variations in signal strength, of course, affect sonar and other instruments utilizing underwater sound. Because of the obvious practical importance of understanding such a phenomenon in any application of underwater sound, considerable effort has been spent in trying to analyze this transmission variability. Several excellent summaries (1, 2) have been written on the subject.

Some of the mechanisms that have been discussed in the literature as possible causes of fluctuation (2) are as follows: (a) relative motion of projector and hydrophone; (b) interference between direct and reflected sound (in deep water); (c) interference between rays bent by thermal, micro- or macrostructure; (d) focusing and defocusing by thermal inhomogeneities (lens action); (e) reflection and scattering from inhomogeneities in the sea; and (f) interference between direct, surface-reflected, and bottom-reflected sound (in shallow water).

In general, some types of fluctuations are caused by tilting or turning of the beam pattern of the transducer. In other cases, fluctuation may be due to refraction or reflection, a sound beam being bent in a varying fashion so that sometimes it is received and sometimes it is not. A third cause of fluctuation is interference due to phase shifts. This last may include the effects of the other causes, in that the phase shift may be caused by path difference due to reflection or refraction, etc.

The general problem of fluctuation is so complex that it is hardly possible to produce a general theory that will take into account, in terms of known or measurable parameters, all the variables involved under all conditions of transmission. Any general consideration must include, equipment characteristics such as frequency, pulse length, pulse repetition rate, transducer parameters, type of detection (such as peak or average amplitude), and amount of smoothing. In addition, the geometry of transducer depth, range, orientation, and motion with respect to the water must be considered. The boundaries of the medium contribute variable properties: the surface is irregular and time-dependent, and the bottom varies in depth and

[illegible]

*[illegible] cited in Ref. 5.

acoustic properties. Finally there is, in general, an inhomogeneous, nonisotropic volume. The problem, of course, must be idealized and restricted to one mechanism at a time in order to evaluate the importance of each. For the purposes of discussing the recent work in fluctuations, a particular model will be considered, and it is hoped that the physical situation corresponds sufficiently often to this model to be useful.

First, consider that transducer and water depths are sufficient and pulse lengths are short enough so that the direct sound can be separated from sound reflected from the boundaries. The gross thermal structure or gradient will be neglected, as will the effects of reflection, since fluctuation from these causes is fairly well understood and is covered in the standard references such as (1) and (2). In other words, only the effect of inhomogeneities in the volume of the medium which cause small deviations in the velocity of sound from the average velocity in the medium will be considered. For sea water, the most important oceanographic parameters which can cause such deviations are salinity and temperature. In the discussion to follow salinity will be neglected with only temperature variations allowed in the model.

The reason for omitting salinity variations from the considerations are primarily pragmatic. Compared to temperature variations, little is known about salinity inhomogeneities in the sea. Further, as will be seen below, an accounting of temperature variations alone are sufficient in many cases to understand the observed fluctuations in acoustic transmission.

These small temperature variations within the volume of the sea are often termed "thermal microstructures" and, for the purposes of this report, will be defined as temperatures deviating less than 0.5°C from the average.

Even under these rather severe limitations, in order to describe the effects of volume inhomogeneities on acoustic propagation, considerable knowledge of the characteristics of the microstructure is required. Unfortunately, the experimental observations of such fine temperature structure shows wide variations in its character. However, these observations can be separated into two extreme situations which result in correspondingly different analyses.

Observations of small scale temperature structure in relatively small bodies of water protected from the open ocean by land masses has revealed the existence of temperature layers on the order of a meter thick extending horizontally for hundreds of meters with temperature excursions of tenths of a degree centigrade. The size, shape, and horizontal extent of these layers are slowly varying functions of time. Such layers form natural sound channels which can cause considerable local perturbations in the sound field depending upon the geometry of the acoustic observations with respect to the layers. When transmission is between fixed points these layers can create considerable time variations in the acoustic level, primarily by vertical migration over periods in the order of tens of minutes. The analysis of the sound field perturbations is a direct approach, requiring detailed knowledge of the temperature structure which, unfortunately, is difficult and time consuming to acquire.

In contrast, observations of deviations from the average temperature in horizontal travel of a submarine made in coastal waters have indicated "blobs" or patches more or less randomly varying in temperature and size.* On the basis of a few statistical parameters describing average water, an analysis can be made relating these parameters to statistical properties of the acoustic field providing that certain assumptions are met.

Both the statistical approach and the direct calculation on the basis of layering has met success in understanding fluctuations under conditions in which the prescribed limitations of each have been met. In the following sections the theory and the experimental results of each will be briefly discussed. However, the paucity of experimental data on most regions of

*One might conveniently imagine that the above-mentioned layers are strongly perturbed by the relatively strong action of the wind and tidal currents in coastal waters resulting in the breaking up and randomly distributing of the layers of different temperatures.

interest does not allow ready numbers to be assigned characterizing fluctuations in a given locality under even these restricted conditions.

STATISTICAL THEORY

The model of the medium to be considered here is one in which the index of refraction varies in a statistically describable manner either from point to point or with time at any particular location. It is first assumed that

$$\mu(x, y, z) = 1 + \alpha n(x, y, z), \tag{1}$$

where $\mu(x, y, z)$ is the index of refraction at position (x, y, z), α is the rms deviation of μ from unity, and $n(x, y, z)$ is the variable component of μ.

Denoting a space average by the symbol $\langle\ \rangle$, α and n are chosen so that

$$\langle n(x, y, z) \rangle = 0, \tag{2}$$

$$\langle n^2 \rangle = 1. \tag{3}$$

It is further assumed that

$$\alpha \ll 1. \tag{4}$$

The second parameter defined is the space autocorrelation coefficient. This is given by

$$R(x - x', y - y', z - z') = \langle n(x, y, z)\, n(x', y', z') \rangle \tag{5}$$

and is assumed to be a function only of the coordinate differences $x - x'$, $y - y'$, $z - z'$. The statistical process producing the microstructure resulting in these small variations in index of refraction is assumed to be a stationary process, so that a kind of working hypothesis can be made. That is, time averages at one space location over long periods of time are equal to space average over large regions of space for the function $n(x, y, z)$ characterizing the variation in index of refraction. Time averages will be denoted by barred quantities.

There is some experimental justification for this model. Several series of measurements have been made of the thermal microstructure of the ocean. In each, a sensitive, short-time-constant electrical thermometer was mounted on a submarine to obtain a relatively stable platform. The submarine then cruised at constant depth while continuous recordings were made. The fluctuations of temperature with respect to the mean were obtained, and from these data, α and $R(\rho)$, ρ being the coordinate difference, could be calculated. References (1) and (2) discuss some of the earlier results. Urick (3, 4), working at Key West with a probe whose time constant was 0.4 second, found large patches of "inhomogeneous" water whose average "size" was several yards. However, the time constant of his probe prevented the observation of temperature variations smaller than a few yards. Using a probe with a 0.02-second time constant Liebermann (5) made extensive measurements along the coastal waters from Southern California to Alaska. A typical example of his data shows α^2 to be of the order of 5×10^{-9}. The form of the correlation coefficient was found to be a monotonically decreasing function of the coordinate difference, which could be written as

$$R(\rho) = e^{\left(-\frac{\rho}{a}\right)} \tag{6}$$

or

$$R(\rho) = e^{\left(-\frac{\rho^2}{a^2}\right)} \tag{7}$$

where "a" is a measure of the average "patch" size and is of the order of 60 cm.

Two other statistical quantities should be defined as measures of the fluctuation of the sound field. These are the coefficients of variation of the intensity, I, and the pressure amplitude, p:

$$V_I^2 = \frac{\overline{I^2} - \overline{I}^2}{\overline{I}^2} \tag{8}$$

$$V_A^2 = \frac{\overline{p^2} - \overline{p}^2}{\overline{p}^2}. \tag{9}$$

There have been several applications of this general model to fluctuation. Bergmann (6) applied a perturbation calculation based upon the equations of ray acoustics. He obtained an expression for the variation of intensity, which may be represented approximately by

$$V_I^2 = \frac{r^3}{15} \alpha \int_0^\infty \nabla^2 \nabla^2 R(\rho)\, d\rho. \tag{10}$$

Since this is a high-frequency approximation to wave theory, the frequency does not appear as a parameter. The important consideration is the predicted $r^{3/2}$ variation of V_I with range. Since it is a ray theory, it can be interpreted as the result of the focusing and defocusing action of the microstructure.

Others using this same model for the medium, have obtained similar perturbation solutions for the wave equation. Pekeris (7) and Ellison (8) assumed plane waves traveling through the medium. Mintzer (9, 10) applied the same general method in greater detail to the case of spherical waves under the condition of pulse operation. This more complete and more general treatment by Mintzer will now be considered.

Mintzer (9) places his transmitter at the origin and his receiver at a position $\vec{r^1}$ from the origin. Using Eq. (1), he then expands the time-independent wave equation including terms of first order in obtaining

$$(\nabla^2 + k_o^2)\, \alpha = -2k_o^2\, \alpha n p. \tag{11}$$

Here $k_o = \omega/c_o$ where c_o is the average, or unperturbed sound velocity.

Applying the Born approximation to this equation, he obtains for the spherical solution

$$\alpha(x, y, z) = \frac{e^{ik_o r}}{r} - \frac{k_o \alpha}{2\pi} \int_{\text{all space}} n(x', y', z') \frac{e^{ik_o |\vec{r} - \vec{r}'|}}{|\vec{r} - \vec{r}'|} \frac{e^{ik_o r'}}{r'} dv'. \tag{12}$$

Here the first term is the normal spherical solution of the wave equation. The second term represents the total contribution due to scattering by the inhomogeneities, where $\vec{r}'$ is the location with respect to the transmitter of a differential scattering volume with index-of-refraction deviation from unity of $n(x', y', z')$.

The introduction of the correlation coefficient comes when p^2 is computed for the coefficient of variation of the pressure. A cross-product term is obtained, which includes a double integration over all space of

$$\langle n(x', y', z')\, n(x'', y'', z'') \rangle,$$

which is

$$R(x' - x'', y' - y'', z' - z'')$$

by definition. By an ingenious process of approximation based on the orders of magnitude of α and a, Mintzer arrives at the final result, which is

$$V_A^2 = 2k_o^2 \alpha^2 r \int_0^\infty R(\rho)\, d\rho, \tag{13}$$

where the path of integration is along the direction of the vector connecting the source to the receiver. The expression given in Eq. (7) for $R(\rho)$ yields

$$V_A = (\pi^{1/2} k_o^2 \alpha^2 a)^{1/2} r^{1/2}. \tag{14}$$

We may note several interesting features of this result. First, the coefficient of variation for the pressure is determined from two measurable medium parameters, α and $R(\rho)$. Second, there is a frequency dependence proportional to f, since $k_o = 2\pi f/C_o$. Finally, a range dependence of $R^{1/2}$ is predicted.

In his second paper, Mintzer (10) examines the region of validity for his first calculation by including terms in α^2. He finds that the first calculation should be valid for

$$k_o r \ll \frac{1}{k_o a \alpha^2}. \tag{15}$$

Other approximations are made, including an extension to the high-frequency limit, where a comparison with Bergmann's ray calculation is made.

COMPARISON WITH EXPERIMENT

Careful measurements of sound transmission at 24 kc using a pulse method were made by Sheehy (11) off San Diego. He obtained data over many successive "pings" at sufficient depth to separate the direct ray from the surface-reflected ray. Sufficient data were taken at each of many ranges from 30 yards to 4000 yards to enable a calculation to be made of V_A. Figure 1 is a reproduction of a figure from Mintzer's first paper (9), showing a best curve through Sheehy's experimental data and the prediction given by Eq. (14) for the wave calculation and Eq. (10) for Bergmann's ray calculation, both employing the values for $R(\rho)$ and a from Liebermann. Note that the range dependence of $r^{1/2}$ predicted by Mintzer agrees with the best line through the experimental data; further, that the quantitative agreement between the theory and the average of the experimental data is very good considering the uncertainty in $R(\rho)$ and a and the wide scatter of the experimental data. The range dependence for ray acoustics does not agree with

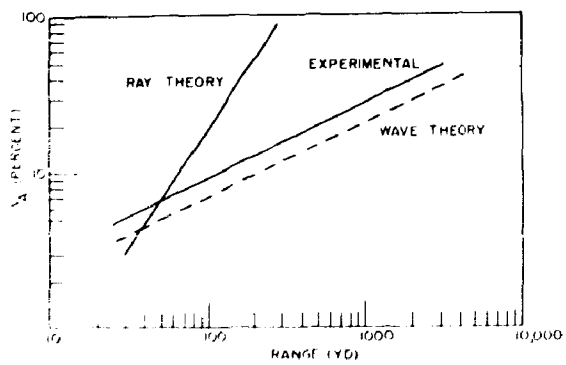

Figure 1 - Coefficient of variation as a function of range

the experimental data, indicating that at 24 kc for the experimental ranges considered the high-frequency approximation is not valid.

LAYER THEORY

In the statistical approach the microstructure was thought to be arranged in small patches randomly positioned in space and undergoing random changes of positions with time allowing only calculations of average acoustical quantities. In the layer theory, the model of the mediums is much different. Here it is assumed that the microstructure is arranged in stable horizontal layers that preserve their size, shape, and position over times of the order of tens of minutes. For acoustic experiments of shorter duration than this stable period the layers can then be assumed fixed in space and the acoustic field at all points in space can, in principle, be directly calculated from the layer characteristics and the geometry of the transducer position.

The experimental evidence for the existence of such layers is unfortunately confined to only two geographic areas. Galle (12) in 1940 through 1944 made a series of observations in the Baltic Sea. His work, published in 1953, discusses these results and a theoretical interpretation of the mode of layer formation. Garrison (13) has made similar observations in Dabob Bay, located in Puget Sound, Washington. Figure 2 shows a typical layer traced for a distance of 140 yards over a time of 56 minutes.

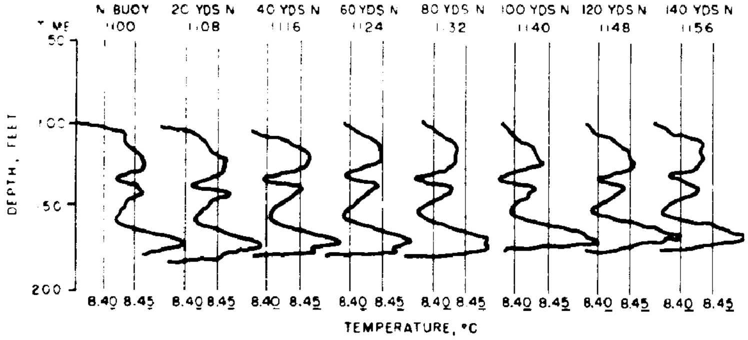

Figure 2 - Temperature profiles as a function of depth
(Dabob Bay, N End, March 22, 1955)

To readily obtain an estimate of the effect of such layers on sound transmission advantage may be taken of the small deviation of the index of refraction from the average value throughout the medium. A single layer is assumed extending horizontally throughout all space, with an average value of 1 and a maximum excursion from the value of a. Then

$$\mu = 1 + a n(z), \tag{16}$$

where $n(z)$ is a function of depth only and is normalized to one at the maximum excursion. The dimension z is chosen to be zero at the depth of the transmitter and assumed to be much less than one. A perturbation calculation on the ray approximations of the Eikonal Equations is followed* after Bergmann (6). Defining L_1 as the difference between the actual sound level (in nepers) and the level caused by spherical spreading, Bergmann's Eq. (20) becomes

$$L_1 = a\int_0^r \left(\frac{1}{r} - \frac{1}{\rho}\right) \rho^2 \nabla_\rho^2 n(z)\, d\rho \tag{17}$$

* 1 neper = 8.6 db

where the integral is taken along the line from the source to the receiver located at $\vec{r}$ with respect to the transmitter. This can be rewritten as

$$L = \frac{\alpha r^2}{z^2}\left[-n(z) - n(o) + \frac{2}{z}\int_o^z n(z)\,dz\right]. \qquad (18)$$

Once the shape function of the layer, $n(z)$, is available from experimental data, the perturbation level L_1 can readily be calculated.

Unfortunately for this simple approach, no simple validity criterion is available. Being a perturbation calculation, the dependence of Eq. (18) cannot be valid for ranges which allow L_1 to be too large a fraction of the inverse-square level. However, as will be shown in the next section, comparison with experimental values are surprisingly good up to values for L_1 of the order of 10 db.

COMPARISON WITH EXPERIMENT

Figure 3 gives an example (12) of the application of Eq. (18). The temperature distribution on the right, shows a predominant layer at 150 feet in depth. This was approximated by a gaussian curve with the parameters noted on the figure. The actual relative sound level is shown by the light, irregular line on the right measured at 525 yards with 60 kc pulses. The predicted level is the smooth heavy line with reasonable agreement.

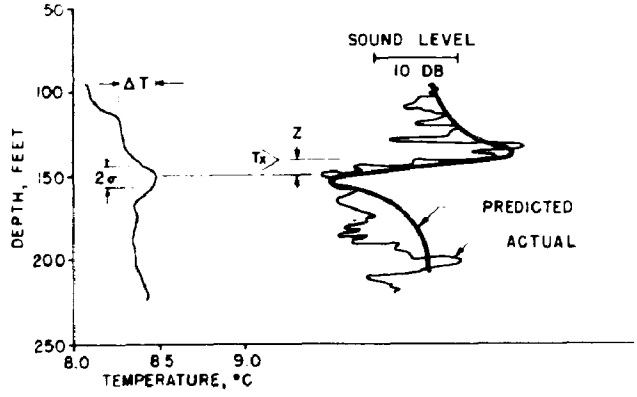

Figure 3 - Comparison of predicted and measured acoustic variations as a function of depth at a constant range (Dabob Bay, March 2, 1955, range - 525 yd., T_x depth - 140 ft)

Figure 4 shows a more complicated example (14). The actual temperature distribution is shown on the left with the dotted line and the resultant approximation to it by a series of gaussians shown with the solid line. The actual sound level and the predicted level is shown to the right for a transmitter at 240 feet in depth and a range of 520 yards. Again, a reasonable agreement is obtained between the predicted sound level and the actual level.

The two foregoing examples are typical of those situations in which the structure was truly layered and which therefore allowed the application of the theory of this section. It should be emphasized, however, that such an ideal situation does not always occur. Layers existing strongly at one point can fade out and become extinct in moving several hundred feet horizontally. Further, influx of tidal currents and the excitation of internal waves (12) can distort the thermal pattern radically over a time of 20 to 30 minutes.

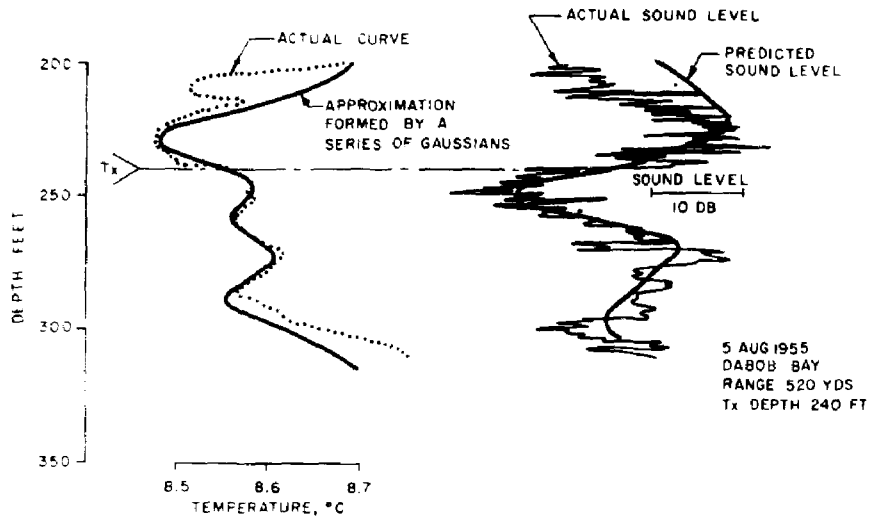

Figure 4 - Sound level variations predicted by thermal layers (Dabob Bay, August 1955, T_x depth - 240 ft)

CONCLUSIONS

In the preceding discussion, fluctuation in direct sound transmission has been associated with the thermal microstructure existing between the transmitter and the receiver. Two convenient models of the arrangement of the microstructure throughout the volume have been considered, both of which have the support of experiments in certain local areas. However, the extrapolation of these data and prediction techniques to other localities is not possible until more extensive studies of the thermal microstructure and its process of formation are made in many different oceanographic situations. The designer and operator of acoustic equipment, then, is not well supplied with the kind of information on fluctuations he may desire. He knows that he may expect in direct transmission variances of the kind shown in Fig. 1. Further, he is aware that small temperature layers of the kind shown in Figs. 2, 3 and 4 can cause acoustic "holes" which extend essentially horizontally and have a magnitude of the order of 10 db at several hundred yards, depending upon the transducer and layer geometry. However, he has neither a way to choose between these alternate viewpoints in a given application nor a reasonable value of the pertinent parameters needed to apply these theories. Further, information concerning other important functions such as probability distributions of amplitudes and rapidity of fluctuations with time, is not available for general applications. Rather, the chief contribution of the work discussed in this section lies in the foundation established from which to continue the study of fluctuations.

Future experimental and theoretical work must be done. However, it must be emphasized that acoustic data alone, without a corresponding study of oceanographic conditions including the microstructural arrangement in the medium, is of little value. Indeed, a strong effort made to understand the basic processes involved in the production of this microstructure and the probable distribution of this structure throughout geographical regions of acoustic interest would greatly clarify the present situation.

REFERENCES

1. "Physics of Sound in the Sea," STR Div. 6, NDRC, Vol. 8, Ch. 7, 1946

2. "A Survey Report on Basic Problems of Underwater Acoustics Research," Panel on Underwater Acoustics of the Committee on Undersea Warfare, NRC, Ch. 5, 1950

3. R. J. Urick and C. W. Searfoss, "The Microthermal Structure of the Ocean Near Key West, Florida, Part I. Description," NRL Report S-3392, 1948

4. R. J. Urick and C. W. Searfoss, "The Microthermal Structure of the Ocean Near Key West, Florida, Part II. Analysis," NRL Report S-3444, April 1949

5. L. Liebermann, "The Effects of Temperature Inhomogeneities in the Ocean on the Propagation of Sound," J. Acoust. Soc. Amer., 23:563-570, 1951

6. P. G. Bergmann, "Propagation of Radiation in a Medium with Random Inhomogeneities," Phys. Rev., 70:486-492, 1946

7. C. L. Pekeris, "Note on the Scattering of Radiation in an Inhomogeneous Medium," Phys. Rev., 71:268-269, 1947

8. T. H. Ellison, "Propagation of Sound Waves Through a Medium with Very Small Random Variations in Refractive Index," J. Atm. and Terrest. Phys., 2:14-21, 1951

9. D. Mintzer, "Wave Propagation in a Randomly Inhomogeneous Medium I," J. Acoust. Soc. Amer., 25:922-927, 1953

10. D. Mintzer, "Wave Propagation in a Randomly Inhomogeneous Medium II," J. Acoust. Soc. Amer., 25:1107-1111, 1953

11. M. J. Sheehy, "Transmission of 24-kc Underwater Sound from a Deep Source," J. Acoust. Soc. Amer., 22:24-28, 1950

12. K. Kalle, "Zur Frage der Innern Thermischen Unruhe des Meeres," Deut. Hydrograph. Z., Band 6, Heft 4/5/6, 145-170, 1953

13. G. F. Garrison and D. S. Potter, "The Influence of Oceanography on Torpedo Ranging in Dabob Bay and Hood Canal," APL, Univ. of Wash., APL/UW/TE/55-40 (Confidential), August 26, 1955

14. Monthly Report for Project 8, APL, Univ. of Wash., December 1955

15. S. R. Murphy, L. Beck, Y. Igarashi, and D. C. Whitmarsh, "A Summary of Recent Information on the Acoustics of the Sea with Application to Acoustic Torpedoes," Joint ORL, NOTS and APL, Univ. of Wash. Report, ORL Penn State Univ. Serial Nord 7958-308 (Confidential), September 1955

LOW-FREQUENCY DEEP-WATER TRANSMISSION

LONG-RANGE SOUND TRANSMISSION IN DEEP WATER

C. B. Officer
Woods Hole Oceanographic Institution

INTRODUCTION

This chapter covers the general subject of long-range sound transmission in deep water. The main concern is with transmission from a shallow, near-surface source, propagation from a deep source to a deep receiver via the SOFAR channel being covered elsewhere in the volume. A brief discussion of the various transmission paths from a shallow source to a receiver at distance and a review of the criteria that have been developed over the past few years from both theoretical considerations and field measurements to determine over what ranges and frequencies each of these paths is available and to determine their dependence on environmental factors are given. The results are applicable to the problems involved in the long-range detection of and by submarines.

Historically, this work begins with, and is heavily dependent on, three excellent papers (9, 10, and 60) that were published shortly after World War II. Since then the research in this field has progressed in several directions. Work has continued on the study of SOFAR propagation (58, 2, 6, and 14) with application to the location of submarine topographic peaks (25 and 49). Recognition of the existence of the 35-mile focussing peaks (54, 55, 56, 23, 47, and 20) has led to a continued examination of these convergence regions (5, 7, 26, 46, 44, 18, and 28). Considerable emphasis has been placed on the study of long-range transmission through the surface, isothermal sound channel (50, 35, 51, 29, 52, 53, 48, 30, 57, 36, 45, 32, 33, 1, 31, 11, and 34). Recently the emphasis has shifted to a more general study of sound transmission from a shallow source in deep water and of transmission from deep to shallow water, with particular emphasis on the dependence on oceanographic, topographic, and geologic conditions (59, 21, 15, 37, 13, 40, 16, 4, 3, 43, and 61) which has led an increased interest and research on bottom reflectivity (19, 27, 37, 40, 44, 16, 42, 24, 8, and 62) and to prediction of long-range transmission conditions for moderately complex areas (22, 38, 12, 39, and 41).

As might be expected, it is essential to have an adequate knowledge of the physical factors affecting sound transmission of the area under consideration. The most important are the sound-velocity structure in the ocean, the bottom topography, and the bottom reflectivity. The sound-velocity structure in the ocean is usually determined from bathythermograph lowerings and hydrographic stations of water-bottle samples collected at depth. The bottom topography is determined from surveys which in many cases require precision echo sounding and accurate navigational control. The bottom reflectivity as a function of angle of incidence and frequency is determined from seismic reflection profiles. Additional information to an understanding of bottom reflection phenomena are obtained from seismic refraction profiles and deep sea cores.

Note: Paper received September 1955

CRITERIA DETERMINING LONG RANGE SOUND TRANSMISSION IN MODERATELY DEEP TO DEEP OCEAN AREAS

There are four possible types of paths for sound to travel from a near surface source to a receiver at distance in deep ocean. These are illustrated in Fig. 1.

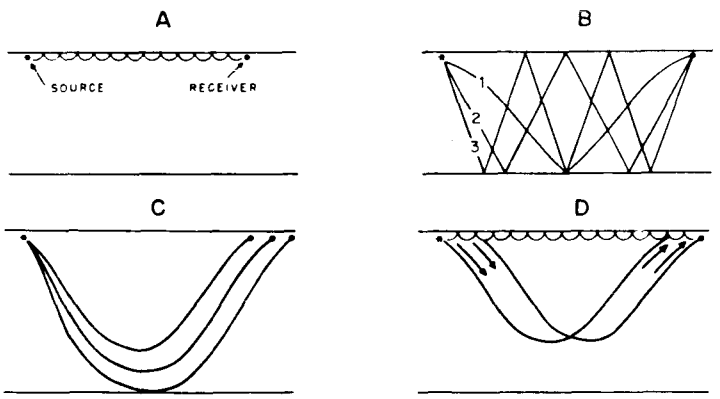

Figure 1 - Ray diagrams of four types of deep water transmission

Transmission Through the Surface Sound Channel (Fig. 1A)

If there is mixed, isothermal water near the ocean surface, a slight posjtive sound-velocity gradient will be developed down to the depth of the main or seasonal thermocline, thus forming a sound channel with the ocean surface as shown in Fig. 2A. This sound channel when developed usually extends down to a modest depth of around 100 to 300 feet. The frequency content of the energy trapped is a function of the channel thickness; for a 100-ft channel, energy is trapped down to a frequency of 3000 cps; for a 300-ft channel down to 1000 cps. The efficiency of the channel is also dependent on the attenuation from absorption losses in sea water and scattering losses from the rough sea surface, both of which give an increased attenuation with increasing frequency. The absorption loss has been given (32 and 33) in decibels per kiloyard as

$$\alpha = 0.6 \frac{f_m f^2}{f_m^2 + f^2}$$

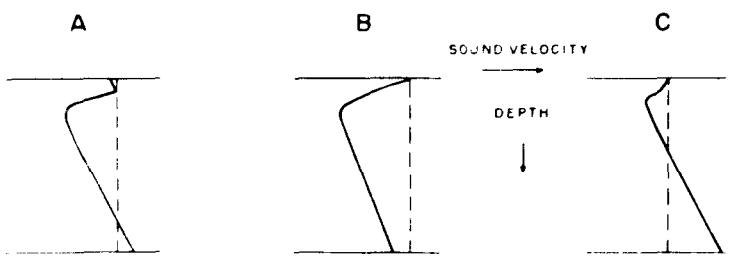

Figure 2 - Characteristic sound velocity sections

where f is the frequency in kilocycles per second and $f_m = 2.19 \times 10^7 . \ e^{[-6300/T + 524]}$, T in degrees Fahrenheit, in agreement with theory and laboratory experiments. For frequencies around 16,000 cps, the scattering loss from sea-surface roughness has been given as 5-db loss per range interval of the ray, taking the maximum surface-to-surface distance in the channel, for each Beaufort unit increase in wind force. Thus, the combined effects of the increased loss with decreasing frequency due to leakage out of the channel and the increased loss with increasing frequency due to absorption and scattering produce an optimum frequency for best transmission. Prediction (57) of the overall attenuation for various thicknesses of the isothermal channel is shown in Fig. 3. These predictions have been verified (36) as to the value of the optimum frequency as a function of channel thickness and the magnitude of the attenuation at both lower and higher frequencies. This type of transmission is generally unimportant for the lower frequencies (500 cps and below) but can in some cases be the most important path at higher frequencies. This type of transmission will exist for the sound-velocity sections of Fig. 2A but is not allowed for the sound velocity sections of Figs. 2B and 2C.

Transmission Via Bottom and Surface Reflection (Fig. 1B)

This type of path is allowed with any sound-velocity structure or bottom depth. The important criterion in determining its effectiveness is the amount of energy that is returned from the bottom upon each reflection. There has been some confusion as to the reflectivity of

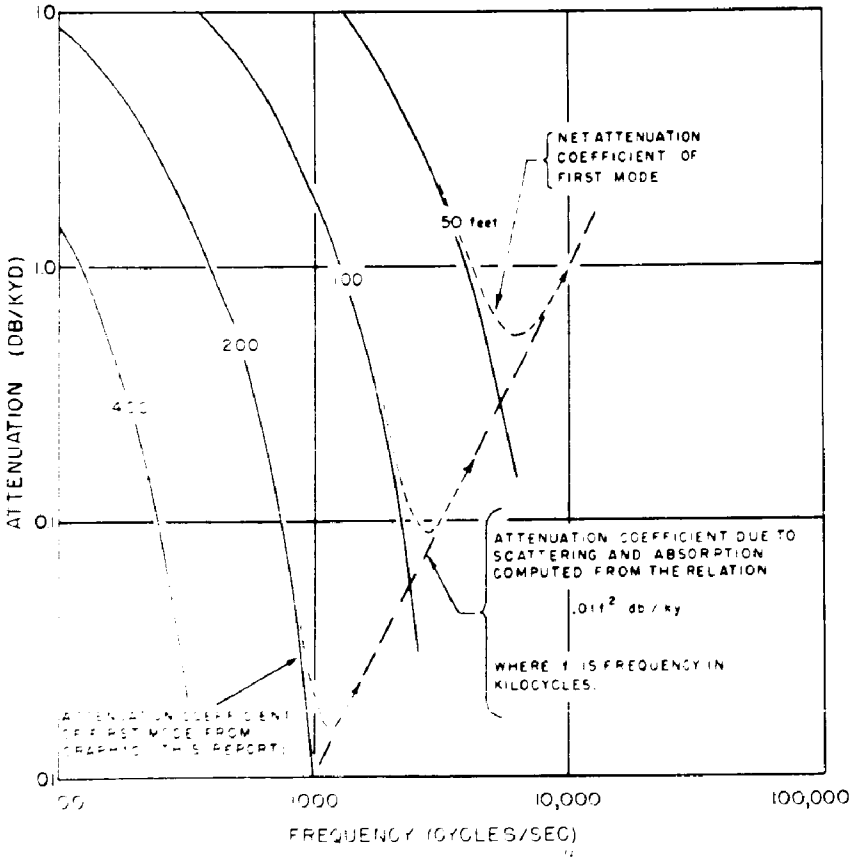

Figure 3 - Surface sound channel attenuation as a function of frequency and channel depth (57)

the bottom, several investigators having reported negligible bottom reflection losses as a function of angle of incidence or frequency. This generally is not true; usually there is a considerable bottom-reflection loss, which is a function of both angle of incidence and frequency. As one follows a given order of reflection, say the first order, (Curve 1 of Fig. 1B), out in range, the angle of incidence on the bottom will decrease from near vertical to a more grazing angle; the percent of energy returned from the bottom is predicted from simple theory to increase with range to 100% at some intermediate angle, known as the critical angle, and remain the same with continuing decrease in angle of incidence. This effect, due to partial transmission into the bottom, is observed, but in general the reflectivity even beyond the critical angle is not unity. For a long-range transmission run, the increased losses at the steeper angles of incidence are such that the higher orders of reflection are not observed until the range of their critical angle ray is reached. This phenomenon has been used (62) to determine the critical angle, giving values in agreement with that expected from seismic velocity measurements of the bottom sediment.

As one continues to follow a given order, say the first order, beyond the critical angle, a range will be reached beyond which that reflection will not be received. This is due to the velocity structure in the ocean. The ray which carries a given order of reflection out to its maximum range is known as the limiting ray. The range interval between the critical-angle ray and the limiting ray is a good criterion for the distance over which a given order of bottom reflection is received well. In Fig. 4 the critical angle and limiting rays, and the range intervals for best reception by one and two bottom reflections are shown for a moderately deep ocean and a horizontal bottom.

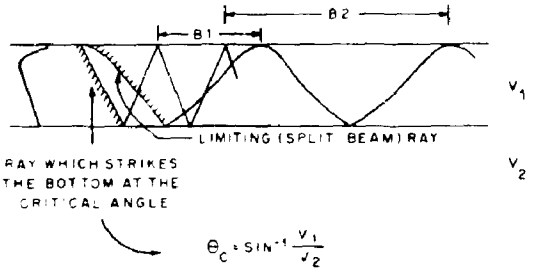

Figure 4 - Critical angle and limiting rays and range intervals of best reception by bottom reflection

Of considerable interest, then, in this type of transmission is the bottom reflectivity over the range interval of best reception. Figure 5 is a graph of the average energy lost per cycle of bottom and surface reflection over this interval plotted as a function of frequency for various geologic areas (37, 40, 24, and 16). All the graphs show an increase in loss with increase in frequency. This is probably due to the combined effects of scattering from bottom and surface roughness and of local interaction across the boundary between the ocean and the highly porous sediment. At the lower frequencies, below 300 cps, another mechanism is dominant. A close examination of the bottom reflections at these frequencies shows that the arrival consists of one or more subbottom reflections as well as the bottom reflection, and further that as the angle of incidence decreases from near vertical the portion of the energy reflected from the bottom decreases, and that reflected from below the bottom increases and becomes the dominant energy return (42 and 62). Owing to the steep velocity gradient in the sediment, the subbottom reflections eventually become a subbottom refraction. This sequence of events is theoretically understandable in terms of reflection from and propagation in a highly porous sedimentary material. Over the ocean basin areas of the Western Atlantic the total energy returned from the subbottom and bottom is nearly unity at frequencies below 200 cps (Fig. 5). Over the depositional areas of the gentle rise from the ocean basins to the North American continent the loss is greater at corresponding frequencies.

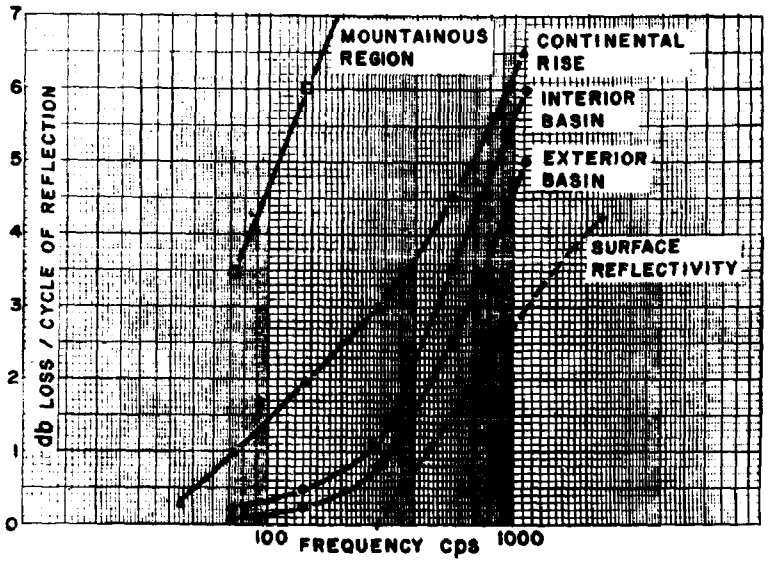

Figure 5 - Reflection loss for angles of incidence more grazing than critical as a function of frequency and geologic area (40)

In dealing with bottom-reflected rays, complications can arise from variations in submarine topography. One of the more obvious effects is either partial or total blocking of the incoming signal. Out from a hydrophone off the Bahamas there is a change in bottom topography such that in progressing from a northeast to a north bearing somewhat over half of the bottom-reflected rays are cut off, giving a corresponding drop of about 4 db in received signal (21). Out from the hydrophone at Oahu there is considerably greater topographic variation such that on an arc run at 50-miles range the signal varied by 22 db with a maximum variation of 10 db over an arc of 3 to 4° (4). In a somewhat similar situation a transmission run over the mountainous region southeast of Bermuda (24) showed losses considerably higher than those observed over level bottoms (Fig. 5).

A less obvious effect is that of long-range transmission over a gentle slope, such as the continental rise. Upon each cycle of bottom and surface reflection the direction of the rays is changed by twice the inclination of the bottom. Thus, on transmission upslope the bottom-reflected rays are steepened and energy is shifted from the region between the limiting and critical-angle rays down to angles of incidence steeper than critical with the result that additional energy is lost into the bottom. For example, in the case shown in Fig. 6B the limiting ray has an angle of incidence on the bottom of 5° with the horizontal and the critical-angle ray 29°; this gives an angular coverage of 24° for best transmission by bottom reflection. If the bottom slope is 2°, the rays will be steepened by 4° upon each bottom reflection and after the sixth reflection all the energy will be shifted down into the region of poor transmission, so that beyond the range at which only the seventh or higher-order reflections are received, all the energy will have had to take at least one reflection steeper than the critical-angle reflection.

Similarly for transmission downslope the energy is shifted to more grazing angles of incidence and some of the energy is changed to RSR, Fig. 1C*, and SOFAR rays. Another effect is that of focussing and defocussing due to bottom curvature. In Fig. 6C a case of focussing from a concave bottom is illustrated. In general such focussing is observed. Over transmission runs where there is also a good echo-sounding traverse, increases and decreases in the intensity of the individual orders of reflection can be associated with particular topographic features (37 and 40).

*See also p. 57

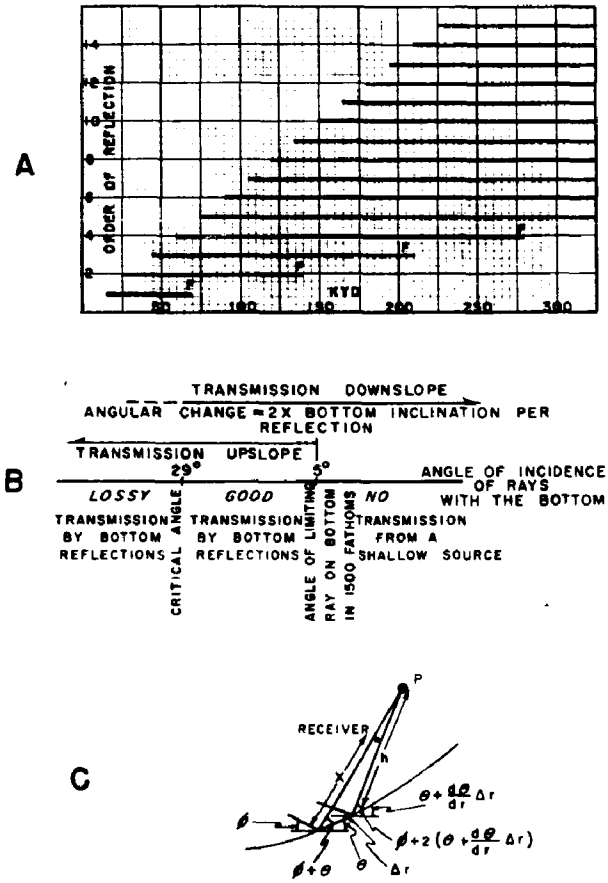

Figure 6 - (a) Transmission diagram, (b) transmission changes over a sloping bottom, and (c) focussing by the bottom (37)

A convenient method for estimating the effect of transmission upslope or downslope or through a section of ocean in which there is a horizontal variation in sound velocity, such as the Gulf Stream region, is that of the transmission diagram (37). On such a diagram the interval of best reception for each order of reflection is plotted against the range. Each line should be marked with the percent of energy returned after its appropriate number of reflections for the frequency interval of interest, the reflectivity values being obtained from graphs such as Fig. 5. In Fig. 6A a diagram is shown for the simple case of a deep Atlantic station at low frequencies with a horizontal bottom. For upslope transmission the intervals for succeeding orders will be less than that shown in Fig. 6A and eventually become zero. The measured intensity at any range then is the sum along a vertical line of the contributions from the appropriate bottom reflections plus a spherical ray spreading term ($1/R^2$). This must be corrected in general for ray focussing and defocussing effects due to the sound-velocity structure in the ocean, particularly for the more grazing rays, and for effects due to bottom curvature. For upslope transmission, the regions to the left in the diagram (which represent energy which has taken only one, two, etc. reflections steeper than critical) with their appropriate reflectivity must also be included. The method has been useful in predicting and verifying experimental results over a sloping bottom (37) and through a region of horizontal variation in sound velocity (3).

Transmission Via a Refraction at Depth in the Ocean Without Bottom Reflection (Fig. 1C)

This type of path is allowed only when the sound-velocity condition is met that the maximum velocity near the surface is exceeded at depth in the ocean. This condition follows directly from Snell's law for a variable-velocity medium. In the sound-velocity sections of Fig. 2 this type of ray is allowed for Figs. 2A and 2C but not for Fig. 2B. If the depth were three-quarters that shown for Fig. 2A or one-third that for Fig. 2C, this type of ray would not be allowed for these cases either. As shown in Fig. 1C this type of ray is received over a limited range interval for each cycle of refraction at depth; this inverval is dependent on the thickness of water below the point where the maximum velocity near the surface is reached at depth; Fig. 2C would thus give a longer interval than 2A. For typical sound-velocity sections in the Pacific this type of ray first appears at a range of approximately 30 nautical miles (Fig. 7), and continues out to a range dependent on the depth of water. If, for example, this ray first appears at a range of 3 units and disappears at a range of 4 units for the first cycle, it will reappear again at a range of 6 units for the second cycle and disappear at 8 units, then reappear again at 9 units for the third cycle and disappear at 12 units, then reappear at 12 units for the fourth cycle and so on, so that beyond a range of 9 units there is continuous coverage by one or more cycles of this type of ray, overcoming in part the apparent deficiency in coverage which would result from the consideration of a particular order of refraction alone. Each of these zones may consist of two parts, an intense focussing peak, F, followed by a broad region of moderately high intensity, RSR. This RSR region is of the order of 6 db more intense than the corresponding bottom reflections, RE, at the same range. Figure 8, a graph of computed ray intensity from a shallow source to a shallow receiver for a mid-Atlantic station (with a deep, 1000-ft, isothermal channel), illustrates these regions. Values for the intensity increase

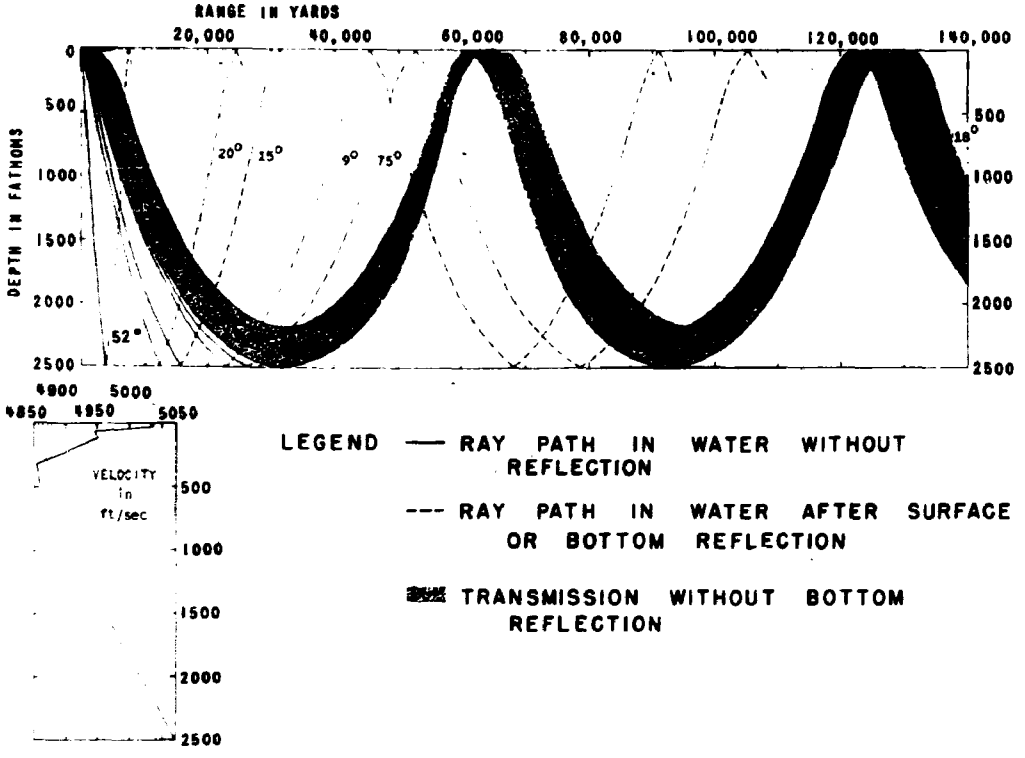

Figure 7 - Ray diagram for transmission by a refraction at depth in the ocean (54). Surface water isothermal to 300 ft.

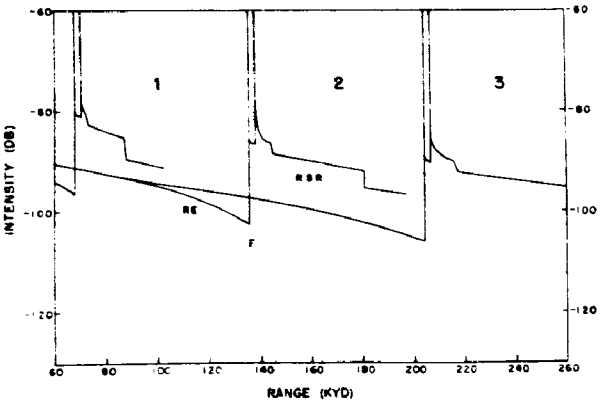

Figure 8 - Computed ray intensities for bottom reflections, focussing peak, and RSR region (unpublished, Brockhurst, WHOI)

in the neighborhood of the focussing peaks have been quoted as 20-30 db (55), 5-10 db (26), 15-20 db (7), 18 db (1), and 18 ±9 db (18). It is difficult from some of the references to determine whether the measurements were at the focussing peaks or the nearby RSR region, but it is surmised that the lower values refer to the RSR regions, the highest values being restricted to the narrow peaks.

A graph such as shown in Fig. 9 is of value in determining the extent of the RSR region and the existence of a focussing peak. Here the angle of emergence of a ray from a shallow source is plotted against the range at which the ray reappears at the surface. The heavy curve corresponds to the rays which have been returned by a refraction at depth in the ocean, the light curves to the bottom reflections. In this case deep refractions exist for water depths greater than 2200 fathoms. With increasing depth of refraction down to 2400 fathoms the range decreases, and then with continuing increase of depth the range increases. The focussing peak, F, is located at the knee of the curve. This is understandable qualitatively in that at this point there is an intense crowding of rays within a narrow range interval. For this case, if the depth of water is greater than 2400 fathoms a focussing peak will exist; if less, no intense focussing

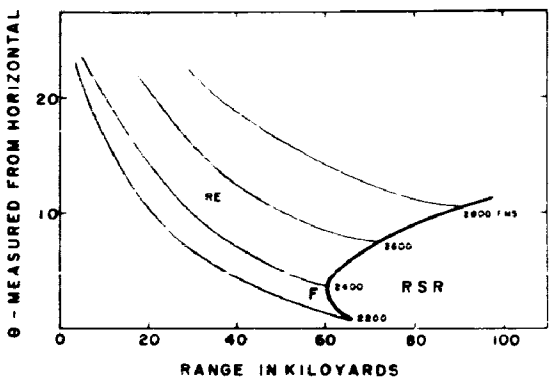

Figure 9 - Graph of angle of emergence from a shallow source as a function of range to illustrate the focussing peak and the RSR region

peak, F, will exist. The extent of RSR coverage for the first cycle is simply that portion of the curve to the depth of water for the particular case; the extent of coverage for the second cycle will be simply twice this interval located at twice the range and so on. When the sound velocity conditions are such as to allow this type of transmission, it is in general the most intense arrival at all frequencies, due in part to the focussing effects that occur along the ray paths and in part to the lack of bottom reflection losses.

Transmission Via Leakage Into and Out of the Surface-Sound Channel with an Associated Limiting Ray Bottom Reflection or Refraction at Depth (Fig. 1D)

This type of ray is allowed only when a surface-sound channel exists. It is not as intense as its associated cycle of deep refraction or bottom reflection, but does extend at lower intensity the range over which the associated cycle is observed. In a case (24) where a good surface-sound channel existed, (400 ft), this type of transmission extended the coverage of each cycle by as much as 200 kiloyards in the frequency region from 150 to 1000 cps. Similar to surface sound-channel transmission, this type of transmission is generally unimportant at the lower frequencies but can in some cases be an important path at higher frequencies.

REFERENCES

1. H. R. Baker, A. G. Pieper, and C. W. Searfoss, "Measurements of Sound Transmission Loss at Low Frequencies 1.5 to 5 kc," NRL Report 4225 (Confidential), September 1953

2. L. H. Barbour and G. P. Woollard, "SOFAR Triangulation Methods," WHOI Ref. 49-38, August 1949

3. A. P. Boysen and C. L. Walker, "Surface Temperature Correlation with Deep-Water Sound Transmission," USN J. Underwater Acoustics, 5:174-183 (Confidential), July 1955

4. R. J. Bolam, M. J. Sheehy, and R. M. Lesser, "Preliminary Evaluation of Transmission from Shallow Explosive Sources at Kaneohe, Oahu, T.H.," NEL Report 568, (Secret), 1955

5. D. Cole, "Broadband Measurements," USL Tech. Memo. (Confidential), 1950

6. T. P. Condron, "Effect of Sound-Channel Structure and Bottom Topography on SOFAR Signals," NEL Report 233, 1951

7. T. P. Condron and R. W. Schillereff, "Long-Range Sound Transmission with a Shallow Towed Source at 500- and 1000-cps Frequency," NEL Report 323 (Confidential), 1952

8. T. P. Condron, D. L. Cole, and J. F. Kelly, "Comparison of Computed and Measured Intensities for Project AMOS Noisemaker Measurements," USN J. Underwater Acoustics, 5:46-51 (Confidential), January 1955

9. M. Ewing and J. L. Worzel, "Long-Range Transmission," WHOI Interim Report 1, Contract NObs-2083 (Confidential), August 25, 1945. This same information may be found in "Long Range Transmission in Propagation of Sound in the Ocean," Geol. Soc. Amer., Mem. 27, 1945

10. M. Ewing, G. P. Woollard, A. C. Vine, and J. L. Worzel, "Recent Results in Submarine Geophysics," Bull. Geol. Soc. Amer., 57:909-934, 1946

11. J. R. Frederick, J. C. Johnson, and W. H. Kelly, "An Analysis of Underwater Sound-Transmission Data," Engrg. Res. Inst. Univ. of Mich. Report 1936-1-T, Contract N6onr-23221 (Confidential), April 1954

12. R. A. Frosch, "A Preliminary Ray Computation for the Ocean South of Sable Is.," Hudson Lab. Tech. Report 11 (Secret), 1953

13. R. A. Frosch, A. N. Guthrie, H. H. Loar, and H. L. Poss, "A Preliminary Report on Sound Transmission at San Juan, Puerto Rico," Columbia Univ., Hudson Lab. Tech. Report 12 (Secret), October 1953

14. J. A. Greer and H. Westfall, "Long-Range Propagation from a Pulsed Audio-Frequency Source in the Pacific SOFAR Channel," NEL Report 340 (Confidential), 1953

15. A. N. Guthrie and H. H. Loar, "Transmission Tests at USNEF Eleuthera, Part II," Columbia Univ., Hudson Lab. Tech. Report 7 (Secret), January 1953

16. A. N. Guthrie, "Transmission of Sound from Deep to Shallow Water," Columbia Univ., Hudson Lab. Tech. Report 23 (Secret), August 1954

17. A. N. Guthrie and M. C. Rinehart, "Determination of Bottom Characteristics by Reflection," USN J. Underwater Acoustics, 5:184-190, (Confidential), July 1955

18. F. E. Hale, M. A. Pederson, and A. J. Keith, "Long-Range Transmission from Near-Surface Underwater Sound Sources in the Pacific," NEL Report 558 (Confidential), 1954

19. J. B. Hersey and M. Ewing, "Seismic Reflections from Beneath the Ocean Floor," Trans. Am. Geophys. Union, 30:5-14, 1949

20. J. B. Hersey, "Outline Report of Research During the Cruise of the Research Vessels ATLANTIS and CARYN, February to April 1949," WHOI Report Contract NObs-2083 (Secret), 1949

21. J. B. Hersey and C. B. Officer, "Transmission Tests at USNEF Eleuthera, July-August 1952, Part I, General Introduction and Evaluation of Azimuth Dependence," WHOI Ref. 52-100 (Secret), December 1952

22. J. B. Hersey, C. B. Officer, E. T. Booth, and J. L. Worzel, "Procedure for Acoustical Evaluation of Array Sites," Propagation Committee Report (Secret), 1953

23. C. O'D. Iselin, "Preliminary Report on Low-Level, Long-Range Listening Tests on a Snorkelling Submarine," WHOI Report contract NObs-2083 (Secret), 1948

24. H. R. Johnson, "A 320-mile Sound Transmission Run SE from Bermuda," WHOI Ref. 55-27 (Confidential), May 1955

25. B. Luskin, M. Landisman, G. B. Tirey, and G. R. Hamilton, "Submarine Topographic Echoes from Explosive Sound," Bull. Geol. Soc. Amer., 63:1053-1068, 1952

26. K. V. Mackenzie, "Long-Range Sound Transmission in the Deep Bering Sea," NEL Report 280 (Confidential), 1952

27. K. V. Mackenzie, "Short-Range Sound Transmission in the Deep Bering Sea," NEL Report 299, 1952

28. K. V. Mackenzie, "Reverberation from Convergence Zones," USN J. Underwater Acoustics, 5:58-68 (Confidential), January 1955

29. H. W. Marsh, "Theory of Anomalous Propagation of Acoustic Waves in the Ocean," USL Report 111, 1950

30 H. W. Marsh, "Propagation of Acoustic Waves in Surface Sound Channels," USL Tech. Memo. 1110-35 (Confidential), 1952

31. H. W. Marsh, "Propagation of Sound in Isothermal Water," USN J. Underwater Acoustics, 3:115-124 (Secret), July 1953

32. W. C. Meecham, J. C. Johnson, and J. R. Frederick, "An Analysis of Project AMOS Data to Determine the Effects of Oceanographic Conditions on 8- and 25-kc Sound Transmission," Engrg. Res. Inst. Univ. Mich. Report Project M-936, Contract N6onr-23221 (Confidential), March 1953

33. W. C. Meecham, W. H. Kelly, and J. R. Frederick, "An Investigation of the Sound Transmission Loss In and Below an Isothermal Layer," Engrg. Res. Inst. Univ. Mich. Report, Project M-936, Contract N6onr-23221 (Confidential), July 1953

34. W. C. Meecham, "A Statistical Model for the Propagation of Radiation in Refraction Ducts Bounded by Rough Surfaces," Engrg. Res. Inst. Univ. Mich. Report 1936-3-T Contract N6onr-23221 and RAG Brown Univ. Report Contract N7onr-35808, November 1954

35. C. B. Officer, "Energy Losses from an Isothermal Channel," WHOI Ref. 49-40, September 1949

36. C. B. Officer, "Sound Transmission in the Surface Isothermal Channel, Part II, Experimental Measurements," WHOI Ref. 53-18 (Confidential), March 1953

37. C. B. Officer and J. B. Hersey, "Sound Transmission from Deep to Shallow Water," WHOI Ref. 53-32 (Secret), August 1953

38. C. B. Officer, "A Preliminary Evaluation of Sound Transmission Characteristics from Deep to Shallow Water off Cape Hatteras," WHOI Ref. 53-33 (Secret), 1953

39. C. B. Officer, "A Preliminary Evaluation of Sound Transmission Characteristics from Deep to Shallow Wafer off Cape May," WHOI Ref. 53-57 (Secret), October 1953

40. C. B. Officer, L. C. Davis, and J. B. Hersey, "Transmission Tests at USNEF, Eleuthera, 29 July to 1 August 1952, Part III," WHOI Ref. 54-49 (Secret), July 1954

41. C. B. Officer, "Prediction of Long-Range Sound Transmission in the Norwegian Sea Area," WHOI Ref. 55-20 (Confidential), 1955

42. C. B. Officer, "A Deep-Sea Seismic Reflection Profile," Geophysics, 20:270-282, 1955

43. M. A. Pederson, E. R. Anderson, J. F. Kidd, and R. M. Lesser, "Results of a Long-Range 530-cps Underwater Sound Transmission Experiment," NEL Report 559 (Confidential), 1955

44. A. G. Pieper, H. R. Baker, and C. W. Searfoss, "Underwater Sound Propagation Measurements at 1050 Cycles Per Second," USN J. Underwater Acoustics, 4:115-121 (Confidential), October 1954

45. J. Roberg, "Sound Transmission in the Surface Isothermal Channel, Part III, Ray Theory Discussion," WHOI Ref. 52-96, December 1952

46. J. F. T. Saur and H. W. Menard, "On the Probability of Successful Convergence Zone Transmission Over an Irregular Sea Floor," USN J. Underwater Acoustics, 4:99-114 (Confidential), October 1954

47. W. E. Schevill and A. C. Vine, "Report of SONAR Tests Conducted at Pearl Harbor Aboard the USS SEA DOG (SS401)," WHOI Report Contract NObs-2083 (Secret), 1948

48. B. J. Schweitzer, "An Approximate Method for Determining the Distribution of Intensity in the Mixed-Layer Sound Channel," USN J. Underwater Acoustics, 2:67-77 (Confidential), July 1952

49. G. B. Tirey and J. I. Ewing, "Investigation of Existence of Echo Bank by Topographic Echo Technique," Columbia Univ. Lamont Geol. Obs. Tech. Report 7, Contracts NObsr-43355 and N6onr-27124, May 1954

50. R. J. Urick, "Sound Transmission Measurements at 8 and 16 kc in Caribbean Water," NRL Report 3556 (Confidential), November 1949

51. R. J. Urick, "Sound Transmission to Long Ranges in the Ocean," NRL Report 3729 (Confidential), September 1950

52. R. J. Urick, "Sound Trapping in the Ocean by the Surface Mixed Layer," USN J. Underwater Acoustics 1 (No. 15):129-134 (Confidential), January 1951

53. R. J. Urick, "Recent Results on Sound Propagation to Long Ranges in the Ocean," USN J. Underwater Acoustics, 1 (No. 2(s)):57-63 (Confidential), April 1951

54. A. C. Vine, J. B. Hersey, and W. E. Schevill, "Memorandum on the Extension of Sonic Listening Ranges," WHOI Report Contract NObs-2083 (Secret), March 1947

55. A. C. Vine, J. B. Hersey, and W. E. Schevill, "Extension of Sonic Listening Ranges, Preliminary Report," WHOI Report NObs-2083 (Secret), 1947

56. A. C. Vine, J. B. Hersey, W. E. Schevill, and R. L. Rather, "Extension of Sonic Listening Ranges, Preliminary Report of SENNET Tests," WHOI Report Contract NObs-2083 (Secret), October 1947

57. A. Voorhis, "Sound Transmission in the Surface Isothermal Channel, Part I, An Application of Normal Mode Theory," WHOI Ref. 52-90 (Confidential), November 1952

58. G. P. Woollard, "A Manual for SOFAR Observers," WHOI Report Contract NObs-2083, 1947

59. J. L. Worzel, "Long-Range Detection of Submarines, Seventh Partial Report," Com. Sub. Dev. Group II, 21-24 (Secret), 1950

60. R. W. Young, "Example of Propagation of Underwater Sound by Bottom Reflection," J. Acoust. Soc. Amer., 20:455-462, 1948

61. Bell Telephone Laboratories, Reports to BuShips, Code 849 on Project CAESAR and Reports to ONR on Project JEZEBEL

62. J. Nafe and J. Ewing, unpublished, Lamont Geological Observatory

PROPAGATION LOSSES FOR PULSED CW AUDIO-FREQUENCY SOUND IN DEEP WATER

F. E. Hale
U. S. Navy Electronics Laboratory

INTRODUCTION

It will become increasingly apparent to the reader that the approach in this paper is one stressing the possibility of predicting the propagation losses for low audio-frequency sound at ranges appropriate to those frequencies, and with almost complete disregard of fine detail such as closely spaced multiple arrivals and phase. It would seem that one valuable contribution has been to show that for some applications reasonable predictions can be made based on only the oceanographic data ordinarily available. If greater accuracy is required or if oceanographic data are not available, then measurements appropriate to the particular requirement are in order. It is clearly beyond the scope of a single article to do more than touch on the common types of propagation. The purpose is to consolidate and present information permitting a rough prediction for both bottom-reflected sound and sound influenced by the deep sound channel, so that these predictions, combined with knowledge of surface-channel propagation, will provide a complete and reasonably accurate picture of propagation at these frequencies. Prediction of surface-duct propagation for the most part will need to be based on another section of this summary or on other sources.

BOTTOM-REFLECTED SOUND

If the sound-velocity gradients in the oceans could be neglected, then underwater sound would become more predictable. This is seldom the case, but for one type of deep-water propagation such neglect is not so serious as to prevent formulating of rough predictions.

Bottom-reflected sound in deep water, simply by virtue of its steeper paths through the ocean, is affected to a lesser degree by velocity changes with depth than is sound which follows more nearly horizontal paths. If interest can be confined to a particular inclined beam, then the geometry of Fig. 1 applies.

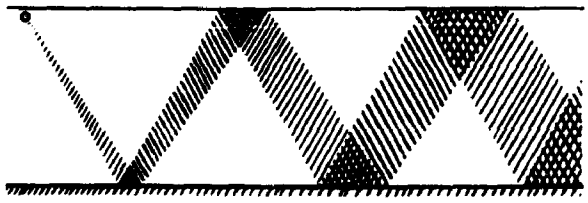

Figure 1 - Steep-angled sound beam resulting in first and second bottom-reflected signals

Note: Paper received December 1955

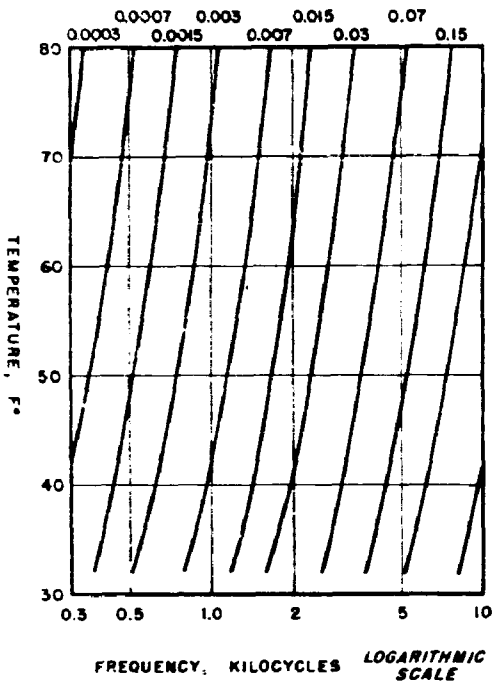

Figure 2 - Sound absorption coefficient in sea water

One may, then, usually predict a propagation loss based on (a) spherical spreading along the slant-range to the point of measurement, (b) the absorption loss from Fig. 2 for the frequency considered (1), and (c) a third empirical term which accounts for reflection losses at the bottom. These reflection losses are frequency dependent and have been compiled to cover the average situation for deep-water bottoms. Losses determined for the Atlantic from the AMOS data (2) are the most extensive and have been plotted with appropriate probable errors (see Fig. 3).

A further loss which may become important is associated with reflection from the surface. Although it has been presented as having very appreciable values at near grazing angles (30) and will certainly be important at higher frequencies and sea states, it has not been necessary for present accuracies to include this loss in treating data of this report.

To determine applicability of the bottom-reflection losses of Fig. 3 to Pacific areas, they have been used in computing propagation losses which were then compared with Pacific area experiments. These experiments were to a maximum 50-mile range, and were extensive although fewer in number than the AMOS tests. Areas were from California and the Hawaiian Islands north to the Bering Sea. A total of 164 averaged measurements in the frequency range 0.2 to 7.5 kc were considered, and averages over range intervals of 5 and 10 miles were commonly used. Bathymetry was not considered in the comparison, but was considered in choosing moderately smooth bottoms for test sites.

The comparison showed that 44% of the losses lay within the probable errors of the AMOS data. This agreement is good, although NEL data did not substantiate the small probable errors at frequencies below 0.5 kc as reported from AMOS. Since variation of data scatter with frequency was not substantiated, it is of interest to note that 73% of all Pacific data lay within ±5 db of computed propagation losses.

In this comparison there was no obvious disagreement for any particular class of data. Various areas and ranges seemed to agree with predicted values about equally well, and so did various frequencies except for the previously mentioned fact that data scatter at lowest frequencies was not so small as predicted.

It is not to be inferred that there will necessarily be general agreement on the validity of this method. Remember that large amounts of data have been drawn upon and small differences eliminated. Reports of individual tests (4, 5, 6) and one analysis of a part of common data (7) led to somewhat different conclusions. Spot check of still another test (8) seems to show good agreement at the longer ranges, with poorer agreement at short ranges where an appreciable directivity correction was used. Perhaps some breakdown by area (3) will be useful for more precise prediction, or the weight of more data can be brought to bear on improvement of the empirical terms.

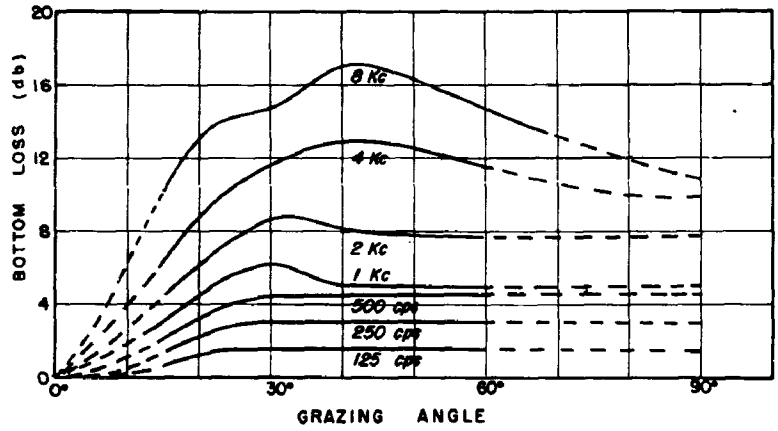

Figure 3a - Bottom losses at lower frequencies as determined from AMOS data

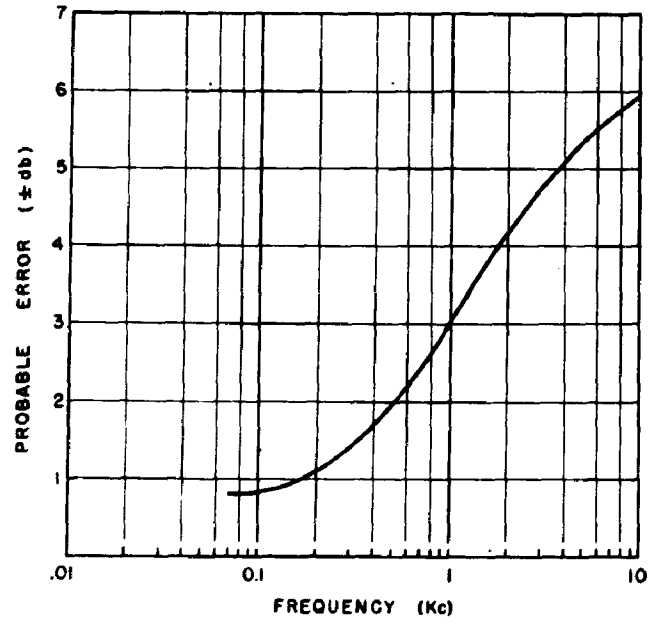

Figure 3b - Probable errors to be associated with AMOS bottom losses

In spite of these differences one must conclude that fair prediction of intensity can be made, based on only moderately accurate indication of a uniform deep bottom. If one needs to know with some precision the range interval in which reflections of certain orders will predominate, and the ranges which limit reflections of lower orders, then considerable knowledge of refractive processes is essential. We will consider these processes in the following, but present Fig. 4 at this time to show an example of computed and experimental propagation loss for bottom-reflected sound. Shaded areas are predicted values and probable error; points are averaged transmission losses for sound with: one bottom reflection (solid), and with two bottom reflections (open circles) with probable error bars. Frequency is 1 kc/s, and water depth is 2000 fathoms.

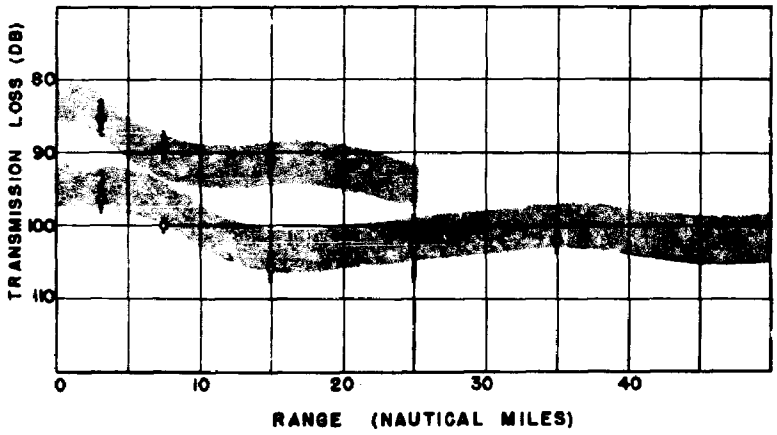

Figure 4 - Bottom-reflected sound: Comparison of USL (AMOS) prediction of propagation loss and NEL measurements

To drop consideration of bottom-reflected sound without mention of some of the more complex bottom properties which influence propagation would be misleading. Advances have been made in analysis of sediment structure and the acoustic implications (9); some consideration has been given to the effect of obstructions such as seamounts, and of hollows in the sea floor (10). A start has been made in considering forward scattering a deep mud bottom and its relation to the backscatter (11). Studies such as these should eventually lead to predictions of higher precision for these propagation losses. Signal distortion is a severe and almost untouched problem.

REFRACTION

Refraction was neglected in the previous section because consideration was given to only relatively steep sound paths in the ocean. In practically all other acoustic data it has been found that refraction plays a major role. Although no really general velocity structure is applicable to the oceans of the world, the presence of a deep-sound channel is to be expected. Even if this general channel structure is cut off by a relatively shallow bottom, some part of the same basic ray structure persists. The tendency of sound energy to refract downward and to cause formation of shadow-zones is well known, and in studies of supersonic transmission the effect of negative gradients in limiting the range of successive orders of reflection from a shallow source was investigated and reported (12). The thermocline exerts a similar influence on low audio-frequency sound, causing first bottom-reflections to be limited in temperate zones to a range of perhaps 15 miles in 1000-fathom water. As water depth increases to depths in the neighborhood of 2000 fathoms, deep-sound channels are formed. Hydrostatic pressures increase velocity so that eventually the near-surface velocity is regained and exceeded.

Skip-distance propagation follows, and regardless of further increasing depth there can be no first bottom-reflection beyond the first skip range. The skip effect may persist to ranges of several hundred miles.

Data on skip-distance propagation in the deep ocean are now plentiful, (13, 14, 15) and ray theory has been developed so that adequate knowledge of velocity structure can be converted into accurate predictions of intensity in convergence zones formed near the surface at skip range intervals (14, 16, 17). Since these predictions require ray tracing or digital computing, the general problem of predicting for many velocity structures, or for variation of vertical structure with range, is still tedious. Some progress in rapid predicting for moderate ranges is being gained by an analog method (3).

Although these and other studies are improving our knowledge of long-range propagation and are pointing out close relationship between acoustics and environmental factors, much of the detailed information cannot be condensed into a form suitable to this summary. On the other hand, there now exist enough experimental data so that the outstanding features of skip-distance propagation can be described adequately for many purposes. A condensed description might be as follows:

Zone Spacing: From about 15 miles in "miniature" deep channel structures at high latitudes to about 35 miles near the equator.

Minimum Spreading Losses: 15 to 25 db less than spherical spreading observed in short-range intervals of about 1/4 mile at the zones.

Zone Widths: About 5 to 10% of the zone range when measured within 300 feet of the surface to points where loss is 10 db greater than minimum. In the case of a highly developed surface channel a long "tail" follows the zone, and portions of this tail may show losses within 10 db of the minimum.

Depth Effect: Zones are wider by a factor of about 1.5 at depths 500 to 1000 feet. Spreading losses usually are roughly 5 to 10 db greater, but a source and receiver configuration permitting paths with no surface reflection can compensate this additional loss.

Prohibitive Condition: Bottom limiting of deep sound channel.

Some of the above descriptive statements are better established than others, and there are different degrees of variability, but it is nevertheless surprising that such a concise description can be made. Based chiefly on Pacific data, these factors seem to describe Atlantic propagation as well (5, 17). An interesting point is that water depth, so long as bottom limiting is avoided, is relatively unimportant. Widening of zones can result from deep bottoms, but with the possible exception of artic regions and a few of the great deeps of the oceans, surface ducts would seem to be more generally effective than increased depth.

On the subject of reliability of this type of propagation, a recent study has shown that interference to skip-distance propagation by seamounts will be largely a matter of ocean area, but that the probability of successful transmission to the first zone will be about 0.8 to 0.9 in one of the poorer areas (18).

Since it would now seem that the major effects of refraction on long-range propagation can be described in simple terms, these ideas can be combined with our knowledge of bottom-reflected sound to present a fairly complete picture of deep-water propagation from near-surface sources. Neglecting direct and surface-channeled sound, one predicts a sound field dominated by first bottom-reflections to a range within a few miles of the first skip-range. Here the once-reflected sound is by paths which are starting to bend upward, so that little energy is incident on the bottom. Consequently the intensity of once-reflected sound decreases; and then with further increase of range there is a sudden rise of intensity as the skip paths (without bottom reflection) become effective and the first-convergence zone is entered. This

same pattern is repeated for bottom reflections and zones of higher order. An example is presented in Fig. 5, showing the same shaded 1st and 2nd bottom-propagation predictions used in Fig. 4, with the addition of shaded-zone predictions based on mean values of the descriptive paragraphs of this section. The shapes of these predicted zones reflect the commonly noticed steep rise of the first and second zones, but no real prediction of shape is intended. To guard against any misconception regarding fluctuation and scatter of data, experimental points representing average loss in only 400-yard range intervals are plotted for a single 1 kc/sec test (19). Open circles are first bottoms and first-convergence zone, solid circles are second bottoms and second zone. Third bottom-reflected signals were below noise level but the third zone is represented by open squared points. Surface-channel loss measurements are represented by the dashed line near zero range, and it can be seen that the experimental zone measurements show the characteristic tails to some degree. As a general comment we can say that the prediction, except for some second bottom reflections near their extreme range, covers the situation of this test.

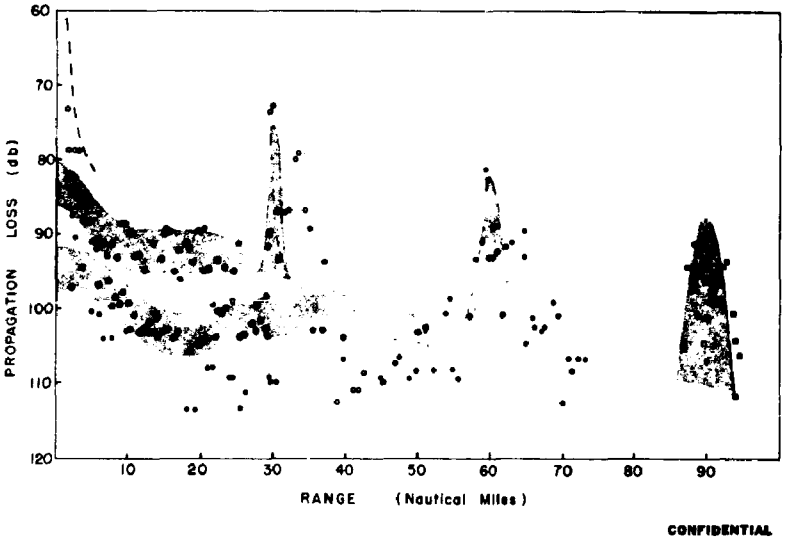

Figure 5 - Predicted and detailed experimental results of a single 1-kc test showing first bottom-reflected and first-zone (0), second bottom-reflected and second-zone (•), and third zone (□) signal losses

Figure 6 gives a pictorial representation of experimental zone structures to greater ranges. The upper sketch represents zone measurements in Hawaiian area 3100-fathom water (15) with a nominal 100-foot surface duct. The dashed line extending to zone 2 indicates the level of bottom reflections. These may be compared with interzone levels of the lower sketch which represent unusually strong "tails" resulting from a 400-foot surface duct. Zones 5 to 8 in this second test were abnormally low because of shielding from a seamount, but zone structure was fairly clear to the extreme range shown here. From this point to the end of the run at 517 miles, zone structure was poor and sporadic signals, which had first appeared between zones 9 and 10, became predominate. The area for this test was off the coast of California and Northern Mexico (10). Frequency for both tests was 530 cps.

Simply for its value in clarifying the effect of frequency on these types of propagation, Fig. 7 shows smoothed results of a single test run at both 1 and 4 kc with source and hydrophone at 50 feet (19). Measurement was also made at 2 kc in this run but the intermediate losses are not plotted because with such drastic smoothing no real additional information results. The difference in loss to the zones (in excess of about 8 db, accountable by absorption difference) can be associated with the greater zone width at 4 kc. A surface duct to 100 feet

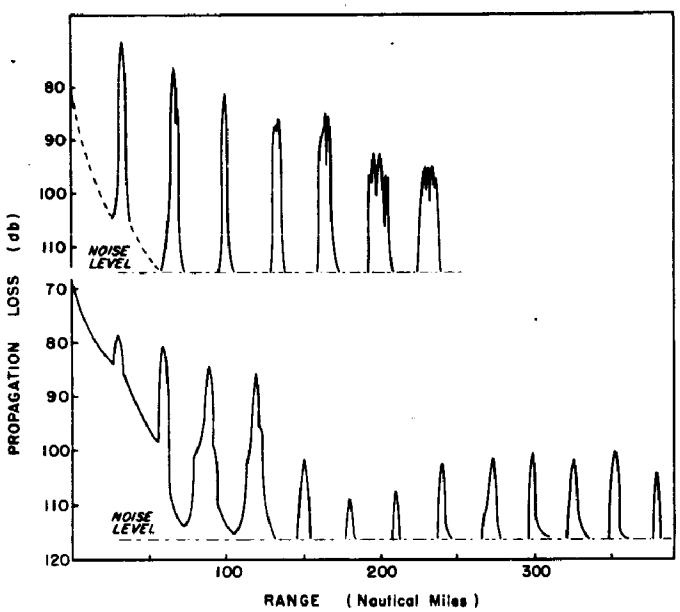

Figure 6 - Gross structure of zones as determined in long range tests off Hawaiian Islands and Continental U. S.

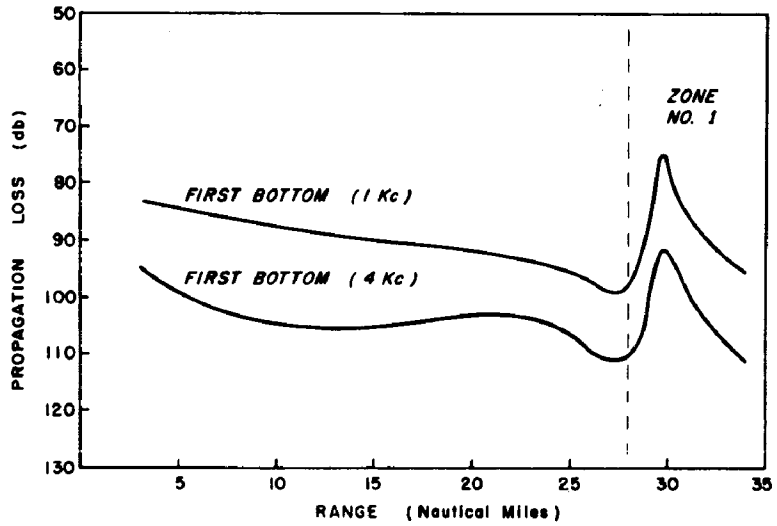

Figure 7 - Smoothed experimental results for first bottom reflected and first zonal signals at 1 and 4 kc

was present in a calm sea and 4 kc signals were so strongly affected that they remained above the bottom-reflection level to about 15 miles. This behavior affected the width of the 4 kc zone.

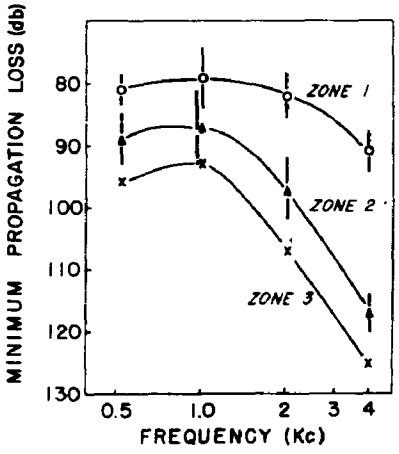

Figure 8 - Mean minimum propagation losses and standard deviations for 76 tests covering the first three convergence zones

Figure 8 summarizes the results of 76 test measurements (29) of zones of order 1 to 3. Most of these tests were in deep water of California and Northern Mexico. The slight tendency toward smaller losses at 1 kc is in accord with theory (16, 17) which shows convergence at caustics increasing with frequency so as to oppose the effect of absorption. For zones 2 and 3 this peaking with frequency should theoretically occur nearer to 500 cps. Bars on the figure show standard deviations where justified by sampling.

The approach here has been one attempting to avoid complications, but some additional points deserve mention. A minor confusion seems to exist on the role of surface reflection in skip-distance propagation. It is difficult to foresee a situation when it will not play an important part. If the source is in a surface duct and frequency is one strongly affected by that duct, then all of the skip-distance sound is surface reflected. The most intense portions of the zones are usually at caustics of surface-reflected sound. Nevertheless, for a source in an effective negative gradient, the beam of sound energy which is near enough to horizontal so that it can be refracted downward without incidence on the surface, may continue in this refracted looping path to extreme ranges. Although the distinction is not important in most actual cases because the surface is a good reflector and present day experiments seldom resolve the two propagation paths, situations such as just noted under the subheading of "depth effect" can bring the distinction into prominence.

As submarines go deeper there will be more interest in these niceties of propagation, and a difficulty which can be foreseen is description of propagation from the region of the thermocline. Some tests have indicated that variation of the thermocline with range and time will cause difficulty in predicting the entire sound field; but reciprocal measurements and a recent NEL test in which a source at 400-feet depth was monitored continuously in range, have substantiated the theory that convergence zones near the surface will be affected to only a minor degree.

Actual zone structure is complex and the convergence or concentration of energy can be examined in terms of ray caustics (16) and multiple arrivals. Experimentally, the signals are normally characterized by low distortion and it is only when pulse lengths have been shortened to 25 milliseconds that any noticeable path resolution has been achieved (20). Broadband and high power requirements on the source have in the past been a difficulty in extending such measurements; but this difficulty has been overcome so that at least one adequate source is available (21) and better measurements can be made.

SURFACE DUCTS

Surface-duct propagation is preferred because of low distortion, but the losses are often extremely variable over only moderate periods of time. Some predictions of the ducts themselves may be made on a statistical basis (22) and the predictions of acoustic behavior of ducted sound and leakage can be made readily from knowledge of duct structure (2, 23, 24). Since all this would require detail beyond the present scope, Fig. 9 has been prepared to give a limited but fairly representative example. This figure is in sketch form so that a ready comparison

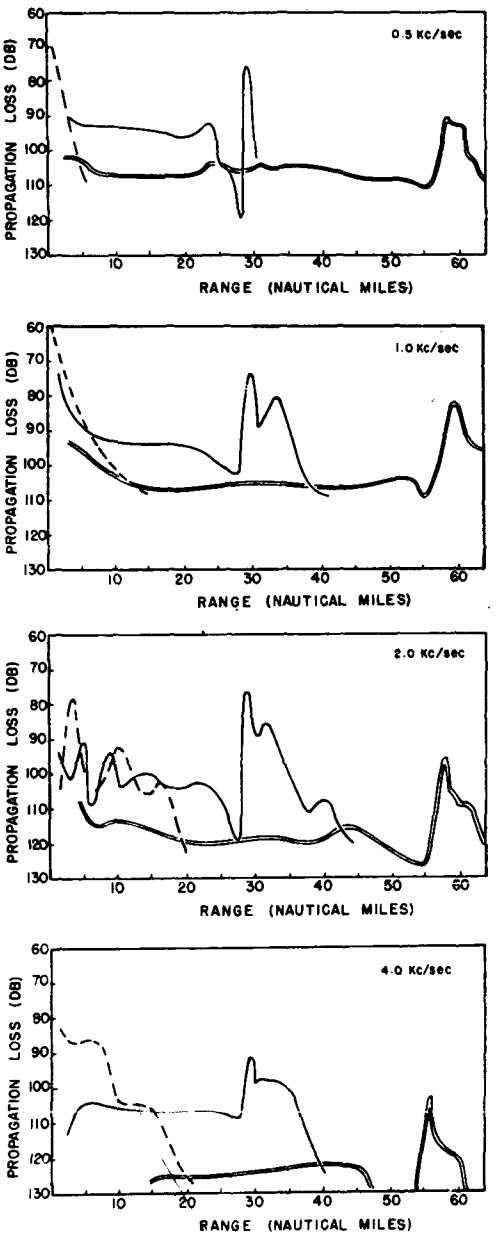

Figure 9 - Comparison of experimental losses for surface duct and other propagation types at frequencies 0.5 to 4 kc. Dashed lines are duct signals, solid lines are first bottom and first zone, double lines are second bottoms and second zone.

can be made with other types of propagation. Dashed lines are duct signals; solid lines are first bottoms and first zone; double lines are second bottoms and second zone. All except the first plot are from the same test run, and the 0.5-kc exception (Fig. 9a) is from a run which immediately followed (19). Channel depths and sound-velocity gradients showed considerable variation in range and time but gave averages of 130 feet and 0.008 reciprocal seconds over the two runs. Sources and hydrophones were at 25- to 50-foot depth, well up in the duct.

The sketches show the increased trapping at higher frequencies, but this is not clearly demonstrated at 4 kc because absorption has become important even at these ranges. There is also indication at 2 kc of an interference beat between the two modes trapped. This effect was demonstrated even more clearly in another test (25). The increased tailing of zones with improved duct propagation is clearly visible.

One must not yield to a temptation to predict surface-duct propagation on the basis of this example. It may be much better, as indicated by Fig. 6b, in which a 400 duct was effective, or it may be much worse. A reasonable prediction will be obtained only by consideration of the probable duct and its effect on the frequency of interest. A point of interest is that for only slightly directional low-frequency sources the presence or absence of a surface duct has only minor effect on other types of propagation. Sound is emitted from the base of the duct in much the same manner as from a source in a negative gradient, and the amount of energy trapped is usually small and may be partially replaced by energy which would otherwise take very steep angles and be propagated in only high-order bottom reflections. This behavior has been verified in tests (8, 10).

DEEP-CHANNELED PROPAGATION

Although skip-distance propagation is certainly channeled, the usual implication of the term implies a more uniformly insonified medium. This condition of uniform insonification is met only when sources are near the deep channel axis. This type of propagation will be next discussed.

It would at first seem that the physical analysis in this case would be relatively simple, but closer inspection of the channel structure shows that such is not the case. Search for a simple model leads one to the idea of spherical divergence to some range comparable with the vertical dimension of the channel, and cylindrical spreading at all greater ranges. This is indeed a useful concept, but it obviously will run into trouble as spreading in time becomes effective. In addition to usual spacial spreading and absorption, a short pulse of channeled sound will lose energy with increasing range because various paths have different average velocities, and even longer pulses will achieve a steady state composed of arrivals of varying phase. Facilities and methods are now fully adequate for investigating this effect-by-ray theory in detail, and the only reason that computations have not been made is that operational use of deep sources has not been attractive. Clearly this difficulty with different velocities is more severe in the case of deep sources because the effective width of the vertical beam of sound is much greater than in the case of skip propagation from a shallow source. The effect in distorting explosive signals is well documented (26).

Although we would prefer a more complete framework for data, we must recognize the fact that its complexity would prohibit its use in making any quick estimates of losses to be expected. For this purpose the results of two unique experiments using pulsed audio-frequency sources and hydrophones near the deep-channel axis (27) are useful in determining limits in the range of parameters which may be applied to simple concepts. Following this approach, we present Fig. 10, which summarizes test results and shows empirical equations applicable to range intervals and conditions shown. Consideration of these test data, and some unpublished NEL information at 7.5 kc, leads to the following conclusions:

(a) The direct measurements are not precise enough to determine an open-ocean attenuation term different from the absorption shown in Fig. 1, but tend to support the absorption figures.

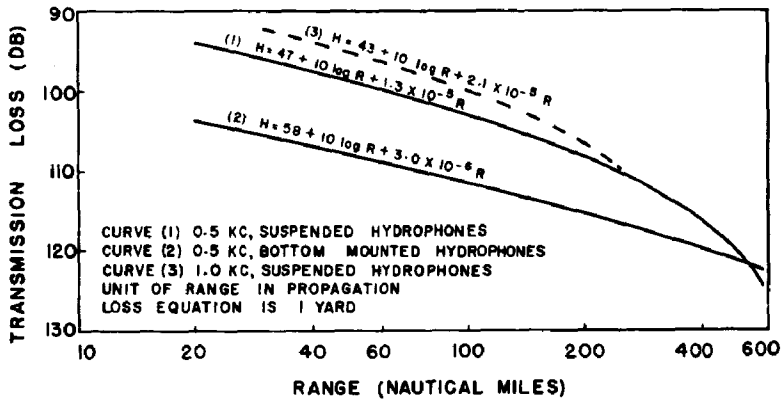

Figure 10 - Deep-channel losses from near-axis sources to ship-suspended hydrophones and to hydrophones bottom-mounted at the Pt. Sur, (California) Transmission Experimental Facility

(b) Cylindrical spreading describes the data in the range interval 20 to 200 nautical miles for pulselengths 0.5 to 5 seconds.

(c) In a range from about 200 to 500 miles these same pulselengths show attenuation much greater than absorption when a wide-angle beam is accepted by ship-suspended hydrophones, but only attenuation moderately greater than absorption when sound paths are restricted by bottom mounting to those near the axis.

(d) Spherical spreading fits the data adequately to about a 5-mile range.

(e) In the deep channel off California, channeled propagation with no shadowing is encountered at about 700-feet depth.

Items (b) and (d) indicate that choice of a particular range as a transition point from spherical to cylindrical spreading is somewhat artificial, but the equations show that it may be effectively set at about 15 miles. This is 7.5 times the channel depth dimension, and hence somewhat greater than might be expected.

Since reporting, a rather striking similarity has been noted between Curve 3 of Fig. 10 and results of a similar experiment made under ice fields of the Beaufort Sea (28). The surface-bounded channel in the Beaufort Sea was similar to the below-axis portion of the deep sound channel encountered in the earlier test, but it is surprising to find that reflection from the water-ice interface of the Beaufort Sea gave rise to almost exactly the same propagation of loss that was encountered in the normal deep channel at 30° north latitude.

Returning finally to our objective of predicting sound fields, we now see that for usual deep-channeled sound, and for that in surface-bounded deep channels as well, a simple but useful method is assumption of spherical spreading loss to about 15 miles and cylindrical spreading to about 200 miles. To these must be added absorption from Fig. 1 and some additional losses if either greater ranges or signal pulses of order less than 1 second are contemplated. The sum of all of these, of course, should be a smaller loss than any encountered by bottom reflections, but the bottom reflections arriving at nearly the same time in the 10 to 20-mile range interval may be at comparable level at low frequencies and may result in interference effects.

SUMMARY AND CONCLUSIONS

In conclusion, it would seem to be more important to emphasize limits on the value of what has been presented than to create any false impression that all propagation is readily predictable. One such limit is range. Although some illustrative data run to much greater ranges, most of the long-range experimental work has been to ranges of only 50 or 100 miles. A related limitation is imposed by changes of velocity structure with range, a problem that has been ignored here. A third troublesome factor is the predictability of the directional characteristics of sources when placed within a few wavelengths of an imperfectly reflecting surface. Reflection coefficients as now stated for both surface and bottom have usually not been checked for more than a few orders of reflection. All these and other factors must be considered in predictions, and there is no intent here to disparage the careful work necessary to improvement of our understanding of physics of sound in the sea. Perhaps the chief value of this summary is that it may provide useful hints of the situations in which some factors may be ignored.

REFERENCES

1. R. T. Beyer, "Nomogram for the Sound Absorption Coefficient in Sea Water," RAG Brown Univ. Tech. Report (Confidential), November 1953

2. H. W. Marsh and M. Schulkin, "Sound Transmission at Frequencies Between 2 and 25 kc/sec," USL Tech. Memo. 1110-110-54 (Confidential), August 1954 (revised)

3. C. B. Officer, "Prediction of Long Range Sound Transmission in the Norwegian Sea Area," WHOI Ref. 55-30 (Confidential), June 1955

4. R. J. Urick, "Recent Results on Sound Propagation to Long Ranges in the Ocean," USN J. Underwater Acoustics, 1 (No. 2(S)):57 (Confidential), April 1951

5. A. G. Pieper, H. R. Baker, and C. W. Searfoss, "Underwater Sound Propagation Measurement at 1050 cps," USN J. Underwater Acoustics, 4 (No. 4):115-121 (Confidential), October 1954

6. H. R. Baker, A. G. Pieper, and C. W. Searfoss, "Measurements of Sound Transmission Loss at 1.5 to 5 kc," NRL Report 4225 (Confidential), September 1953

7. R. J. Urick and B. J. Schweitzer, "An Analysis of the AMOS V Punched-Card Transmission Data," USN J. Underwater Acoustics, 1 (No. 4, Series A):319-325 (Secret), October 1951

8. R. J. Urick, "Sound Transmission to Long Ranges in the Ocean," NRL Report 3729 (Confidential), September 1950

9. G. A. Shumway, "A Resonant Chamber Method for Sound Velocity and Attenuation Measurement in Water Saturated Sediments," and

   W. J. Toulis, "Theory of a Resonance Method to Measure the Acoustic Properties of Sediments"

   Manuscripts submitted to Geophysics

10. M. A. Pedersen, et al., "Results of a Long-Range 530 cps Underwater Sound Transmission Experiment," NEL Report 559 (Confidential), January 1955

11. K. V. Mackenzie, Code 2232, NEL, - Manuscript in preparation

12. "Physics of Sound in the Sea, Part 1, Transmission," STR Div. 6, NDRC, Vol 8, p. 141, 1946

13. T. P. Condron and R. W. Schillereff, "Long Range Sound Transmission with a Shallow Towed Source at 500- and 1000-cps Frequency," NRL Report 323 (Confidential), October 1952

14. F. E. Hale, et al., "Long Range Transmission From Near-Surface Underwater Sound Sources in the Pacific," NEL Report 558 (Confidential), December 1954

15. M. A. Pedersen, "A Long-Range, Low Frequency Underwater Sound Transmission Experiment in 3100-Fathom Water," NEL Report 618 (Confidential), July 1955

16. H. W. Marsh, Jr., "The Use of Ray Methods and First Order Diffraction Corrections," USL Tech. Memo. 1100-61-54, September 1954

17. T. P. Condron, D. L. Cole, and J. F. Kelly, "Comparison of Computed and Measured Intensities for Project AMOS Noisemaker Measurements," USN J. Underwater Acoustics, 5:46-51 (Confidential), January 1955

18. J. F. T. Saur and H. W. Menard, "On Probability of Successful Convergence Zone Transmission Over an Irregular Sea Floor," USN J. Underwater Acoustics, 4 (No. 4):99-114 (Confidential), October 1955

19. C. R. Corpew, "Underwater Sound Transmission Tests of September and November 1954 at 0.5 and 4 kc," NEL Tech. Memo 74 (Confidential), January 1955

20. J. A. Greer and R. D. Adams, "Measurements of Resolved Multipath Signals at the First LORAD Zone," NEL Tech. Memo. 103 (Confidential), April 1955

21. F. X. Byrnes, J. S. Hickman, and G. E. Martin, "Broadband, High-Power, Low Frequency Variable Reluctance Projector Array," NEL Tech. Memo. 145 (Confidential), October 1955

22. USN Hydrographic Office, Sound-Ranging (SONAR) Charts

    H.O. 1400-R N. Atlantic
    1401-R N. Pacific
    2600-R S. Atlantic
    2601-R S. Pacific
    2603-R Indian Ocean (Confidential)

23. M. R. Powers, et al., "Contours of Transmission Loss for Standard Conditions and Correction Charts," USL Tech. Memo. 1110-101-54 (Confidential), August 1954

24. T. P. Condron, et al., "Contours of Propagation Loss and Plots of Propagation Loss at 2, 5 and 8 kc," USL Tech. Memo. 1110-14-55, April 1955

25. D. H. Potts and R. W. Rempel, "An Application of Normal Mode Theory," NEL Tech. Memo. 61, November 1954, also submitted to USN J. Underwater Acoustics, 6 (No. 1):37-45 (Confidential), January 1956

26. "Physics of Sound in the Sea, Part 1, Transmission," STR, Div. 6, NDRC, Vol. 8, p. 213 and 216, 1946

27. J. A. Greer and R. J. Bolam, "Long-range Sound Transmission to Ship-Suspended and Bottom-Mounted Hydrophones," NEL Report 499 (Confidential), June 1954

28. J. A. Greer, "Long Range Underwater Sound Transmission Tests Under Ice Fields," NEL Tech. Memo. 108 (Confidential), May 1955, also submitted to USN J. Underwater Acoustics

29. J. A. Greer, "Shapes and Locations of Convergence Zones," NEL Tech. Memo 102, April 1955

30. H. R. Johnson, "A 320-mile Sound Transmission Run SE from Bermuda," WHOI Ref 55-27 (Confidential), May 1955

SOFAR PROPAGATION

M. J. Sheehy
U. S. Navy Electronics Laboratory

INTRODUCTION

This chapter will deal briefly and qualitatively with the propagation of acoustic signals from explosive charges deep in the ocean to bottom-mounted hydrophones. Specific topics discussed will be the nature of an underwater explosion, the qualitative effects of sound velocity structure and bottom topography on signal shape, and the idea of the transmission loss of such signals. Since most of the experimental work in this field was directed toward the development of a Sofar network, some details of this application will also be given.

Historically, the first experiments known to the writer on the propagation of sound from a deep explosive source to a similarly located receiver were carried out in 1933 and 1935 by the U. S. Coast and Geodetic Survey.* One-half-pound charges of TNT were used, and although no attempt was made to achieve long ranges, the signals were readily detected at a distance of 56 kilometers. The experimenters mentioned that theoretical considerations indicated much greater ranges might be obtained.

In 1937, Maurice Ewing interpreted some of his results during geological survey work in the deep ocean as indicating that signals from small explosive charges deep in the ocean could be detected at ranges of thousands of miles. During World War II, Ewing proposed to the Bureau of Ships that practical use be made of this long-range propagation, and he and his coworkers later showed that it would indeed be feasible to use this phenomenon for locating persons in distress at sea.

NATURE OF THE SOURCE

Since there is considerable literature on the nature of underwater explosions, the subject will not be treated in any detail here. It may be of interest to give a brief account of the sequence of events in an underwater explosion, however, before going on to the propagation of such signals. Reference 14 is particularly recommended to those seeking a complete treatment of underwater explosion phenomena.

Once an explosion is initiated the intense heat and pressure developed at the detonation point within the material sets up the reaction in adjacent material. This reaction is propagated through the material by means of a "detonation wave" which travels through a high explosive such as TNT with a speed of several thousand meters per second.

Note: Paper received January 1956

*See Refs. 13, 50, 51. To document this chapter properly would require repeated references to many reports. Rather than do this, the author has chosen to list a fairly complete bibliography at the end, and to acknowledge here his extensive use of Refs. 14, 15, and 48 in writing this chapter.

The first cause of disturbance to the surrounding water is the arrival of this detonation wave at the boundary between the material and the water. This initiates an intense pressure wave in the water called the shock wave. For the case of a high explosive, the pressure rise at the leading edge of the shock wave can be considered discontinuous, followed by a roughly exponential decay of at most a few milliseconds duration for charges of ordinary size.

An approximate value for the peak pressure in the shock wave for an explosion of TNT can be obtained from the empirical expression

$$P_m = 2.25 \left(\frac{W^{1/3}}{R}\right)^{1.13} \times 10^4 \text{ lbs/in.}^2$$

where W is the charge weight in pounds and R is the distance from the charge in feet. Naturally this expression does not hold for large values of R where absorption, refraction, etc., have to be considered. Other expressions for P_m exist in the literature, and in general yield peak pressures in the neighborhood of those of the above formula.

The energy in the shock wave decreases rapidly near the charge as the wave progresses outward, approximately 50% being dissipated within a distance of 25 charge radii. Theoretical consideration result in an estimated 1060 cal/gm for the total energy of explosion for TNT; 53% of this, or 562 cal/gm at 1 charge radius, represents the total energy radiated by the shock wave.

The rapid dissipation of energy near an explosive charge represents a wastage of available energy to heat, and occurs at the steep gradient of the shock front. The fact that one-quarter of the total energy of explosion is lost in the near field of the charge illustrates what has been referred to as the inefficiency of the shock wave for the transmission of energy.

The initial high pressure in the gas bubble which results from the detonation process is considerably decreased when the shock wave has been emitted, but is still higher than the equilibrium hydrostatic plus atmospheric pressure. The gas bubble accordingly expands rapidly and, because of the inertia of the outward flowing water, the expansion continues beyond the point at which the sum of the hydrostatic and atmospheric pressure is the same as the gas pressure in the bubble. This pressure difference ultimately halts the expansion and the bubble begins to contract. The contraction continues until the compressibility of the gas in the bubble checks the inward flow of water. Thus the inertia of the water plus the elastic properties of the gas and water provide the conditions for an oscillating system, and the bubble undergoes repeated expansion and contraction. This motion results in the emission of pressure pulses which are of maximum amplitude at times corresponding to minimum bubble volume. These are referred to as bubble pulses. The peak pressure of the first bubble pulse is only 10-20% of that of the shock wave, but the duration of the pulse is much greater.

A considerable amount of the energy still present is lost at the time of each pulse, and, as a result, only the first one or two pulses are usually of practical significance. Less than 10% of the total energy of explosion is left in the bubble after the second contraction.

For a TNT explosion the period between the shock wave and the peak of the first bubble pulse is given approximately by

$$T = \frac{4.35\ W^{1/3}}{(d + 33)^{5/6}}, \text{ seconds}$$

where d is the depth of the charge in feet and W the charge weight in pounds. Periods between successive bubble pulses become progressively shorter.

Thus, very briefly, an underwater explosion puts acoustic energy into the medium in the form of a shock wave having a high peak pressure, a virtually discontinuous pressure rise at the leading edge and a roughly exponential decay, followed by a series of pressure pulses of much smaller amplitude and of progressively decreasing amplitude and period.

As an example, the peak pressure in the shock wave and the period between it and the first bubble pulse for an explosion of four pounds of TNT at a depth of 2000 feet are, respectively, 177.6 db re 1 μ bar at 1 yd and 0.012 sec, based on the expressions given above.

EFFECT OF SOUND VELOCITY STRUCTURE ON PROPAGATION

A pronounced thermocline in which the temperature decreases with depth down to depths of a few thousand feet exists in most areas of the deep ocean. This feature, coupled with the increase of hydrostatic pressure with depth, produces a sound velocity profile which decreases to a minimum value and then increases with increasing depth (Fig. 1). Sound rays in the deep ocean will be refracted toward this region of minimum velocity in accordance with Snell's law.

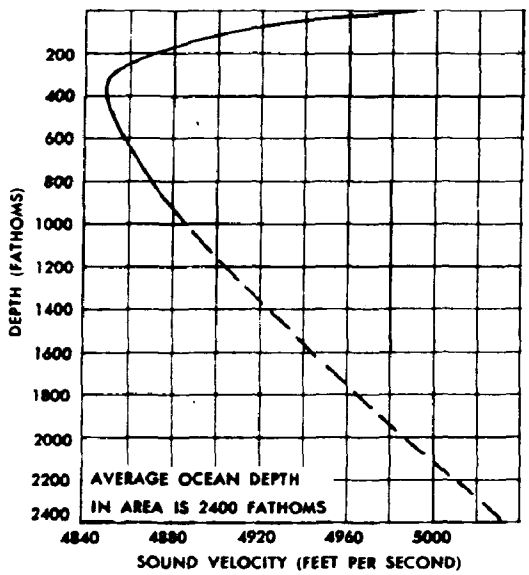

Figure 1 - Sound-velocity profile in middle latitudes

We shall be concerned here with the propagation of signals originating at or near the level of minimum sound velocity. Ray paths from such a source position are shown in Fig. 2 together with a schematic representation of the sound-velocity profile. For the case shown, all sound rays departing within ±11.3 degrees of the horizontal travel via completely-refracted paths; they are not reflected from either the surface or the bottom of the ocean. Energy traveling by such paths does not suffer losses at the boundaries of the medium, and is said to be channeled.

As shown in Fig. 2, the ray of this type which becomes horizontal at the depth of maximum velocity is called the limiting ray. The angle this ray makes with the horizontal at the minimum-velocity depth is the limiting-ray angle and is a measure of the strength of the sound channel; the greater this angle, the more energy travels via completely-refracted paths. The case illustrated by Fig. 2 is that of a strong, well-defined sound channel such as generally exists in low- and midlatitude waters.

When the relationship between the velocity profile and the ocean depth is as shown on this figure, there are also some rays which are reflected from the surface but not from the bottom. (These are not shown on the figure.) Since the ocean surface may be considered a near-perfect

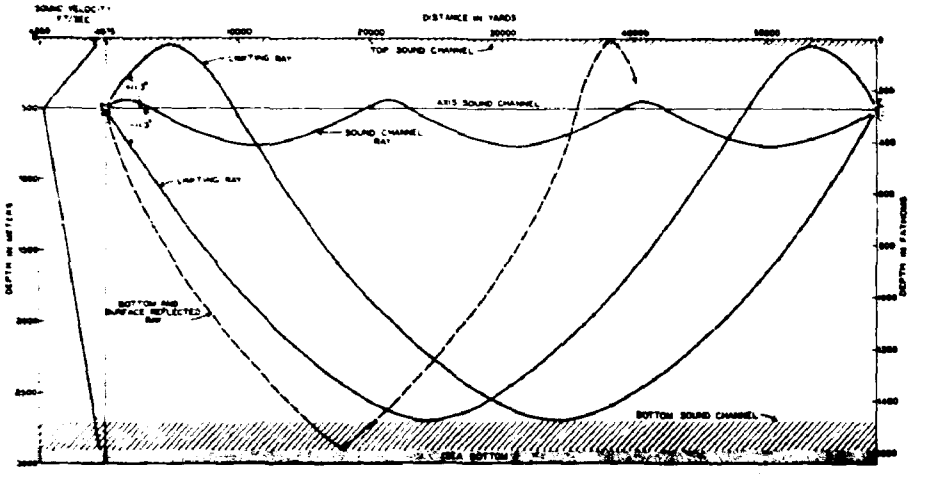

Figure 2 - Ray paths for sound-channel transmission

reflector for low-frequency sound, energy traveling such paths may, for practical purposes, also be considered channeled. Such ray paths do not exist unless the ocean depth is greater than the depth at which the sound velocity again reaches its maximum near-surface value.

The dashed ray path in Fig. 2 is representative of those which are reflected from both the surface and the bottom. Energy traveling such paths will suffer losses depending upon the sound frequency, the angle of incidence on the bottom, and the acoustic properties of the bottom. Although these losses are generally considered negligible at angles of incidence greater than the critical angle, this angle may be quite large, or even nonexistent, for some bottom types.

Energy from a deep source may thus be propagated by many paths, some involving large departures from the sound-channel axis and some small. The energy travels along the various sound rays with different mean horizontal velocities, and is thus spread out in time during propagation. A typical relationship between the mean horizontal sound velocity per refraction cycle for the completely-refracted rays and the angle at which the ray path crosses the sound-channel axis is shown on Fig. 3 for the case of a strong sound channel.

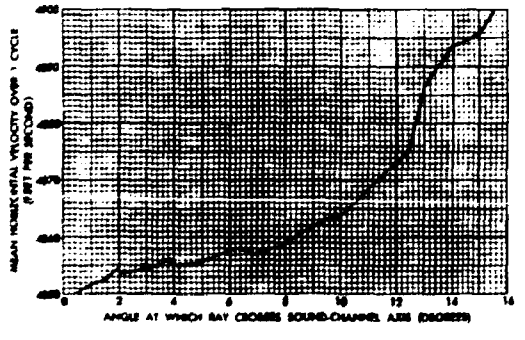

Figure 3 - Ray travel velocity versus axial angle for a Pacific oceanographic station

At long ranges under these conditions the first sound to arrive has traveled the longest actual path and has also made the fewest axial crossings; the next sound has traveled a slightly shorter path involving one more axial crossing, etc. When both source and receiver are on the sound-channel axis, the final sound to arrive is that which has traveled along the axis.

The time separation between subsequent arrivals becomes shorter and

shorter, and since most of the energy also travels by the low-angle paths, the received signal builds up in intensity until the final signal component arrives, at which time the signal abruptly ceases.

A typical long-range signal in the North Pacific under conditions of a well-defined sound channel is illustrated by the longer-range ones shown in Fig. 4. The presentation here, and in similar figures in this chapter, is that of power level versus range. The signal was received by a hydrophone located on the continental slope at approximately the depth of minimum velocity, was brought to shore through several miles of cable, amplified, passed through a 500-cps lowpass filter, rectified, logarithmically compressed, and then recorded in the form shown.

When the sound-channel structure and bottom topography along the travel path remain reasonably constant, or are known in sufficient detail, the total signal duration can be computed on the basis of individual ray travel times and agrees well with experimental measurements. In midlatitude regions of the North Pacific the maximum signal duration rate is about 4 seconds for every 1000 nautical miles of travel. In the Atlantic, duration rates of 12 seconds per 1000 miles have been obtained. When such conditions are known, the signal duration can be used as a rough measure of the range of propagation, provided, of course, background noise conditions permit a reasonably accurate measurement of the total signal duration. An example of the change in signal duration and appearance with range along essentially the same bearing and under conditions of a strong sound channel is shown on Fig. 4. It will be noted that, as the range increases, the signal peak shifts to the right and the buildup increases in duration.

The depth of the sound-channel axis and the limiting-ray angle vary with location. In the North Pacific, for example, the surface waters in high latitudes are cold, and thus the velocity difference between the surface and the axis is small. This velocity difference increases with

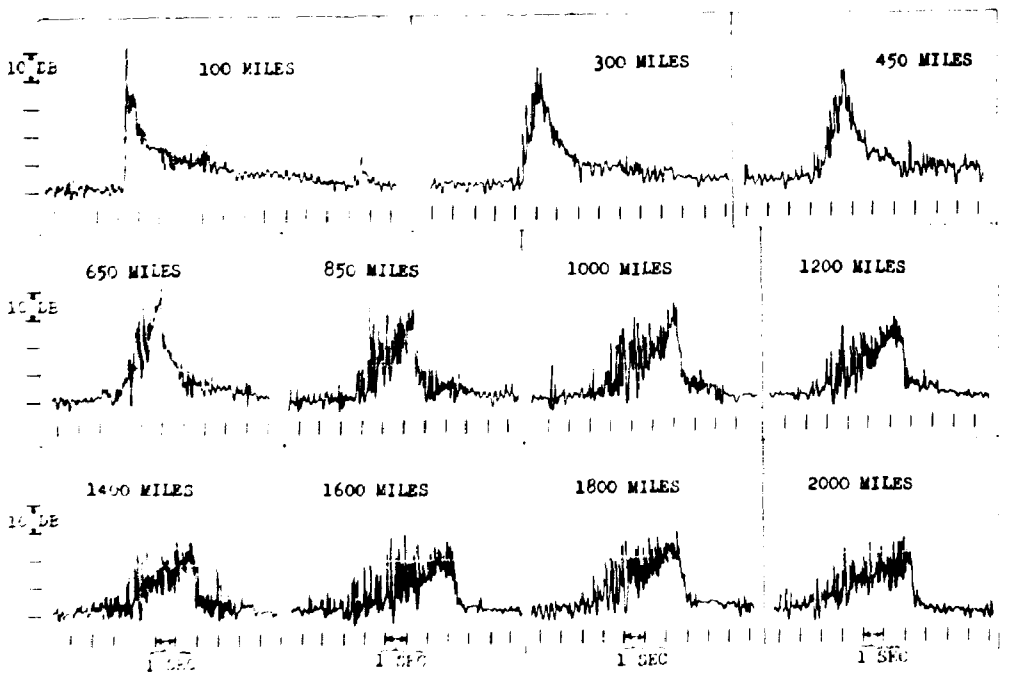

Figure 4 - Change in shot characteristic with range (miles). Records taken at Kaneohe Station. Detonation depth, 550 fathoms. Middle latitudes.

decreasing latitudes; hence the limiting-ray angle also increases. In low- and midlatitudes in the Pacific more energy is therefore channeled from explosions near the axis than is the case in high latitudes. Figure 5 shows representative examples of sound-velocity profiles in different locations in the North Pacific.

It may be of interest to consider briefly the propagation of signals along a path on which the sound channel gradually becomes stronger. When a signal originates where a weak sound channel of shallow axis depth exists, only a small percentage of the energy can initially travel by completely refracted paths. As the signal enters waters in which the channel axis deepens

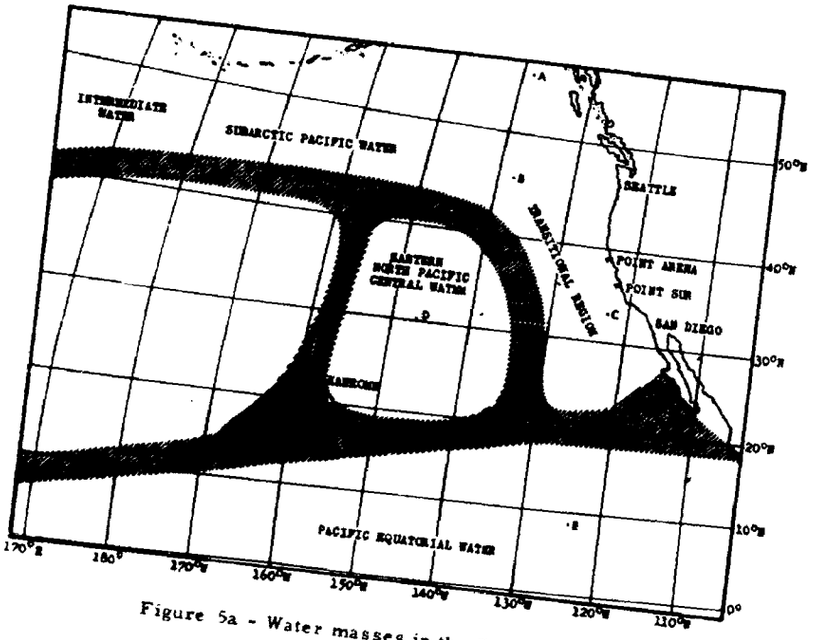

Figure 5a - Water masses in the Pacific Ocean

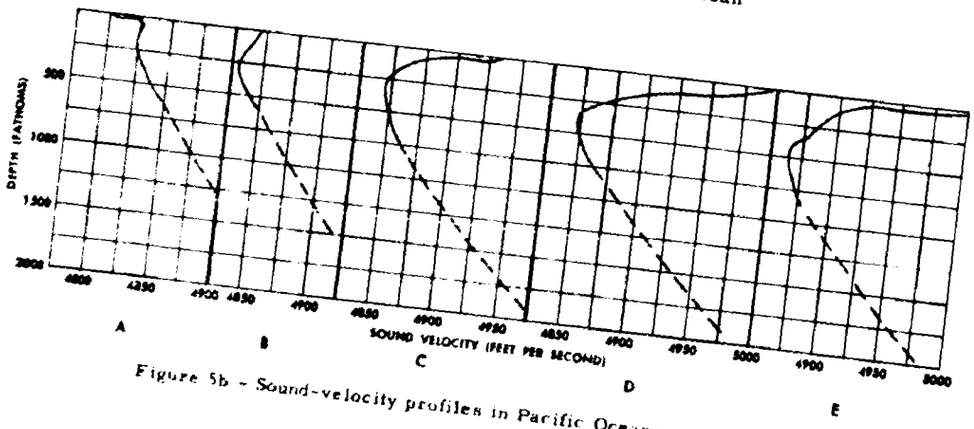

Figure 5b - Sound-velocity profiles in Pacific Ocean water masses

and a stronger channel develops, some rays which were originally surface-reflected can now travel by completely refracted paths. Also, since bottom-reflection losses are generally small for low frequencies at below grazing incidence, energy which has been reflected only a few times from the bottom may travel completely refracted paths as the channel develops. Thus more energy will be propagated than would have been the case had the channel not become more clearly defined.

The reverse situation exists, of course, for transmission along a path on which the channel becomes weaker. Energy which initially traveled by refracted paths only now suffers increasingly from bottom reflections, and less energy is propagated than would have been the case had the channel not weakened.

If no sound channel exists in deep water, a condition prevailing in very high northern latitudes in which the cold surface waters often result in a continuous increase of sound velocity with depth, all the ray paths are refracted upward and reflected from the ocean surface. If the ocean depth is great enough, a considerable amount of sound energy may travel via non-bottom-reflected paths to long ranges because of the near-perfect reflection at the surface. Very little energy will be propagated, however, by ray paths involving numerous reflections from the bottom at angles of incidence less than the critical angle.

Sound-velocity conditions near the sound-channel axis, in mid-latitude waters at least, seem to show remarkably little time variation. Signals from bombs detonated semi-monthly over a period of 16 months offshore of Kaneohe Bay were analyzed to determine the variation in total travel time between the Hawaiian area and the West Coast. The standard deviation of the travel times was only 2.7 seconds, and it was believed that this variation was caused primarily by small differences in location of the bomb drops. There was no evidence of any change in the speed of sound transmission along the channel axis over this long a time.

EFFECT OF BOTTOM TOPOGRAPHY ON PROPAGATION

The effect of the bottom along the path, and also at the receiver, must be considered. Since energy traveling via bottom-reflected paths will be lost after a few reflections unless they occur below grazing incidence, long-range signals necessarily contain only the energy that has traveled by these and by non-bottom-reflected paths. As the ocean depth decreases, more of the energy traveling by high-angle paths is absorbed by the bottom. Since the sound traveling by these paths makes up the front part of the signal, the received signal will be of sharper buildup and shorter duration. The peak amplitude of a long-range signal, however, when both source and receiver are on the axis of a strong sound channel, will not be markedly affected by small changes in ocean depth, since the signal peak under these conditions results from the energy that has traveled by low-angle paths near the channel axis.

An obstacle, such as a seamount, rising above the surrounding ocean floor can intercept those rays which reach depths greater than the summit of the obstacle. This means, again, that the large-angle rays at the source are the ones most likely to be intercepted, and thus we would expect a seamount to alter the shape of the received signal by removing, or at least attenuating, the early portion of it. The higher the seamount, the greater will be the amount of energy removed from the front part of the signal. It is not likely that diffraction of that sound which passes close to the sides of the seamount without obstruction will replace that intercepted, since the amount of energy carried by these high-angle paths is low.

Many of the bombs used in Sofar tests in the Pacific were dropped at locations where the propagation path to one of the stations was over a known seamount. Figure 6 shows some signals recorded under these conditions compared to those recorded under normal conditions at comparable ranges. It will be noted that the effect on the top three signals has been that predicted; a portion of the leading edge is missing on those which have passed over seamounts enroute to the receiver, but the peak amplitude has not been significantly affected. These signals were propagated through midlatitude waters where a strong sound channel exists.

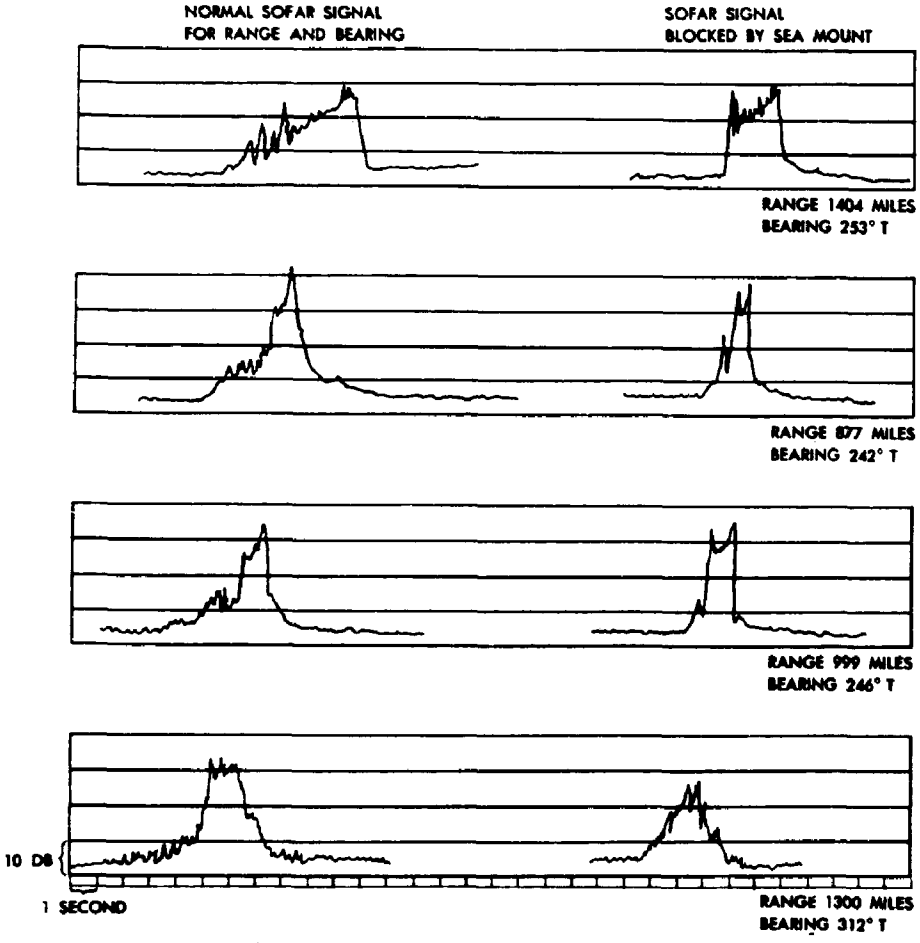

Figure 6 - Distortion of SOFAR signals by sea mounts

The fourth example on the figure is the signal from a bomb detonated in northern waters and off the sound-channel axis. The signal is therefore made up primarily of energy traveling via high-angle paths, and thus it is not surprising that the effect of the seamount has been to attenuate the entire signal rather than just the front part. Incidentally, the shape of these two signals is typical of those propagated through northern waters or from a source considerably off the channel axis.

Bottom topography near the receiver is also of importance to signal shape and duration, and thus to the total energy of the signal. As the bearings from the receiver to the source position approach the arc-of-reception limits at a station, the duration rate decreases rapidly.* This is illustrated in Figs. 7 and 8 in which are shown the average signal duration rates at the West Coast stations as a function of bearing from each station. In each case, although not shown here, the maximum duration rate is closely associated with the maximum rate of bottom slope.

*The arc of reception at a station is the ocean sector from which signals can be received. Outside of this area long-range signals cannot be received, and even short- and moderate-range signals are markedly attenuated. The duration rate is the rate at which the signal builds up to its maximum amplitude as the range is increased along a given bearing.

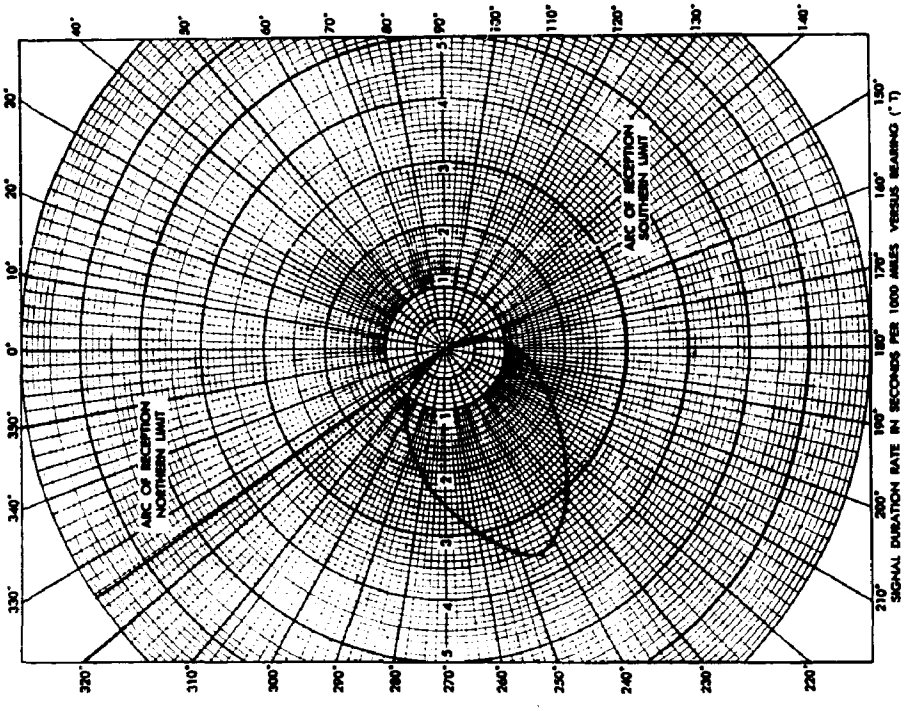

Figure 8 - Polar diagram of signal duration rate at Point Sur

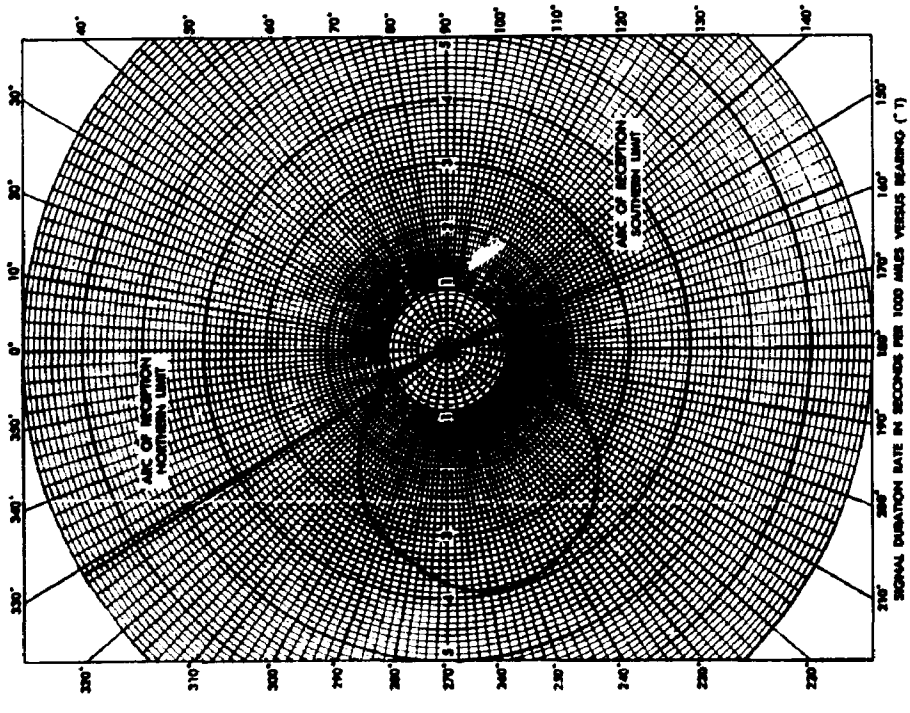

Figure 7 - Polar diagram of signal duration rate at Point Arena

As the bearing changes so as to require energy to reach the hydrophone via a slantwise traverse up the continental slope, the duration rate decreases. Under these conditions, most of the sound energy reaches the hydrophone after repeated reflections from the continental slope. Energy traveling by high-angle paths suffers more from such reflections than that traveling by low-angle paths; consequently the front portion of the signal again is the first to be affected. Thus, the signal is shortened and the duration rate decreases. Finally, the arc-of-reception limits at the station are reached as the bearing becomes nearly parallel to the continental slope, or until gross features of the bottom topography seaward of the slope cut off the signal. In the former case, signal energy fails to reach the hydrophone for two reasons, (1) bottom losses associated with repeated reflections from the bottom at decreasing angles of incidence, and (2) at each such reflection occurring slantwise up the slope the ray path is reflected out of its present perpendicular plane into one directed slightly more seaward. A sufficient number of such reflections, depending upon the original ray direction, the first angle of incidence on the bottom, and the bottom slope, can divert the energy traveling by such paths away from the hydrophone location.

TRANSMISSION LOSS

In determining the divergence factor in transmission loss, it seems clear that we are dealing with cylindrical spreading. Certainly, at ranges of interest to us in this type of propagation, virtually the only sound energy propagated will be that which has traveled by completely refracted paths. Thus both the peak sound pressure of the signal and the total sound energy passing through a vertical section of unit width through the sound channel should vary as the inverse first power of the horizontal range.

It might seem that long-range propagation experiments of this type could yield values for the attenuation of low-frequency sound in sea water. Unfortunately, this has not been the case. There are three limiting factors: (1) the extent to which environmental conditions must be known over very long travel paths before an individual experiment can be analyzed properly; (2) the length of time required to conduct a propagation experiment out to ranges of a few thousand miles, during which some of the environmental conditions may change and certainly equipment responses will vary; and (3) the very small magnitude of the quantity to be measured.

At long ranges, say more than several hundred miles, virtually all of the sound energy received from a 4-pound charge of TNT lies below 200 cycles per second. Since the theoretical value for the absorption of sound in sea water at 100 cycles per second is of the order of 0.1 db per 1000 nautical miles, it is clear that remarkable experimental control would have to be exercised to measure the attenuation of sound in the sea at this frequency, even though it may be more than an order of magnitude higher than the absorption. Over the interval of time required for a propagation run, changes in environmental conditions and equipment responses might easily overshadow the factor being measured.

A lower limit to the transmission loss, however, can be based on cylindrical spreading and the theoretical values of the absorption of sound in sea water. As a further refinement, some presently unpublished data at NEL, obtained from a different type of experiment, indicate a value of approximately 1.5 db per 1000 nautical miles for the attenuation of 100-cps sound in the sea.

As a final remark, whenever transmission losses associated with long-range, deep-sound channel propagation are discussed, the term must be defined rather carefully. In other types of underwater-sound-propagation experiments, ranges are limited to a few hundred miles at most, and in many cases a single-frequency source emitting pings of several cycles duration is used. In these experiments the signal is not markedly spread out in time, and transmission losses can be based on average or peak sound levels at the signal frequency.

For explosions however, what starts as a signal of very short duration and broad frequency spectrum is spread out in time many hundredfold and is materially altered in frequency content. The frequency bandwidth with which the transmission losses are associated - whether the losses are based on total signal energy considerations, on peak or average sound pressures, or on the energy carried by certain ray groups - must be specified.

THE SOFAR APPLICATION

A Sofar network has the purpose of furnishing information on the location of anyone in distress at sea, and is thus intended to be an important part of an air-sea rescue system. Ships and aircraft operating in areas covered by Sofar networks would be equipped with bombs containing four pounds of TNT and having a suitable fuze mechanism. Whenever a distress situation arose, one of these bombs, set for detonation at the sound-channel axis, would be dropped into the sea. The sound produced by the explosion would be received at the shore stations, and the location of the explosion determined by triangulation procedures based upon differences in times of reception at the stations.

At the present time there is no Sofar network, although individual stations still exist. The Navy Electronics Laboratory completed the installation of three stations forming the Northeast Pacific Sofar Network in September 1948, and the network subsequently underwent an engineering evaluation by NEL and an operational evaluation by the Commandant, Twelfth Naval District. These evaluations showed that the network performed its function satisfactorily, but it was considered too expensive to operate during peace time. The three stations, located at Point Arena and Point Sur, on the coast of California, and at Kaneohe Bay, Oahu, still exist but are not manned.

At each station a group of crystal hydrophones is mounted in a stainless steel cage in the form of a regular tetrahedron situated on the ocean floor at a depth of approximately 2000 feet, i.e., near the depth of minimum sound velocity in the Pacific. The hydrophones are connected to the shore equipment by means of several miles of Navy Type 115P submarine cable. At the shore end of the cable the incoming signals are amplified, filtered, rectified, logarithmically compressed, and then recorded as power levels on a large sheet of paper fastened to a revolving drum. The signals are also routed to a loudspeaker system for aural monitoring, and a timing trace is recorded adjacent to the signal trace so that signal arrival times can be accurately determined. This timing trace is calibrated daily against official radio time signals so that all stations are synchronized.

The area covered by the Northeast Pacific Sofar Network is shown in Fig. 9. It has been demonstrated that within this area more than 99% of the bombs detonated are received at all stations, and that the location of the sources can therefore be determined.

The detonation depth was not found to be a critical factor. Although the sound-channel axis is at a depth of approximately 2000 feet in much of this area, signals originating as shallow as 900 feet and as deep as 4000 feet had peak intensities at the stations only a few decibels lower than the signals detonated near the axis.

With the three stations located as they are the accuracy of signal-source location varies somewhat within the network. In the southeasterly portion the accuracy is of the order of 10 to 20 miles because of the poor triangulation baseline offered by the location of the West Coast stations. Partly for the same reason, the accuracy in the far northern region is somewhat worse, ranging from 20 to 100 miles. An additional reason for the larger error in these regions, however, is that the signals do not have the usual sharp cutoff typical of long-range signals, and the time of arrival is therefore more difficult to determine. As mentioned earlier, the lowest signals on Fig. 6 are typical of those from high latitudes.

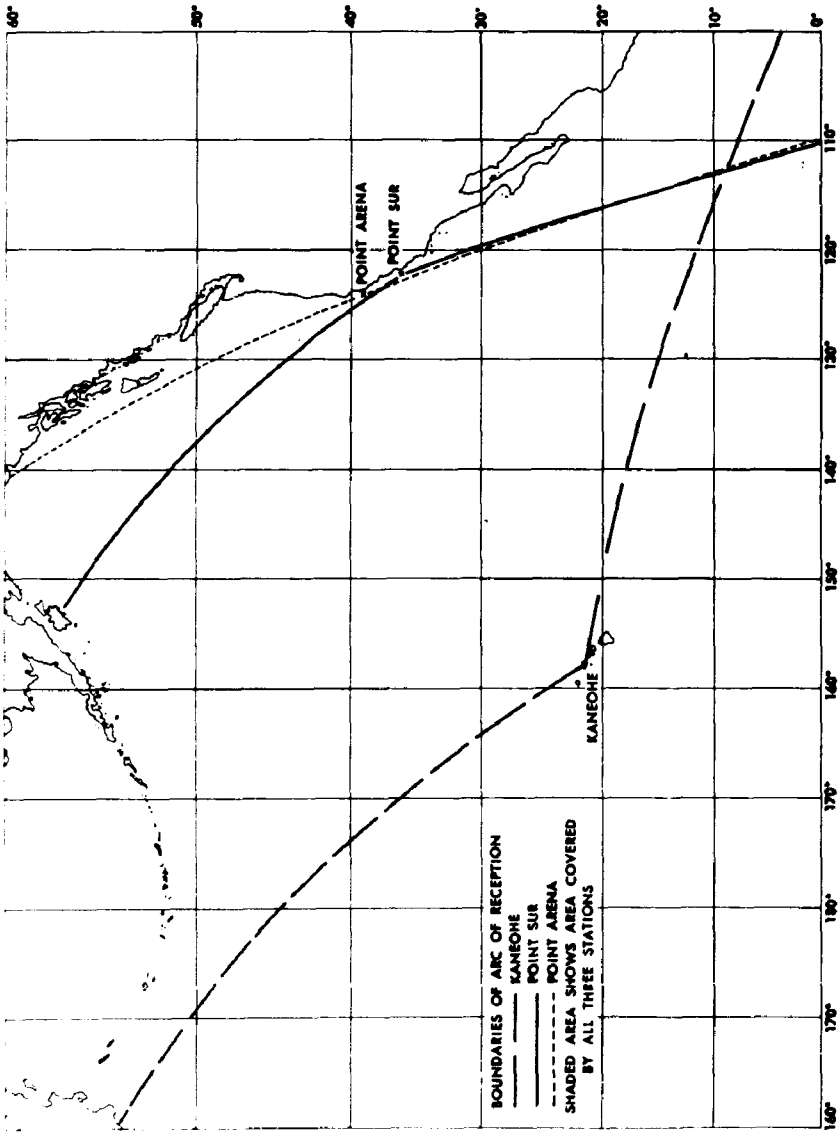

Figure 9 - Arcs of reception and area covered by SOFAR network

In the midlatitude region between the West Coast and the Hawaiian Islands the accuracy is good, of the order of 3 miles. This is considered to be a good measure of the inherent accuracy of the Sofar network, and is believed to be comparable to any other present long-range navigational technique.

A four-pound charge of TNT was shown to be entirely adequate to insure reception of signals originating within the network, and the Mark 22 Underwater Sound Signal was accordingly developed by the Bureau of Ordnance specifically for Sofar applications.

The maximum range at which these four-pound signals can be detected has not been established. They have been detonated offshore of Japan and received at Point Sur, 4340 nautical miles distant, 15 to 20 db above background noise.

REFERENCES

1. E. R. Anderson, "Distribution of Sound Velocity in a Section of the Eastern North Pacific," Trans. Am. Geophys. Union, 31:221-228, April 1950

2. A. B. Arons, "Secondary Pressure Pulses Due to Gas Globe Oscillation in Underwater Explosions II Selection of Adiabatic Parameters in the Theory of Oscillation," J. Acoust. Soc. Amer. 20:277-282, 1948

3. A. B. Arons, J. P. Slifko, and A. Carter, "Secondary Pressure Pulses Due to Gas Globe Oscillation in Underwater Explosions I Experimental Data," J. Acoust. Soc. Amer. 20:271-276, 1948

4. A. B. Arons and D. R. Yennie, "Energy Partition in Underwater Explosion Phenomena," Rev. Mod. Phys., 20:519-536, July 1948

5. A. B. Arons and G. K. Wertheim, "Viscous Attenuation of the Fourier Components of a Shock Wave from Explosion of a Half-Pound Charge in Sea Water," WHOI Ref. 50-32, September 1950

6. L. A. Barbour and G. P. Woollard, "SOFAR Triangulation Methods," WHOI Ref. 49-38, August 15, 1949

7. M. E. Brady and O. W. Schreiber, "The SOFAR Project: Interim Report No. 1," NEL Report 33, December 1, 1947

8. L. M. Brekhovskikh, "Propagation of Sound in an Underwater Sound Channel," Doklady Akad. Nauk SSSR, 69:157-160, November 11, 1949. (Also Ann. Telecommun. 5 (No. 29389), April 1950

9. J. D. Browder and T. P. Condron, "Interim Report No. 2: The SOFAR Project: Completion of Northeast Pacific Network," NEL Report 117, March 6, 1949

10. Bureau of Ordnance, "Signal (Underwater Sound) Mark 22, Mod 0 and 1," Ordnance Pamphlet 1729, April 6, 1950

11. Bureau of Ships, "Operator's Manual for SOFAR Monitoring Stations (Research Phase)," NAVSHIPS 91,287, January 30, 1950

12. D. C. Campbell, "Motion of a Pulsating Gas Globe Under Water: A Photographic Study," DTMB Report 512, May 1943

13. B. V. Carlson, "Detection of Explosions by SOFAR Stations," NEL Report 378, May 15, 1953

14. R. H. Cole, "Underwater Explosions," Princeton Univ. Press, 1948

15. T. P. Condron, "Effect of Sound Channel Structure and Bottom Topography on SOFAR Signals," NEL Report 233, April 19, 1951

16. S. Cornell, "SOFAR Bombs and Detonators," WHOI Interim Report 2, September 1, 1947

17. R. S. Dietz and M. J. Sheehy, "Transpacific Detection by Underwater Sound of Myojin Volcanic Explosions," J. Oceanog. Soc. Japan, 9(No. 2):1-31, September 1953

18. R. S. Dietz and M. J. Sheehy, "Transpacific Detection of Myojin Volcanic Explosions by Underwater Sound," Bull. Geol. Soc. Amer. 65:941-956, October 1954

19. K. Dyk and O. W. Swainson, "The Velocity and Ray Paths of Sound Waves in Deep Sea Water," Geophysics, 18:75-103, January 1953

20. "The U. S. Navy Has Announced SOFAR (Sound Fixing and Ranging)," Electronic Markets, No. 32, p. 11, March 1946

21. M. Ewing and J. Worzel, "Long-Range Sound Transmission: Interim Report No. 1, March 1, 1944 - January 20, 1945," WHOI Report 9 (Confidential), August 1945

22. M. Ewing, E. Newhouse, and R. McCurdy, "Summary of SOFAR Operations at Eleuthera," WHOI Memo for File, September 19, 1945

23. M. Ewing, G. P. Woollard, A. C. Vine, and J. L. Worzel, "Recent Results in Submarine Geophysics," Bull. Geol. Soc. Amer., 57:904-934, 1946

24. M. Ewing, J. L. Worzel, and C. L. Pekeris, "Propagation of Sound in the Ocean," Geol. Soc. Amer. Memoir 27, October 15, 1948

25. R. Halley and O. W. Schreiber, "Hydrophone System Calibration at the Point Sur SOFAR Station," NEL Internal Tech. Memo 46, December 5, 1952

26. C. Herring, "Theory of the Pulsations of the Gas Bubble Produced by an Underwater Explosion," NDRC Report C4-Sr-20-010, OSRD Report 236, October 1941

27. "Sound Transmission Conditions in the Arctic Ocean Related to SOFAR," Hydrographic Office Publication No. 15,159, October 1949

28. W. S. Latham and W. F. Saars, "Long Distance Sound Ranging Equipment (SOFAR) Installation and Operating Notes," USL Report 55, August 21, 1946

29. W. S. Latham and W. F. Saars, "Maintenance Manual for the Experimental Long Distance Sound Ranging Equipment (SOFAR)," USL Report 61, September 15, 1946

30. D. F. Leipper and E. R. Anderson, "Sea Temperatures, Hawaiian Islands Area," Pacific Sci., 4 (No. 3):228-248, July 1950

31. B. Luskin, M Landisman, G. B. Tirey, and G. R. Hamilton, "Submarine Topographic Echoes from Explosive Sound," Bull. Geol. Soc. Amer., 63:1053-1068, 1952

32. R. McCurdy, "Status of Underwater Sound Receiving Station at Eleuthera," WHOI Memo for File, April 4, 1945

33. R. McCurdy, "Summary of Developmental Work to Date on the Equipment for the Long Range Sound Transmission Program," WHOI Memo for File, December 6, 1945

34. R. McCurdy, "Long-Range Sound Transmission," WHOI Interim Report 3 on Contract No. NObs-2083, March 20, 1946

35. T. McMillian, "SOFAR Semi-Monthly Bomb-Drop Schedule Near Kaneohe, Oahu, T.H.," NEL Memorandum, July 20, 1950

36. STR Div. 6, NDRC, Vols. 7 and 8, 1946

37. M. F. M. Osborne and A. H. Taylor, "Non-Linear Propagation of Underwater Shock Waves," Phys. Rev. 70:322-328, September 1946

38. R. W. Rempel, "Some Signal Inversion Probabilities in the Northeast Pacific SOFAR Network," NEL Report 303, June 1952

39. L. D. Rosenberg, "A New Phenomenon in Underwater Sound," Doklady Akad. Nauk, SSSR, 69:175-176, November 11, 1949 (Also Ann. Telecomm., Vol. 5, 29389, April 1950.)

40. O. W. Schreiber, "Velocity Structure in the Northeast Pacific," WHOI Interim Report 4, July 29, 1946

41. O. W. Schreiber, "Some Sounds from Marine Life in the Hawaiian Area," J. Acoust. Soc. Amer., 24(No. 1):116 (Abst.), January 1952

42. "SOFAR, An Underwater Sound System Developed by Navy in Cooperation with Woods Hole Oceanographic Institution," Science News Letter, No. 49, p. 55, January 26, 1946

43. "Peace Time SOFAR Will Save Lives of Civilians Wrecked on Ocean," Science News Letter, No. 49, p. 324, May 25, 1946

44. "First SOFAR Station," Science News Letter, No. 52, p. 19, July 12, 1947

45. M. J. Sheehy, "Underwater Sound Signals at a SOFAR Station," NEL Report 281, February 20, 1952

46. M. J. Sheehy, "Some Signals of Seismic Origin Received at Pacific SOFAR Stations," NEL Internal Tech. Memo. 62, March 3, 1953

47. M. J. Sheehy, "SOFAR in the Pacific," ONR Research Reviews, March 1953

48. SOFAR Research Group, "Triangulation Tests of the Northeast Pacific SOFAR Network," NEL Report 175, April 27, 1950

49. W. W. Stifler, Jr., and W. F. Saars, "SOFAR (Sound Fixing and Ranging)," Electronics, 21:98-100, June 1948

50. O. W. Swainson, "Velocity and Ray Paths of Sound Waves in Sea Water," Report 2, USC & GS Field Engineers Bulletin, No. 10, pages 1-64, December 1936

51. O. W. Swainson, C. G. McIlwraith, and K. Dyk, "The Velocity and Ray Paths of Sound in Deep Sea Water," USC & GS Report 1, April 1934

52. E. E. Watson, "Cables Laid at Eleuthera," WHOI Memo for File, September 1945

53. W. B. Watkins and W. F. Saars, "Receiving, Recording, and Timing Equipment for Ultra Long Distance Sound Ranging," USL Report 35, January 17, 1946

54. G. P. Woollard, "Bathymetry, Control Positions, and Aspect of Proposed SOFAR Stations in the Pacific," WHOI Memo for File, July 24, 1946

55. G. P. Woollard, "A Summary of Factors Affecting Low Frequency Sound Transmission as used in SOFAR," WHOI Memo for File, August 16, 1946

56. G. P. Woollard, "A Manual for SOFAR Observers," WHOI Memo for File, July 1, 1947

57. "Underwater Explosion Research: Volume 1. The Shock Wave," ONR, 1950

SHALLOW-WATER TRANSMISSION

LOW-FREQUENCY ACOUSTIC TRANSMISSION IN SHALLOW WATER*

A. O. Williams, Jr.
Brown University

INTRODUCTION

Only in the last two or three years has low-frequency sound in shallow water received as much attention as other transmission problems. Therefore this part of the Survey can summarize only the ideas, rather than the numbers and formulas which allow a qualitative interpretation of the observations. A few numbers will be offered, tentatively; these have not been tested in enough cases to warrant empirical assurance, nor are they yet based on solid physical explanation. The situation should improve greatly in the next few years.

We shall be concerned here with values of H/λ, the ratio of water depth to acoustic wavelength, from roughly 0.25 to 10 or 20. The acoustic frequencies vary from a few cycles per sec to 1 or 2 kc, and λ from several hundred feet to a few feet. Chief operational interest in the lower H/λ range is concerned with acoustic mines; in the middle and higher range, passive and active detection of submarines is paramount. H runs from 30 ft (minimum navigable water) to some 600 ft at the edge of the continental shelves.

In this domain of H/λ, sources—though not necessarily receivers—are largely nondirectional. Surface waves or bottom irregularities are not large compared with λ. Moreover, spatial variations in sound speed are often of minor importance, though probably not negligible.

In the past 15 years, a few cases of short-range transmission (1) and the mathematical fundamentals (2) (method of normal modes) have been studied carefully. Understanding of longer-range transmission was possibly hindered by attempts to find simple numbers for propagation laws and transmission anomalies (3), in analogy with high-frequency practice.

In the last three years much more work has been done, particularly with very-long-range transmission. Complete answers are still beyond our reach, but the following statements are believed to be at least qualitatively correct.

NORMAL-MODE THEORY

The wave theory of acoustics is correct in all circumstances, even though the ray approximation is often preferable. In much of the range of H/λ specified above, wave treatment is necessary for full description; for transmission in a region bounded by water surface and bottom, this treatment takes the form of the method of normal modes, which in application to underwater sound is described in several references (1, 2, 4, 5). The essence of this method is that sound of a given frequency may travel through the shallow water simultaneously by one

Note: Paper received December 1954, revised August 1955
*See also reference 20 for another summary of this subject by the same author.

or more distinct modes, which are roughly analogous to the various paths of travel known in ray analysis. In ideally simple cases, each mode signal travels with cylindrical spreading (3-db loss in level per distance doubled), and each with a distinct phase velocity. The multiple reflections at the water surface and the bottom are beyond the critical angle and so ideally involve no loss of energy. (There are complications near the source, as will be seen.) These modes can be numbered: $n = 1, 2, \ldots N$. The mode number n must be distinguished from the number of allowed modes, N. If without other changes the water is made ever shallower, the reflections mentioned just above begin to fall within the critical angle. The highest numbered mode (N) is "cut off," i.e., can no longer be transmitted, then (N-1), etc., until finally even mode number 1 is cut off. In this last case, practically all the acoustic output is lost into the bottom near the source. Exact formulas exist to describe cut-off terms of H/λ, the speeds of sound in water and in the bottom, and the two densities of water and bottom. For the usual ocean conditions, no mode can exist if

$$H/\lambda \lesssim 0.5. \tag{1}$$

The total number N of modes escaping cut-off (and so available to propagate sound) is given roughly by

$$N \approx H/\lambda. \tag{2}$$

If the speed of sound is less in the bottom than in water, no undamped modes are possible and only short-range transmission exists. In the opposite, and probably much more common situation, where the speed of sound in the bottom exceeds that in the water, the phase speed for each mode lies between these two limiting speeds, which characteristically differ by no more than 20 or 30 percent (except in the rare case of a solid-rock bottom).

The amount of sound power put into each mode by a given source depends on the mode number (n), the source depth, the water depth (H), and the acoustic wavelength (λ). An analogy exists in the excitation of various overtones in a plucked string. Likewise, the level detected by a hydrophone depends on its vertical location, as would be true if a vibration pickup were moved along a vibrating string.

When mode propagation exists, a definite part of the sound wave is transmitted in the upper bottom, where it just keeps pace with the "water wave."

The mathematical theory of normal-mode transmission furnishes exact, though not always simple, formulas for all the phenomena just summarized. However, any real body of water is far more complicated than the ideal realm of this theory, and so attempts at precise calculation are hopelessly lengthy, unjustified, or even misleading.

The theory is incomplete in another way; it assumes nondissipative transmission if modes are possible at all. Empirically, a considerable attenuation is found; e.g., a db or two per mile at 150 cps in 100-ft depths. True acoustic absorption in the water is negligible by comparison—e.g., a db per hundred miles at 1 kc, and much less at 100 cps. The physical cause of the observed attenuation must therefore lie in the water surface (i.e., its roughness), or in the bottom, or both. At least three causes can be imagined: (1) scattering by surface or bottom roughness, with consequent loss of power into the bottom from the allowed modes; (2) conversion of longitudinal sound waves into shear modes in the bottom, with consequent dissipation; (3) absorption in the bottom material (where, it will be recalled, a part of the sound must always travel). Theoretical analyses indicate that in each of these three cases the attenuation coefficient increases for shallower water or for greater wavelengths (lower frequencies), and also increases rapidly with the mode number, n.

This outline of the normal-mode method is necessary, because it seems reasonably sure now that the practical characteristics of low-frequency sound in shallow water cannot be understood without appeal to this theory or an equivalent one, with modifications to take account of departures from ideal surfaces and to include attenuation. On the other hand, quantitative agreement between theory and experiment cannot be claimed at present; moreover, the physical meaning of the observed attenuation is undetermined.

SHORT-RANGE PROPAGATION

The typical problem in "near-field" or short-range propagation, associated with acoustic mines, is to predict the sound field at a bottomed receiver when a source relatively near the surface is towed nearby.

At horizontal ranges comparable with the water depth, the sound field is much like that of a simple dipole formed by the combination of the source and its mirror image in the water surface. The acoustic level falls off as inverse square (6 db per distance doubled) within a very few yards of the source, but soon goes over into a much more rapid dipole law, 12 db per horizontal distance doubled. If the speed of sound in the bottom is less than that in the water (perhaps not unusual with low frequencies and muddy bottoms), or if H/λ is too small to allow any normal mode to be set up, this fall-off may continue until the acoustic level is negligible, still at short range; almost all the sound has been lost into the bottom. (But see later comments about layered bottoms.)

If one or more normal modes are possible in the water, this very-short-range dipole field probably merges into a zone extending to horizontal ranges of several water depths, where the fall-off is more nearly 6 db per horizontal distance doubled. At greater ranges, cylindrical spreading (3 db per distance doubled) prevails for the average sound level; the attenuation mentioned in the previous section becomes important only after several miles.

When more than one mode is allowed ($H/\lambda \gtrsim 2$), another complication enters in the form of mode interaction. The several modes travel at different speeds and so at ranges more than a few water depths they get successively in and out of phase with each other. The corresponding constructive and destructive interferences produce great "swings" in the sound level. For example, given two modes with equal sound power in each, the total level theoretically swings from 6 db above that of either mode to -00 db below. Many observations show measured swings of 15 to 20 db.

The spacing Δr of successive minima (or maxima) in this simple case is given roughly by

$$\Delta r \approx 8H^2 f/(3c), \qquad (3)$$

where f is the frequency and c is the speed of sound in the water.

When there are more than two modes, the swings become less regular but about as large and sometimes more abrupt. For example, a change of 15 db with 20 yds change of range may be possible. An enlightening summary (possibly too pessimistic in tone) of these various complexities can be found in Ref. 6.

These swings are most marked with single-frequency sounds. Broadband reception is much more regular—although not perfectly so—because a point of destructive interference for some frequencies is likely to be one of constructive interference for other components.

TRANSMISSION OVER LAYERED BOTTOM

The ocean bottom always has a layered structure. When the upper layers are neither very thin or very thick compared with λ, normal modes can exist in the bottom, whether or not the water depth allows modes to propagate. Examples of the resulting transmission have been studied by the Hudson Laboratories (7); in this case the water was so shallow that all modes were cut off, yet modes existed in two deep sedimentary bottom layers, and sound was propagated to a distance of at least several miles, with evidence of normal-mode interaction.

If the uppermost layer is relatively thin, and not too different from water in its value of sound speed, it acts roughly as an extension of the water in depth. An example is found at one of the acoustic ranges at H. M. Underwater Detection Establishment (Portland, England) where

the layered structure is known to be complicated. The true water depth is 12 fathoms, but better agreement with simple mode theory is achieved by pretending the depth is about 14 fathoms.

On the basis of trials at a number of sites in the United Kingdom, Dr. Flint of H. M. Underwater Countermeasures Weapons Establishment offers a simple rule for ranges out to several hundred yards in water of harbor depth (8). Transmission falls into three categories: (a) The water depth is much too small to allow any mode; then, regardless of layering, propagation follows roughly a dipole law. (b) The water depth easily allows one mode, at least; the dipole law merges into cylindrical spreading, possibly with mode interactions. (c) The intermediate situation exists; then bottom layers, minor changes of depth, etc., become important, and simple answers are impossible.

Much more work must be done in this field. Recent "Inshore Survey" acoustic data published by the Hydrographic Office (9) should be helpful, once information about the bottom structure is added.

OPTIMUM FREQUENCIES FOR TRANSMISSION

Dr. Tolstoy of the Hudson Laboratories has showed theoretically that for any one transmitted mode in shallow water there will be an optimum frequency for transmission (10). It is near the frequency at which the group velocity (velocity of a pulse) is minimum, and so rather low, e.g., 20 or 30 cycles for the first mode. Hudson Laboratories' reports confirm this prediction experimentally (11).

When several modes are possible, there will be several individual optimum frequencies, increasing with the mode number. Moreover, at ranges which make attenuation appreciable there will be a shifting of the "average" optimum frequency to higher values (or conceivably a blurring of the effect). It is noteworthy that Woods Hole Oceanographic Institution, in trials of active submarine detection in shallow water, has observed a tendency for best transmission at a few hundred cycles. A similar tendency exists in some of the long-range transmission data to be summarized below.

These effects may be useful or important in various ways, and a better understanding of them is necessary.

MEDIUM- AND LONG-RANGE TRANSMISSION

Transmission to medium and long ranges is of particular interest in the passive detection of submarines. A reasonable amount of data exists but at scattered localities, and it is not as complete as might be desired. Besides material summarized (3) after World War II, some recent measurements can be mentioned. The Admiralty Research Laboratory (12) has made propagation runs at several sites near the British Isles, with maximum ranges of from 36 to 125 miles. The bottom was usually sand or shell and the water depths 100 to 350 ft. Explosive charges were used as sources and the recorded results were the total energies of arrival in octave bands. In later runs these octaves extended from 25 to 50 cycles up to several kilocycles.

The Bell Telephone Laboratories have made several trials at various sites off the east coast of North America. Shots were used in some cases and a 98-cycle projector in others. Many different water depths are represented. Maximum ranges are from 20 to about 60 miles (the latter only with shots). The data have been so far processed only roughly, for survey purposes.

The Underwater Sound Laboratory at New London has recently published (13) the results of several runs off the northeastern United States. An underwater siren of fundamental 113 cycles was the source; reception was in roughly one-third-octave bands, widely spaced.

Ranges achieved before noise limitation were usually no more than 20 to 30 miles. Both mud and sand bottoms were sought, and quite different BT conditions were included.

Other data exist, and more will soon be forthcoming, but the preceding will serve as examples.

A method of analysis which has moderate empirical success has been mentioned in several reports (14, 15, 16). It is based on normal-mode analysis, with approximate methods of evaluation. (In view of the inaccuracies in experimental work and in our knowledge of the bottom structure, rather drastic approximations are justifiable.) Except at short ranges, normal-mode interactions are unimportant for wide bands received from a shot. At longer ranges the received signal is governed by three factors: (a) cylindrical spreading (3 db per distance doubled), (b) variations in water depth along the path, (c) the attenuation mentioned in the discussion of Normal-Mode Theory above.

In view of factor (a), it is desirable to plot the intensity I or level L of the received signal after correction for cylindrical spreading, i.e., to plot rI or $L + 10 \log r$, with r the range.

Factor (b), changes in water depth, affects propagation in several ways. First, it causes minor deviations from cylindrical spreading, owing to funneling or spreading of the sound. Second, it determines the number of modes allowed. Third, the depth H enters into the stimulation functions mentioned under Normal-Mode Theory above. Finally, as was also mentioned, the water depth appears to affect strongly factor (c), the attenuation.

It was stated earlier that this attenuation appears to vary with mode number. From examination of data over sandy or pebbly bottoms at three different sites, with frequencies from 25 to a few hundred cycles, and in water depths from 100 to about 400 ft, the following formula seems to give representative values for the attenuation α_n of the n-th mode:

$$\alpha_n \approx \frac{10^7 n^2 \lambda^{2.4}}{H^{5.5}} \qquad (4)$$

where α is in db per nautical mile and both the wavelength λ and the depth H are in feet. The proportionality constant apparently does not differ by more than a factor of 2 to 4 from one site to another.

As a numerical example, at a frequency of 100 cycles in water of depth 150 feet, Eq. (4) yields a value of 1.25 db/mile for the first mode (some three modes would exist in these circumstances). It is clear that such an attenuation is important at ranges of tens of miles, and moreover that modes higher than the first are likely to be completely damped out at such ranges. On the other hand, doubling the depth would decrease this attenuation over forty-fold, to a negligible value.

Preliminary analysis of the Underwater Sound Laboratory's data (13) over a mud bottom shows qualitatively similar results. Since there was a marked thermocline in the cases analyzed, and since receivers both above and below this thermocline were used, it was possible to test the general effects of such inhomogeneity in the water. The results are inconclusive at present.

The qualitative success, outlined above, in explaining shallow-water low-frequency propagation is encouraging but far from satisfying. For example, despite its empirical validity Eq. (4) is dimensionally wrong and at present incapable of physical explanation; the extremely rapid variation of with depth is hard to believe. Moreover, each new case requires lengthy analysis; neither wide experience nor physical understanding has yet pointed out simple generalizations with even semiquantitative validity.

For comparison with the empirical Eq. (4) a combination of ray and wave analysis suggests the following formulas for α_n in the three separate cases of attenuation listed earlier.

Scattering: $\alpha_n \propto n^2 \lambda h / H^3$ (5)

Shear loss: $\alpha_n \propto n^2 \lambda^2 / H^3$ (6)

Absorption of longitudinal waves in bottom: $\alpha_n \propto (n^2 \lambda^3 / H^3)\ \alpha_b$. (7)

In Eq. (5), h is a representative dimension of the surface or bottom roughness. In Eq. (7), α_b is the ordinary absorption coefficient of the bottom material, presumably a function of frequency (or wavelength).

Equation (7) and the omitted proportionality constant have been derived (17) from wave theory as well as in the approximate manner used for Eqs. (5) and (6), a fact which strengthens confidence in the latter formulas. In two or three instances, the dependence of α_n on the inverse cube of H has been substantiated by RAG analysis of BTL propagation data. The more sensitive dependence on H indicated in the empirical Eq. (4) may be quite unreal. That is, the abnormally high attenuations in shallow water which seemed to demand so high a power of H may instead have been due to local variations in the bottom material.

The wavelength dependence of α_n in Eq. (4) does not agree particularly well with any of the equations (5)-(7), except in the sense of increasing with increasing λ. A British experiment in the North Sea suggests that α_n is given by

$$\alpha_n \propto n^2 (a\lambda + b/\lambda), \quad (8)$$

a and b being constants of such size that α_n is a minimum about 150 to 200 cycles (the depth was constant, so that no information was gained about dependence on H).

At least in the higher values of H/λ postulated at the start of this article, ray methods have had considerable success. Since some of these results will appear elsewhere in this volume, only two examples will be mentioned here. First, USNUSL has used on its own data (13) a method based in part on ray theory and in part on empirical formulas derived from much analysis of propagation in deep-water surface channels (18). Good agreement with experiment is found at least down to a few hundred cycles.

Teer and Daintith of HMUDE have recently used ray theory on some of the British data mentioned above (19). They take account of source and receiver depths and water depth variations, and allow for losses at each reflection of the rays from the bottom. Agreement with experiment is good at 800 cycles and above, but grows rapidly poorer at lower frequencies. It is at these lower frequencies that the normal-mode attack has enjoyed some success.

In conclusion, several qualitative "predictions" are given in Fig. 1 in the form of graphs showing signal level corrected for cylindrical spreading vs. range, for several water depth characteristics.

REFERENCES

1 J. M. Ide, R. F. Post, and W. J. Fry, "The Propagation of Underwater Sound at Low Frequencies as a Function of the Acoustic Properties of the Bottom," NRL Report S-2113, August 1943

2. M. Ewing, J. Worzel, and C. L. Pekeris, "Propagation of Sound in the Ocean," Geol. Soc. Amer. Mem. 27, 1948

3. "Physics of Sound in the Sea, Part I: Transmission," STR Div. 6, NDRC Vol. 8, See Ch. 6, 1946

4. Ibid, Ch. 9, Sec. 4

Constant depth; only one mode allowed; constant attenuation at single frequency.

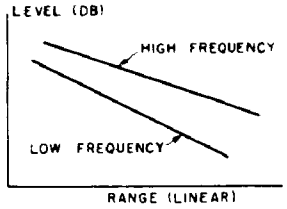

Constant depth – several modes. Higher modes damped out in earlier part of path – thereafter curves approach those of above figure.

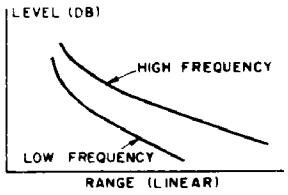

Several modes; depth increases uniformly from receiver to source. Great attenuation in shallow water near receiver. The higher modes generated at the source are cut off on reaching shallower water.

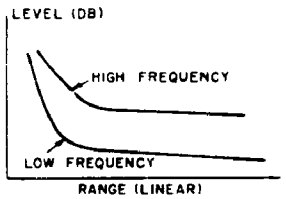

Several modes; H decreases uniformly from receiver to source. Greater attenuation in shallow water near source, partly offset by "funneling" effect.

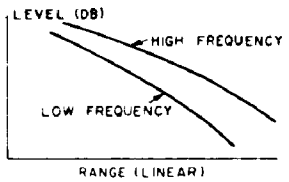

Figure 1 - Typical propagation curves, after correction for cylindrical spreading, that can result from various water depths and mode attenuations

5. H. Merbt and F. M. V. Flint, "The 'Normal Mode' Theory of Propagation of Sound in a Shallow Sea; Theoretical Application and Experimental Results for Very Low Frequencies," Great Britain, Admiralty Mining Est., UCWE Informal Report 1479/49 (Secret), January 17, 1950

6. H. R. Alexander, J. L. Stone, R. W. Morse, and P. J. Westervelt, "A Review of Low-Frequency Acoustic Propagation in Shallow Water with Applications to Minesweeping," RAG Report, jointly with ONR and Princeton Univ. (Secret), February 1953

7. G. E. Becker, R. O. Carlson, R. A. Frosch, and H. L. Poss, "30-cps Sound Propagation in Shallow Water," Project MICHAEL Tech. Report 9 (Confidential), April 1953

G. E. Becker and R. O. Carlson, "15- and 30-cps Sound Propagation at a Location Near the Entrance to New York Harbor," Project MICHAEL Tech. Report 13 (Confidential), Oct. 1953

R. O. Carlson and M. V. Brown, "Shot Refraction Profiles in the Atlantic Coastal Plain 6 Miles East of Ambrose Lightship," Project MICHAEL Tech. Report 14, November 1953

8. T. E. Stringer, "Prediction of Low Frequency Propagation in Shallow Water," UCWE, Informal Report 1636 55, July 1955

9. "Analysis of Mine Countermeasure Data Taken at Charleston in January 1954," Inshore Survey Project (Vamp Survey) H.O. Misc. No. 15359-1 B, Part II (Secret), June 1954

10. W. A. Nierenberg, F. K. Levin, M. V. Brown, and I. Tolstoy, "A Progress Report in Shallow Water Research," Project MICHAEL Tech. Report 21 (Secret), June 1954

11. I. Tolstoy, R. Frasetto, and L. P. Goldberg, "Shallow Water Studies near St. Thomas, V.I.," Project MICHAEL Tech. Report 22 (Secret), July 20, 1954

12. W. W. Reay, "Low-Frequency Sound Propagation in Shallow Coastal Waters," Great Britain Admiralty Research Lab. Report ARL R2/95.80/D, June 1953

13. T. P. Condron, "Summary of Cruise I-4 Siren Data," USL Tech. Memo. (Confidential), August 10, 1954

T. P. Condron, "Completion of Processing of Cruise I-4 Siren Data," USL Tech. Memo 1110-044-54 (Confidential), September 28, 1954

14. A. O. Williams, Jr., "On the Propagation of Sound in Water of Moderate Depth," ONR (London) Tech. Report 88-53 (Confidential), June 5, 1953

15. A. O. Williams, Jr., "A Study of Low-Frequency Sound Propagation in Shallow Water over a Sloping Bottom," ONR (London) Interim JEZEBEL Report 6 (Secret), June 22, 1953

16. A. O. Williams, Jr., "Transmission of Low-Frequency Sound in Shallow Water over a Sloping Bottom," Brown Univ. RAG Tech. Memo 54-2 (Secret), April 1954

17. E. T. Kornhauser and W. P. Raney, "Attenuation in Shallow-Water Propagation due to an Absorbing Bottom," J. Acoust. Soc. Amer., 27:289-692, 1955

18. T. P. Condron and P. A. Barakos, "Analysis of Shallow-Water Sound Propagation in Frequencies from 0.1 to 8 kc," USL Research Report 254 (Confidential), December 15, 1954

19. M. J. Daintith and C. A. Teer, "An Application of Ray Theory to Sound Propagation in Coastal Waters," UDE Report 152 (Secret), May 1955

20. A. O. Williams, Jr., "The Theory of Shallow-Water Sound Propagation - A Survey," USN J. Underwater Acoustics, 5(No. 4):217-226 (Confidential), October 1955

INTERMEDIATE AND HIGH-FREQUENCY ACOUSTIC TRANSMISSION IN SHALLOW WATER

K. V. Mackenzie
U. S. Navy Electronics Laboratory

INTRODUCTION

The range of frequencies discussed will be from about 200 cps to 56 kc. The lower frequencies overlap the upper portion of the range discussed in the preceding chapter (A. O. Williams). Sound at 56 kc and above can be considered as spreading spherically and is essentially limited to short ranges because of the attenuation in the sea water. The depths will be restricted to those greater than five wavelengths (5λ), with a minimum of 15 fathoms and a maximum of about 100 fathoms.

Because several modes are involved, any wave-theory solution is very sensitive to the existing physical environment. The preceding chapter discussed the data in terms of normal-mode solutions. This paper will emphasize the ray-analysis approach. The physical environment with realistic bottom losses and varying velocity profiles over the transmission path appears to be much too indeterminate to permit accurate prediction of transmission losses. However, since many sound paths are involved and the disturbing influences tend to randomize the phases of these, average propagation loss vs range curves can be obtained. The fluctuation about these average curves may be attributed to the interaction of the several modes.

It has been demonstrated that, because of the always present fluctuation, it is impossible to state empirically the best spreading law with any confidence (1). Fortunately, there is a considerable body of experimental data from 25-fathom water, a very common depth, out to ranges of about 40 miles. Very likely active echo ranging at frequencies above 200 cps will not be practical much beyond this range. Possibly active and passive detection will be restricted to ranges less than double 40 miles because it becomes more practical to use electrical cable transmission in place of shallow-water acoustic transmission for greater ranges.

Theoretical curves have been developed that agree quite well with the existing data (2-5), but differ on predicted extrapolations. However, these differences are not of great practical importance in the range of extrapolations required.

BOTTOM REFLECTION LOSSES

The several transmission theories all require an estimation of the bottom losses which are the most important factor in shallow-water transmission at low and intermediate frequencies. This section will discuss the acoustic-energy loss for a single reflection. For frequencies above 200 cps the deeper sediments probably have little influence. The simplifying assumption of a flat, fluid bottom appears to describe the losses adequately.

Note: Paper received January 1956
Information in this chapter may be considered Confidential except where individual paragraphs or figure titles are marked Secret.

If we consider the bottom fluid as dissipationless, then we have Lord Rayleigh's classical formula

$$r = \left| \frac{pq - \sqrt{1 - (p^2 - 1)\cot^2\phi}}{pq + \sqrt{1 - (p^2 - 1)\cot^2\phi}} \right|^2 \tag{1}$$

where r is the ratio of reflected to incident energy.

$$p = \frac{\text{sound velocity in bottom}}{\text{sound velocity in water}} = \frac{c_1}{c}$$

$$q = \frac{\text{density of bottom}}{\text{density of water}} = \frac{\rho_1}{\rho}$$

ϕ = grazing angle of incidence.

The following remarks follow from Eq. (1). When $p > 1$ there is a critical angle

$$\phi_c = \cos^{-1}\left(\frac{1}{p}\right) \tag{2}$$

where the radical becomes imaginary and the loss becomes and remains zero for $\phi < \phi_c$. The phase angle w between the incident and reflected sound in this region is

$$w = 2\tan^{-1}\frac{\sqrt{(p^2 - 1)\cot^2\phi - 1}}{pq}. \tag{3}$$

When $pq = \sqrt{1 - (p^2 - 1)\cot^2\phi}$, the reflection loss is infinite, giving an angle of intromission

$$\phi_I = \tan^{-1}\sqrt{\frac{1 - p^2}{(pq)^2 - 1}} \tag{4}$$

where all of the sound enters the bottom. This angle exists as pointed out by Lord Rayleigh whenever $q > 1/p > 1$ or $q < 1/p < 1$.

When $p > 1$ and $pq \geq 1$, the reflection takes place with no change in phase for $\phi > \phi_c$. If $p > 1$ and $pq < 1$, an intromission angle as well as a critical angle exist. The reflection takes place with no change in phase for $\phi_c < \phi < \phi_I$ but with a reversal in phase for $\phi > \phi_I$.

When $p < 1$ and $pq > 1$, the intromission angle exists and the reflection takes place with a reversal in phase for $0 \leq \phi < \phi_I$ but with no change in phase for $\phi > \phi_I$. When $p < 1$ and $pq < 1$ no intromission angle exists and the reflection takes place with a reversal in phase for all angles.

When $p = 1$, there is no angle dependence and the loss $= 20 \log |(q - 1)/(q + 1)| = 20 \log |(\rho_1 - \rho)/(\rho_1 + \rho)|$ where ρ_1 is the density of the bottom and ρ is the density of the water. There is no reversal in phase on reflection if $q < 1$.

A typical example for fluid "red clay" is shown in Fig. 1. The solid curve gives the loss per reflection vs grazing angle when $p < 1$. The loss rises from normal incidence as ϕ decreases until it becomes infinite at 9.49°, the angle of intromission, and then decreases to zero. The dashed curve was computed for $p > 1$ and corresponds to the more usual case. The critical angle is at 7.22°. There is not much difference in the two curves between 30° and 90° and, in fact, a loss of $-20 \log |(\rho_1 - \rho)/(\rho_1 + \rho)| = 18.7$ db is a fair approximation to either over this range of angles.

However, for long-range, shallow-water transmission the losses at small grazing angles must be considered. For the solid curve of Fig. 1, the reflection takes place with a reversal of phase for $0 \le \phi < \phi_I$. The loss varies with ϕ as shown. For the dashed curves the reflection is perfect for $\phi \le \phi_c$ but the phase changes with ϕ according to Eq. (3).

When the bottom fluid is not dissipationless but attenuates the sound, it is necessary to use a complex velocity for the bottom fluid. This modification to Lord Rayleigh's equation was developed by R. W. Morse (7, 8) and is

$$r = \frac{[T - pq \sin\phi]^2 + S^2}{[T + pq \sin\phi]^2 + S^2} \qquad (5)$$

where

$$T^2 = \frac{1}{2}\left(\sqrt{A} - B\right) \text{ and } S^2 = \frac{1}{2}\left(\sqrt{A} + B\right)$$

when

$$B = p^2 \cos^2\phi - 1 + \left(\frac{\alpha c_1}{2\pi f}\right)^2$$

and

$$A = B^2 + 4\left(\frac{\alpha c_1}{2\pi f}\right)^2 .$$

The attenuation $\alpha = 0.1151\beta$ where β is the attenuation in db/ft, c_1 is in ft/sec and f is in cps.

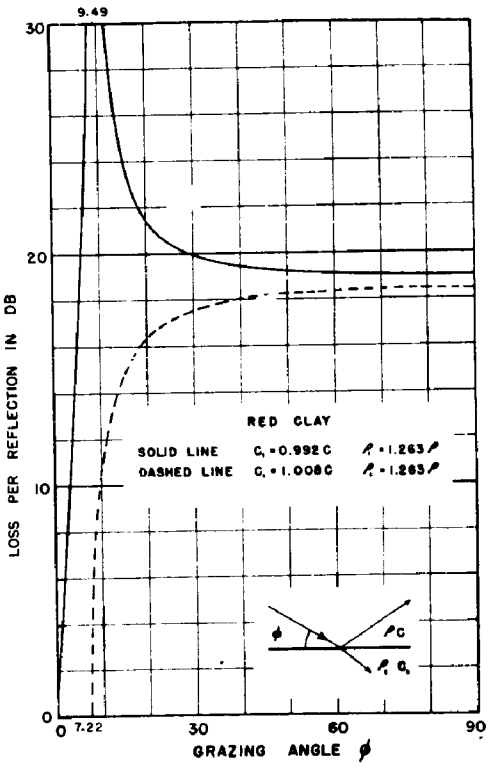

Figure 1 - Loss per reflection in db vs grazing angle calculated with Lord Rayleigh's equation

Available theory (7, 9) predicts that the attenuation should vary as the square root of the frequency. Measurements have been made with innundated 30-mesh sand which verify this dependence from 55 to 365 kc (10). These results are summarized by

$$\beta = (0.79 \pm 0.09)\,(f_{kc})^{\frac{1}{2}} \text{ db/ft.} \qquad (6)^*$$

This equation is consistent with values reported for sand by other investigators at 500 kc (11) and near 30 kc (12). The velocities and attenuation have been recently measured and reported for a number of bottom sediments (12, 13). These values were used (5) with Eq. (5) to compute the reflection loss vs the grazing angle for silt and for fine sand. The computed curves for silt are shown in Fig. 2. Here values of $p = 1.02$, $c_1 = 4896$ ft/sec, $q = 1.64$, and $\beta = 1.5$ db/ft at 30 kc were used. The solid curve is for a dissipationless bottom. The other curves were computed from Eq. (5) with an attenuation extrapolated as $f^{1/2}$ from 30 kc. The value at 200 cps was 0.12 db/ft. It can be seen that even a small attenuation can have a most serious effect on the loss at small grazing angles. The loss curves are frequency dependent because the imaginary part of the complex velocity is $\alpha c_1/2\pi f$ and if α varies as $f^{1/2}$ then the imaginary part varies inversely as $f^{1/2}$.

*In Eq. (6) f is in kilocycles for convenience in computing.

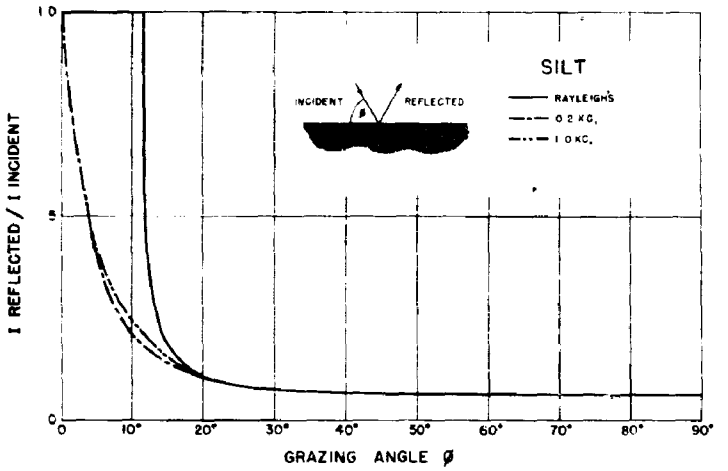

Figure 2 - Ratio of reflected to incident energies vs grazing angle for silt for Rayleigh's equation with and without attenuation in the silt estimated to be typical for Area IV of the Chukchi Sea

The curves computed for a fine sand are shown in Fig. 3. Here $p = 1.33$, $c_1 = 5540$ ft/sec, $q = 2.00$, and $\beta = 4.34$ db/ft at 30 kc, or, extrapolating $f^{1/2}$, $\beta = 0.35$ db/ft at 200 cps. This figure shows the difference between 0.2-kc and 1-kc loss more clearly than Fig. 2. A further curve was added because computed transmission curves, to be discussed later, when compared to actual transmission curves indicate that the extrapolation of β should be as the first power of the frequency. This is shown as the modified curve. (With this extrapolation the attenuation per wavelength is constant.) The value of β used was 0.03 db/ft at 200 cps. For small angles less than 0.1 radians, the ratio for sand-modified can be expressed as $r = 1 - 0.726\phi$, where ϕ is in radians.

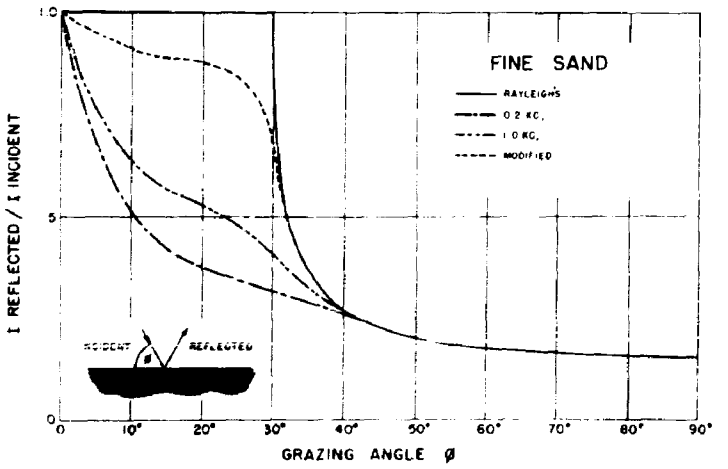

Figure 3 - Ratio of reflected to incident energies vs grazing angle for fine sand for Rayleigh's equation with and without attenuation in the sand estimated to be typical for the Bering Sea. The modified curve is for attenuation extrapolated as the first power of the frequency.

Another equation for reflection from a plane, locally-reacting impedance surface used during the war (14) was

$$r = \left| \frac{\zeta \sin \phi - 1}{\zeta \sin \phi + 1} \right|^2 \tag{7}$$

where, in general, ζ was a complex number given by $\zeta = \xi + i\eta = Z/\rho c$, in which Z is the specific acoustic impedance of the bottom, assumed to be independent of the angle of incidence. This equation had the advantage of predicting losses for small grazing angles. Propagation studies had indicated that such losses existed. Typical curves are shown in Fig. 4 for $|\zeta| < 1$ and $|\zeta| > 1$. When $|\zeta| \to \infty$, we have perfect reflection with no phase reversal for all angles as from an infinite impedance surface. When $|\zeta| \to 0$, the reflection is perfect but with a reversal of phase for all angles. The minimum occurs at $\phi = \sin^{-1} |\zeta|^{-1}$ when $|\zeta| > 1$. The value of r at the minimum is

$$r_m = \frac{\eta^2}{4\xi^2 + \eta^2}$$

and this is zero when $\eta = 0$.

Although the attenuation makes considerable difference in bottom loss curves computed from Eq. (5), the same values used in Eq. (7) yield curves only a little different from one another. The curves computed from Eq. (7) for the same values used to compute Figs. 2 and 3 give bottom losses that drop rapidly with grazing angle to a value near zero and then rise slowly to about the same value at 90°. If the bottom does not behave purely as a locally-reacting surface but supports some shear waves there will be a dependence of Z on the incident angle.

The bottom reflection loss vs grazing angle has been reported by several observers (15-24). The results generally conform to the Rayleigh type curve but sometimes only slightly resemble it (18, 19). The losses for small grazing angles in deep water is discussed in a preceding paper (F. E. Hale). Perhaps, in some cases, the phenomena are more complicated. It was shown (25), for example, that for small grazing angles the loss due to coupling of the shear waves in the sea bed is $K(\rho - 1)\phi$ db/reflection where K is dependent on the nature of the sea bed. Perhaps in some experiments the sound comes by multiple paths in the water. It was shown (26) that the normal loss cannot be obtained by taking the difference between the first and second echo with only spreading and attenuation corrections. This difference is dependent on the ping length and a correction for reverberation must be made to obtain the specular components. One thing seems certain; whatever the mechanisms for a realistic bottom loss, the loss will be roughly proportional to the grazing angle for the small grazing angles effective in long-range, shallow-water transmission.

Other measurements, while not covering a range of angles, are important. Bottom-reflected sound observed in deep water (27) behaves approximately as predicted by Eq. (7) with

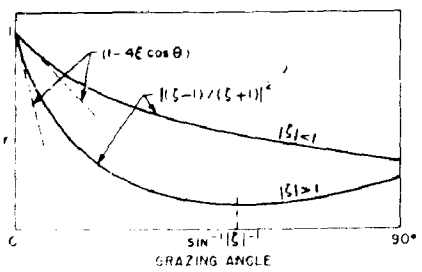

Figure 4 - Ratio of reflected to incident energies vs grazing angle for a simple impedance surface. $\zeta = Z/\rho c$

a value of $\gamma = 0.5$. However, this is not a sensitive test. Curves computed with Eq. (1) do just as well (16). Short-range interference between four bottom-reflected rays, assuming loss independent of angle (28), could be fitted to transmission curves to obtain an "average" loss for small angles. The reflection loss for 24-kc sound near a grazing angle of 9° was measured for a variety of bottoms (29). These values could be used with the assumption that the loss is proportional to the grazing angle to describe the behavior at 24 kc. Some recent fits of curves predicted in Ref. 2 to World War II 200-cps UCDWR data (30) gave γ ranging from 0.60 to 4.18. The curves based on $N = 1.5$ were fitted by eye to the 200-cps data over a range greater than that for which the theory is valid (2). The fits are only fair in the predicted valid region. The same procedure was used for 7.5 kc data and values of γ from 4.5 to 35 were obtained; but, for this frequency the valid range was from 560 yards to 92 kiloyards and even a correction for sea water attenuation of 0.5 db/kyd could not make the data fit over this range. It is to be noted that the value of γ is very sensitive to the fit obtained and for these reasons the reported values of γ are not considered to be significant for 7.5 kc.

There is evidence (31, 32) that the specific acoustic impedance and bottom-reflection loss varies with the season, probably because of biological activity. Strong dispersion in the velocity with frequency was also indicated, with a minimum normal-incidence loss near 200 cps for winter and near 500 cps for the summer. (For further discussion see Ref. 7.) The phase shift at reflection indicated that $p < 1$ below the critical frequency and $p > 1$ above it.

Further study on the nature of bottom reflection is necessary. Perhaps even more complete formulae can be developed. Accurate acoustic measurements at small grazing angles are needed. Other measurements of physical properties are made in soil-mechanics. It is hoped that the acoustic properties can be correlated with other physical properties so that predictions of acoustic behavior may be made with some confidence from more easily measured physical properties.

A stumbling block in comparing the results of several investigators has been the very loose descriptive terminology of the bottom material. Several classification schemes have been used over the years. The one used by a number of investigators was that recommended by the Hydrographic Office (33). Mud is defined as 90% smaller than 0.062mm; Sand-and-mud, as between 10% and 90% smaller than 0.062mm; and sand as less than 10% smaller than 0.062mm, and 90% smaller than 2.0mm. There are two disadvantages to this system. The first is that the word mud is used very loosely by many people and the second is that recent measurements (12, 13) indicate that a more accurate classification is necessary for the finer sediments. It is suggested that the nomenclature be that of the Wentworth scale and the sand-silt-clay ratio be the system recommended by Shepard (34). Here clay is smaller than 0.0039mm; silt, between 0.0039mm and 0.062mm; and sand, between 0.062mm and 2mm. This system is shown in Fig. 5. It is essential to make a complete analysis including the separation of the clay fraction from the silt, as has been done by some observers (35). When the practical analysis is known, the bottom can be described in the suggested system and acoustic measurements can be compared with some confidence. It is suggested that use of the misleading word MUD, which has been used by some to describe everything from a slightly silty sand to clay, be discontinued. The acoustic properties of these materials are very different (12, 13). The adoption of the proposed nomenclature and some statement of the bottom condition, viz: firm, gassy, etc., or preferably the density of an 'undisturbed' sample, will increase the reliability of the comparison of acoustic results.

TRANSMISSION LOSSES

Intermediate Frequencies

The term intermediate frequencies will be used to denote the range from 0.2 kc to about 5 kc. This region has small attenuation due to the sea water. The transducers for the lower frequencies are, in general, nondirectional in the absence of bounding surface. Intermediate frequencies are probably of greatest interest to the Navy in the long-range, active detection of submarines.

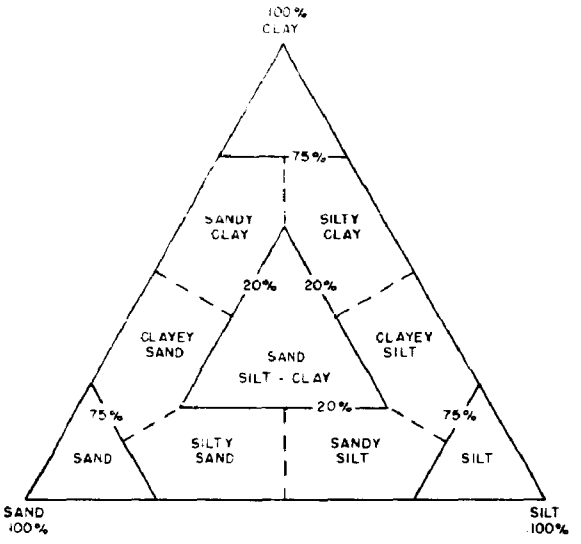

Figure 5 - System for describing sand-silt-clay sediments (32).

The work up to the end of the last war is summarized in the familiar "red" books (27, 36). It was concluded that over level bottoms, with isothermal water or in the presence of downward refraction, the transmission loss can be adequately represented by

$$L = L_o - 15 \log R - 2.5 \times 10^{-4} (f_{kc} - 2) R + C \qquad (8)$$

above 2 kc, there being little correlation of transmission loss with refraction conditions, depth of water, and surface roughness. With strong upward refraction an increase of attenuation with increasing sea state has been observed. Subsequent work has been done to obtain new data and to analyze further the older data. The propagation-loss-vs-range curves for the different investigators are very similar, although different conclusions are reached as to the nature of the propagation. It was shown (1) that the available data did not allow a significant choice to be made between the several theories, even when the "free-field" source level was known. Data obtained with explosive sources are even less amenable to this distinction because the source level, an effective parameter, is more uncertain.

The experimental data exhibit the same general behavior for a given frequency. These will be presented next and afterwards the theories will be discussed as a means of extrapolating the empirical results to greater ranges and/or different water depths.

During the summer of 1949, a joint United States-Canadian scientific expedition was made into the Bering and Chukchi Seas for the purpose of obtaining oceanographic and underwater-sound-transmission data. Measurements were made with a number of frequencies from 0.2 kc to 56 kc over the phenomenally flat 25-fathom water of the Bering and Chukchi Seas. Some of the results from the report (1) on these measurements are shown in Figs. 6, 7, 8, and 9 for the lower frequencies and for different locations. The sound-velocity profiles are shown in the inserts. The anomaly, defined as the departure from simple spherical spreading, is plotted vs the log of the range in kiloyards. Simple spherical spreading yields a horizontal line and cylindrical spreading gives one sloping upwards 3 db per distance doubled.

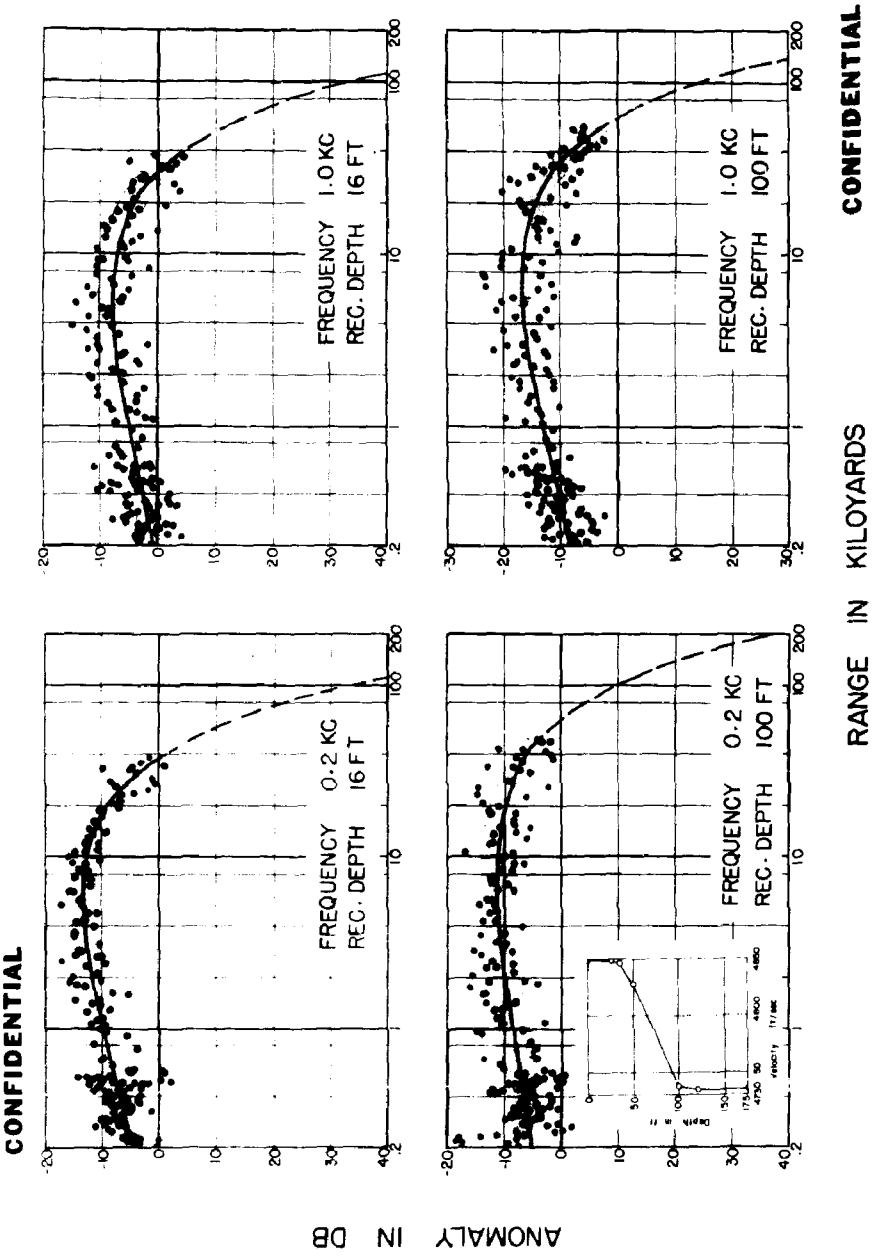

Figure 6 - Anomaly vs range for 0.2- and 1.0-kc sound for Area I of Bering Sea. Inset shows velocity profile existing at time of measurements. Silty-sand bottom, 0.2-kc source at 15-foot depth and 1.0-kc source at 90-foot depth.

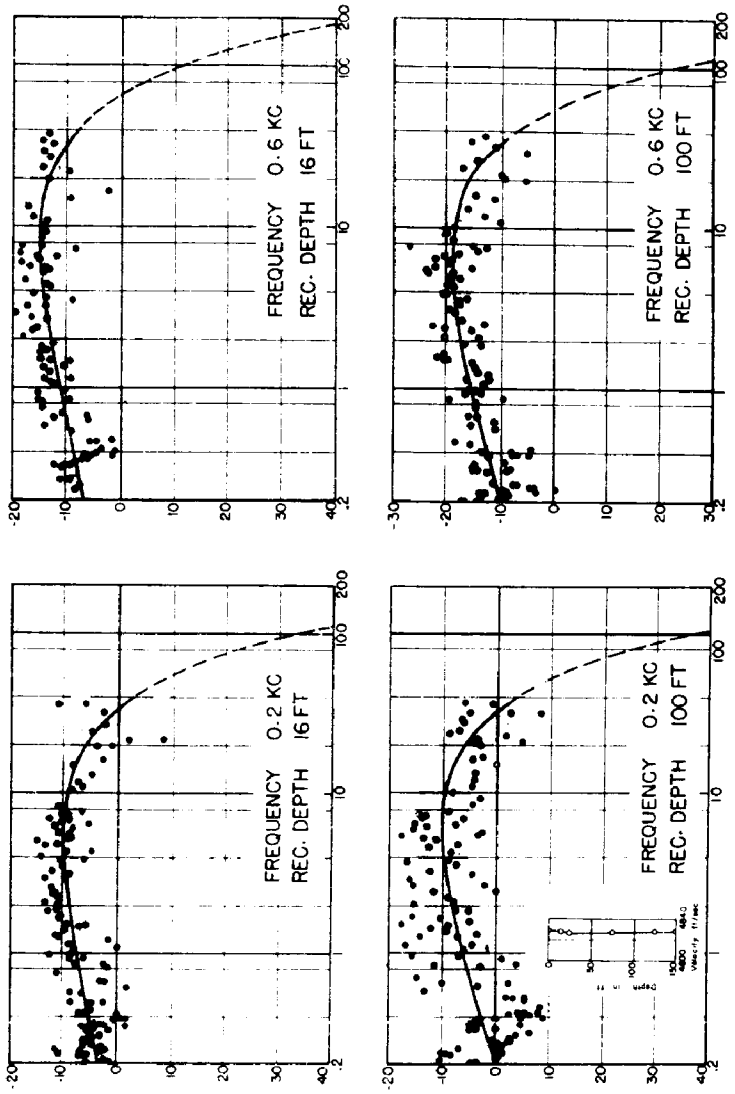

Figure 7 - Anomaly vs range for 0.2- and 0.6-kc sound for Area II of Bering Sea. Inset shows velocity profile existing at time of measurement. Silty-sand bottom. Both sources at 15-foot depth.

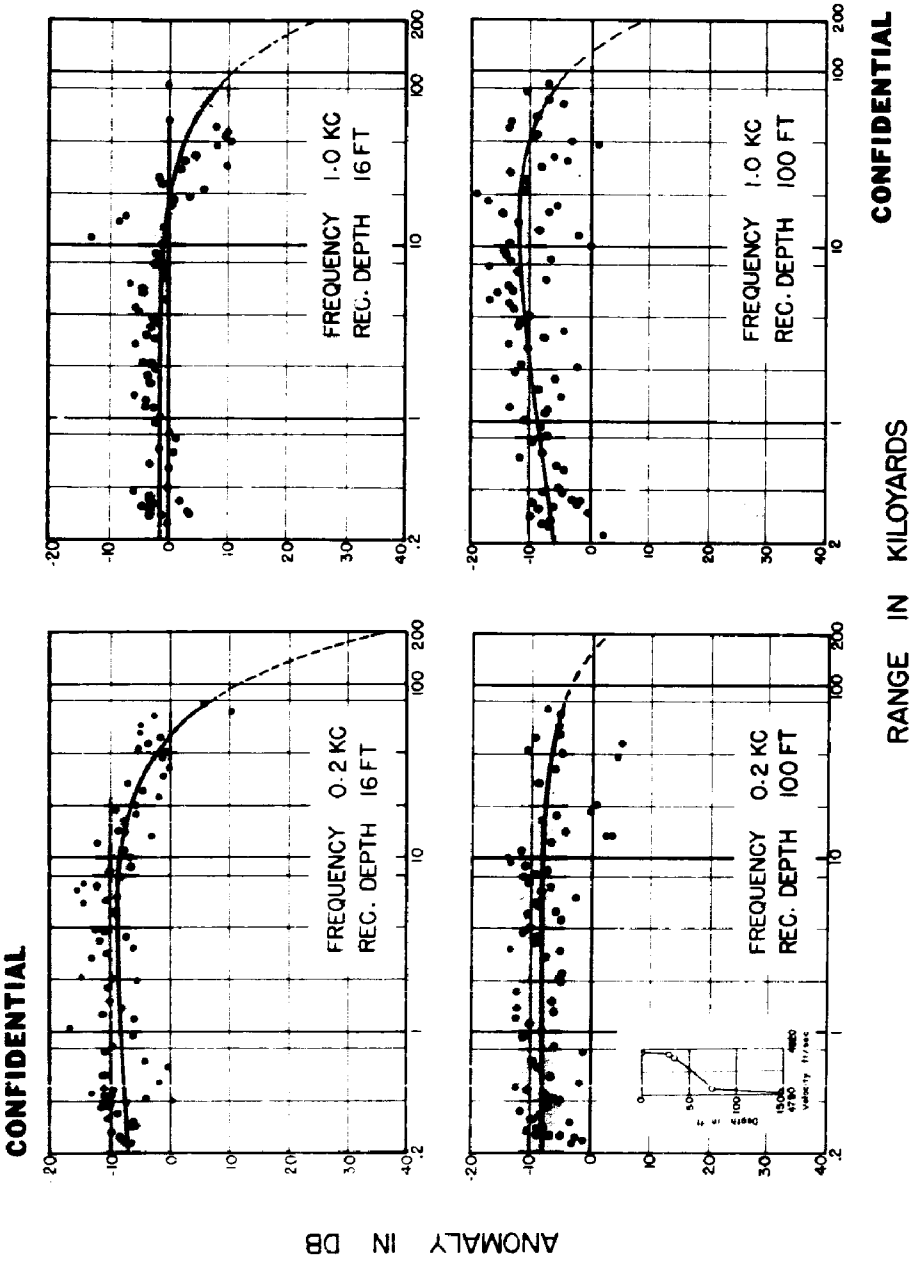

Figure 6 - Anomaly vs range for 0.2- and 1.0-kc sound for Area III of Bering Sea. Inset shows velocity profile existing at time of measurement. Silty-sand bottom, 0.2-kc source at 15-foot depth and 1.0-kc source at 90-foot depth.

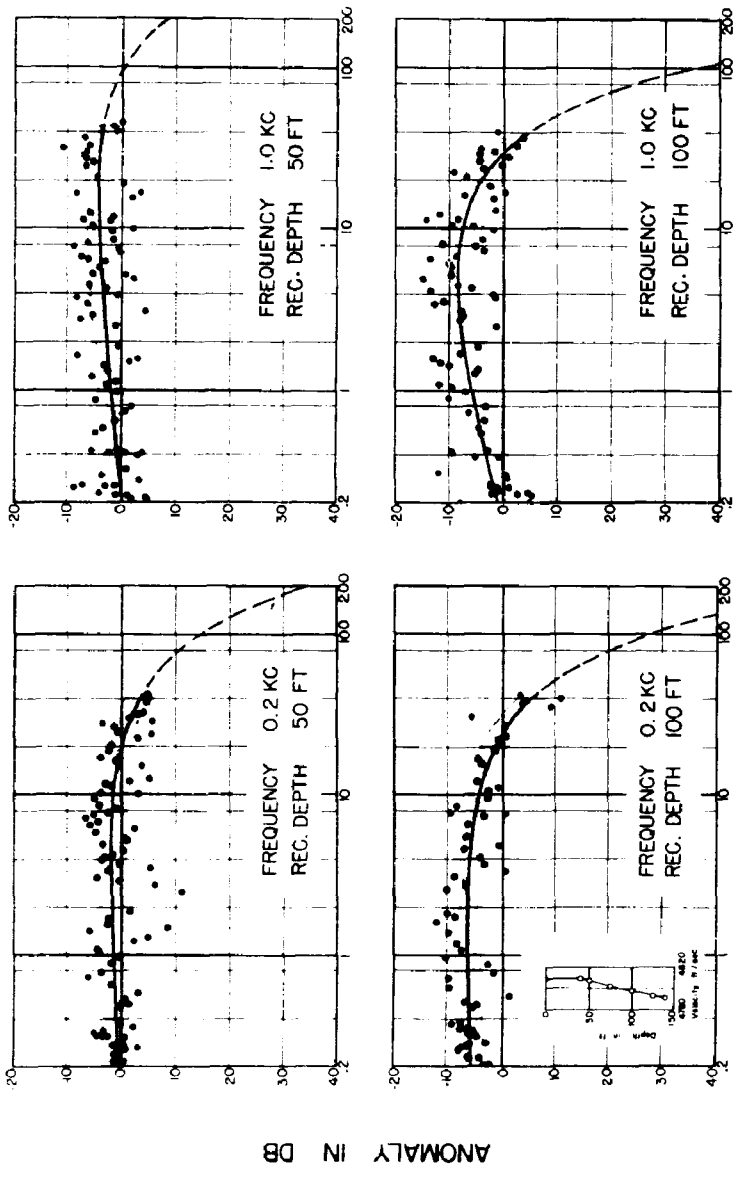

Figure 9 - Anomaly vs range for 0.2- and 1.0-kc sound for Area IV of Chukchi Sea. Inset shows velocity profile existing at time of measurements. Sandy-silt bottom, 0.2-kc source at 15-foot depth and 1.0-kc source at 90-foot depth.

Figures 6, 7, and 8 are for runs over the silty-sand bottom, Fig. 9 is for runs over a sandy-silt bottom. The least square fits are shown. For these fits, the power of spreading, apparent source level, and attenuation were simultaneously solved for. The spreading appears intermediate between spherical ($N = 2$) and cylindrical ($N = 1$). The velocity profile does not appear to have a pronounced effect on the propagation.

The depth of the receiver did not appear to have much influence at these frequencies. Consequently, fits were made combining data for all the receiver depths. The data for all of the areas were then combined to get an average behavior. In Fig. 10a is shown the attenuation calculated when cylindrical spreading ($N = 1$) was assumed and the apparent source level and

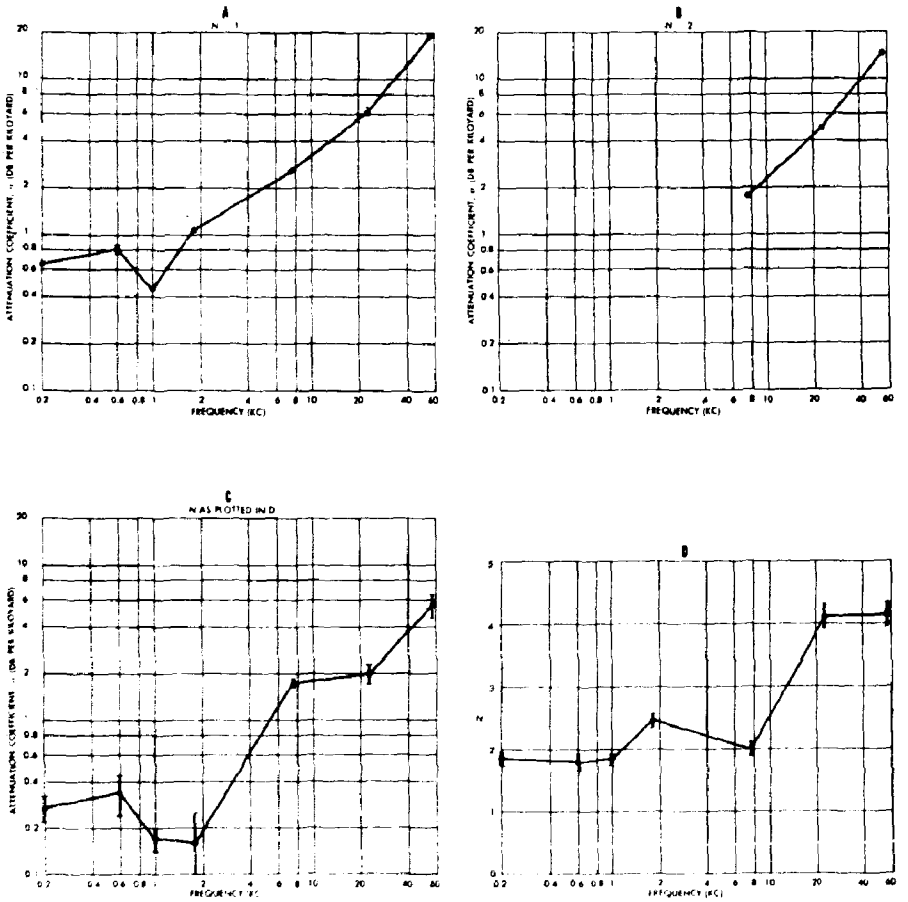

Mean attenuation coefficients for all areas vs frequency for (A) $N = 1$, (B) $N = 2$, and (C) N as plotted in D.

Figure 10 - Average of all Bering and Chukchi Sea areas attenuation coefficients vs frequency for N = 1, 2, and for N as plotted

attenuation were solved for. In 10b is shown the attenuation when spherical spreading (N = 2) was assumed. In Figs. 10c and d are shown the attenuation and the power of energy spreading N when both of these as well as the apparent source level were simultaneously solved for. For the lower frequencies the spreading appears almost spherical and the attenuation essentially constant. Above 1 kc the attenuation appears to vary about as the first power of the frequency up to 56 kc where the attenuation is the same as deep-water values. The received level, L, is calculated from

$$L = L_o + 10\,N \log R + a \times 10^{-3} R \qquad (9)$$

where L_o is the free-field source level at 1 yard, N is the power of energy spreading, R is the range in yards, and a is the attenuation in db/kyd.

The results from a wartime survey (37) are shown in Fig. 11. This is reasonably consistent with Fig. 10. Data (38, 39) recently obtained in the east (Fig. 12) led to the tentative conclusion (3) that the spreading was cylindrical and that the attenuation varied as $f^{1/2}$. However, the smooth curves shown, obtained from Bering and Chukchi Sea data, are for N = 1.9, or practically spherical spreading. The fact that a spherical-spreading curve fits presumably cylindrical-spreading data emphasizes the present difficulty of determining the power of

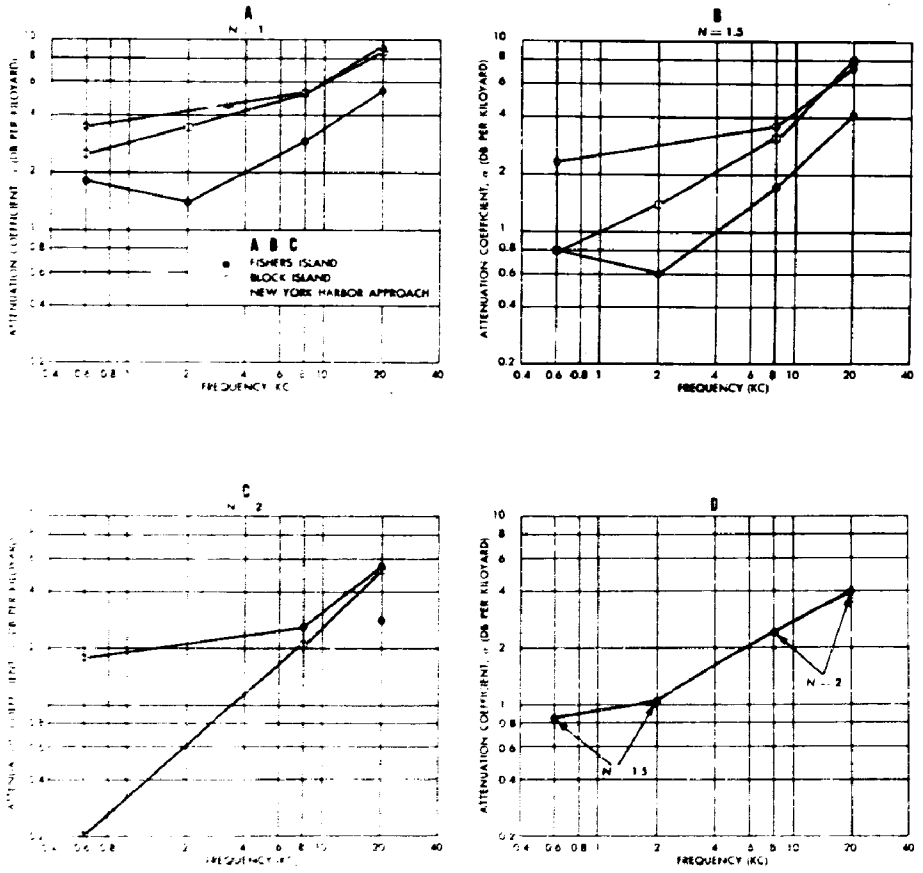

Figure 11 - Long Island Area (Survey 1944) attenuation coefficients vs frequency for N = 1, 1.5, and 2

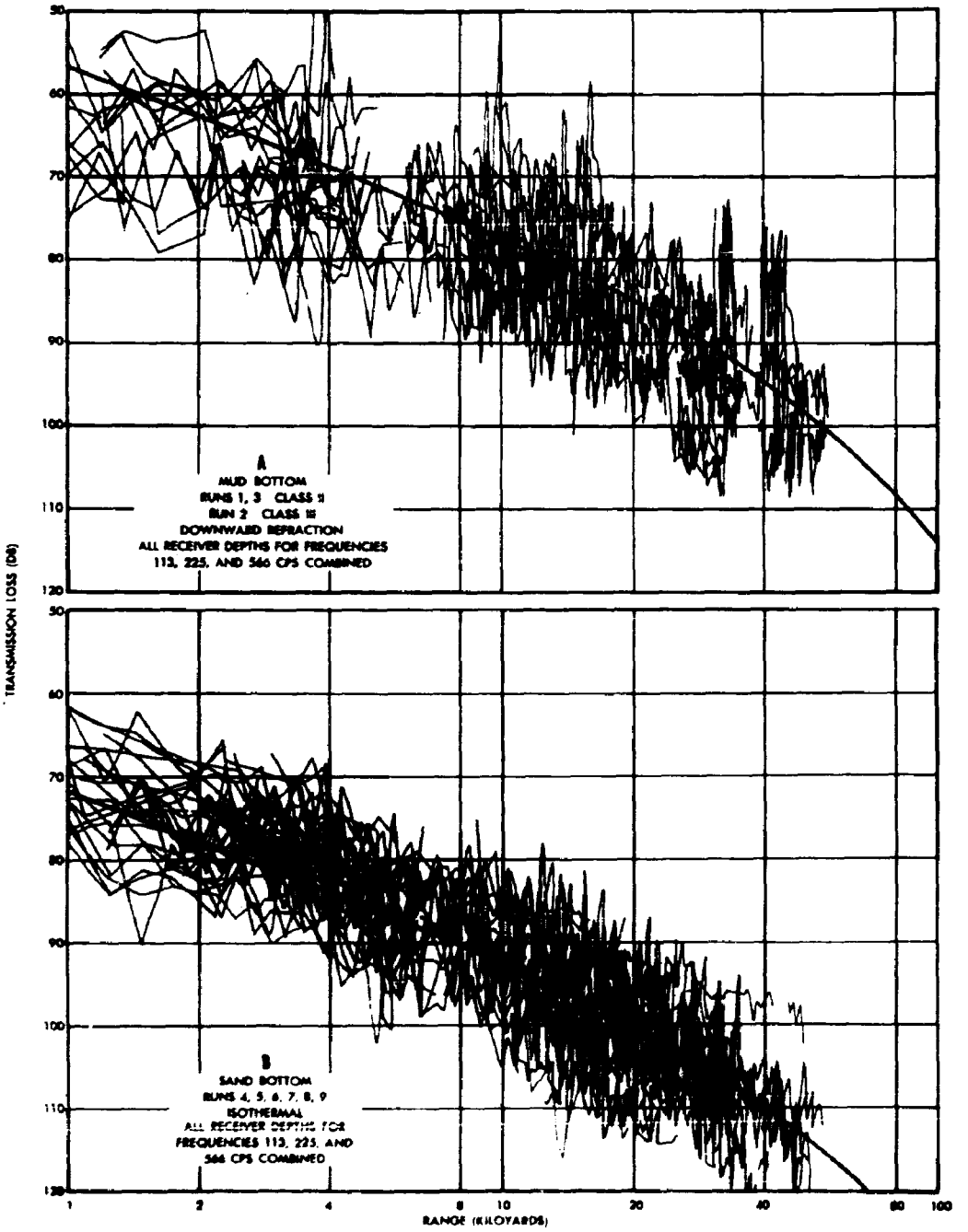

Figure 12 - USNUSL Martha's Vineyard (Survey 1954) for sand and mud with generalized curve for 200 cps from Shallow Bering and Chukchi Seas. The generalized curve has been shifted arbitrarily downwards 5 db for mud and 20 db for sand.

spreading from available experimental data. No reason is apparent why the loss should be less over the sand than over the mud but the spreading appears to be the same for practical purposes.

A body of unpublished UCDWR data has been analyzed in a similar manner to data of Ref. 1 because there were three types of bottom: rock, sand, and mud. Most of these data was taken in water 40 to 50 fathoms deep. Some runs were made over sand and rock where the depth was only 15 fathoms. The same general behavior was obtained. The mud appears to have about the same attenuation as the sand but its transmission curve lies about 4 db below that for sand. The attenuation is greater for the rock but the transmission curve agrees with that for sand in the range 100 to 300 yards. The attenuations are greater in 15-fathom water.

It was concluded from some low-frequency UCDWR data published (40) that, for the example given, the initial parts of the bottom-reflection transmission curve represent coherent interference of bottom-reflected sound. The spreading for 200-cps sound in 50-fathom water appears to be spherical except that the anomaly is -6 to -8 db (greater level than simple spherical spreading). It was also pointed out that cylindrical spreading with an attenuation of 1 db/kyd also fits moderately well out to 30 kiloyards.

In the previous paper by A. O. Williams on low-frequency propagation, Eqs. (5) and (7) gave the losses for scattering proportional to the wavelength, for conversion to shear proportional to the wavelength squared, and for longitudinal bottom absorption (for a single mode) proportional to the third power of the wavelength. All of these predict losses inversely proportional to some power of the frequency. The loss due to sea-water is proportional to the frequency squared. The behavior of the attenuation vs frequency (Fig. 10) is not unreasonable. The previous paper by A. O. Williams also quoted some unpublished British work which expressed the attenuation as the sum of $l\lambda + m/\lambda$ with a minimum about 150 or 200 cps. These results agree very well with the curves on Fig. 10, which indicates that the attenuation is essentially constant from 200 to 1000 cps. This supporting evidence is important, because if the attenuation has essentially a constant minimum value from 150 to 1000 cps nothing could be gained on transmission loss by using 200 cps instead of 1000 cps for active echo ranging. (SECRET)

Some recent data (41) obtained with explosive charges as acoustic sources indicated a systematic decrease in transmission loss between 50 and 400 cps. This decrease also tends to verify a minimum. The bottom was very irregular. Considerable variation with bearing was observed and the losses were greater than the standard 100-cps Nantucket reference curve which is for 33-fathom water south of Nantucket. This standard reference curve has approximately cylindrical spreading with an attenuation of 1 db/mile. Because the Halifax transmission was uniformly poorer for all bearings, some caution should be used in generalizing transmission behavior. (SECRET)

Theory

A theoretical discussion is given to form the basis for extrapolating the empirical curves. This will emphasize the ray theory approach. The normal-mode methods are discussed in a preceding paper (A. O. Williams). One of the earliest papers (2) predicted that the power of spreading should be

$$L = L_0 + 5 \log \left(\frac{\pi}{2} D\right) - 15 \log R \qquad (10)$$

for the high-frequency zone defined as the zone for which $10\ D < R \leq (2\pi D^2/\lambda)$ and $z \geq (R/D)^{1/2}\lambda$ where

D = depth of water
z = receiver depth
$\cdot$ = real part of $Z/\rho c$.

When $R \geq (2\pi D^2/\lambda)$, a transition zone is entered where the sound field is very complicated and no rapidly converging series is available. This treatment predicts that for the lower frequencies, the power of spreading would change with range from $N = 1.5$ to $N = 1.0$ as the range increased. The observed spreading may be closer to spherical, $N = 2$.

A recent theory (3) satisfactorily explains the results obtained on the east coast (38, 39). When the water is isothermal (mild upward refraction) good agreement was obtained between the data and curves calculated from the AMOS formulas (18) for surface channels in deep water. This indicates that for upward refraction, the energy that is scattered by the bottom has no significant effect. The range, the projector depth, and the receiver depth are scaled to the depth of the isothermal layer and the propagation is described for three zones. The first is a direct radiation zone with simple spherical spreading; an absorption term; and a depth-loss term which depends on frequency, source depth, and receiver depth. In the second zone sound has been reflected at least once from the surface and propagation loss includes an additional depth-loss factor. The third zone where energy has been reflected two or more times from the surface follows a cylindrical spreading law and the attenuation is due to surface scattering loss, α_s. This surface scattering loss for frequencies from 113 cps to 7100 cps is the same as obtained for deep water.

$$\alpha_s = 4.5 \sqrt{\frac{f_{kc}}{d}} \text{ db/kyd}$$

where d is the depth in feet.

For downward refraction the predominant field involved the bottom reflection alone. By analogy, the calculations were made by measuring from the ocean's floor instead of its surface. When the velocity gradient is not equal in magnitude to that found in an isothermal layer, the rays, source depth and receiver depths are scaled to twice the distances, R_m, covered in one loop by the limiting ray. The loss in the third zone where sound has been reflected twice from the bottom, the spreading is cylindrical with a bottom-reflection loss, α_B, of

$$\alpha_B = \frac{6.2 \sqrt{f_{kc}}}{2 R_m} \text{ db/kyd.}$$

The constant of 6.2 was obtained for mud bottoms.

When a 35-foot isothermal layer overlayed a downward refraction condition and $f > 500$ cps, the propagation loss was observed to be greater for the deeper hydrophone. At lower frequencies where the wavelength was of the order of the channel depth, the channel was not effective and the bottom-reflected field was predominant for both hydrophone depths. For the higher frequencies, good fits were obtained by assuming leakage from the isothermal layer. For the lower frequencies good fits for data over mud were obtained with assumed cylindrical spreading and an attenuation of

$$\alpha = \frac{10.7 \sqrt{f_{kc}}}{2 R_m}.$$

The constant 10.7 is 4.5 plus 6.2. This simple theory predicts better transmission at 113 cps than at 1 kc. However, other mechanisms (not considered) can increase the effective attenuation at the lower frequencies. For great ranges, it is the attenuation that is important in determining the loss. The difference between cylindrical or spherical spreading is only 3 db per distance doubled - that is between 40 and 80 miles.

The multimoded case becomes easier to handle by ray theory. The assumption that the phases of the arrivals are random for the higher frequencies and the longer ranges is more appealing than the assumption that the conditions could be idealized enough to be able to specify the many phases.

This approach (4, 5) has the added advantage that arbitrary velocity profiles and realistic bottom losses can be considered. It is assumed that the average transmission curves can be calculated by adding the effects of the usual string of double images powerwise (random phase) and that the values are the same for any receiver depth. Calculations made with this concept or with a flux concept from a single doublet yield the same results for the isovelocity case. The flux concept enables calculations for any arbitrary gradient to be easily made.

The sources for the intermediate frequencies are assumed to be omnidirectional in a free field. Because of the surface image, the effective vertical directivity patterns are computed from

$$db = 6 + 20 \log_{10} \left| \sin \left(\frac{2\pi fd}{c} \sin \theta \right) \right| \tag{11}$$

where f is the frequency in cps,
d is the source depth in feet,
c is the sound velocity in feet per second, and
θ is the vertical angle with the surface.

For a source near a rigid boundary the expression would be

$$db = 6 + 20 \log_{10} \left| \cos \left(\frac{2\pi fd'}{c} \sin \theta \right) \right| \tag{11a}$$

where d' is the distance of the source from the boundary. This is a good approximation to use for the smaller grazing angles used in long-range propagation when the source is near the bottom.

Some resulting patterns for a near-surface source are shown in Fig. 13 for the parameter fd. If the source is near the bottom the nulls on Fig. 13 become maxima and the maxima become nulls. For the near-bottom source then there is a stable maximum for the smaller grazing angles and in general doublet directivity is of much smaller importance than for a

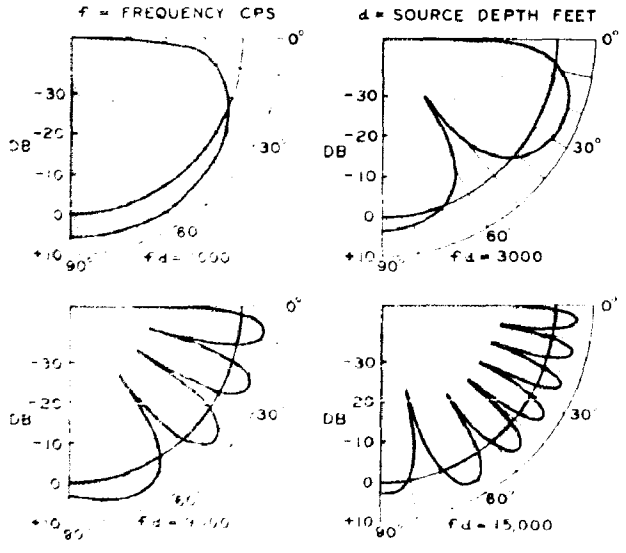

Figure 13. Effective directivity of doublet formed by near-surface source and its surface image

near-surfac source. Surface waves or broadband due to short pulse length or explosives may alter these patterns by smoothing out the maxima and minima for the larger angles. One important characteristic is the stable null for $\theta = 0$ for all values of fd. Since long-range transmission involves only small angles, the directivity must be considered. It should be noted that the near-surface source vertical patterns shown are effective only once, when the sound first impinges on the bottom. After this the sound goes merrily on its way with its many bounces.

The intensity for any given order of bottom bounce is proportional to the ratio of incident and reflected intensities raised to that order. The ratios used were taken from Figs. 2 and 3, which give realistic bottom losses. (The approximation of $R = a\phi$ would be good only for the greater angles.) The product of the directivity and these ratios raised to large powers converges, although the integral using Eqs. (5) and (11) expression appears unmanageable. This type of calculation with a converging series can be handled quite well on IBM machines.

Some computed transmission curves for near-surface sources are shown in the following figures. These curves are based on Figs. 2 and 3 (computed from Eq. (5)), which are estimates for the bottom of the Bering and Chukchi Seas. These estimates were made from the recorded bottom types and measurements (12) on similar types near San Diego. The attenuation due to the water was not used because it is small at the lower frequencies. It can be added in later if desired. Figure 14 shows the result for isovelocity conditions. This fd corresponds to a 0.2-kc source at 15 feet. The upper curves, for a simple Rayleigh relationship, have a cylindrical spreading. The vertical difference between the sand and silt curves is due to the different critical angles. The middle curve, for sand-modified, resembles the actual experimental data. The lower curves appear to have greater than spherical spreading. Figure 15 shows similar isovelocity calculations for fd = 15,000. The comparison of Figs. 14 and 15 gives the effect of the doublet directivities shown in Fig. 13.

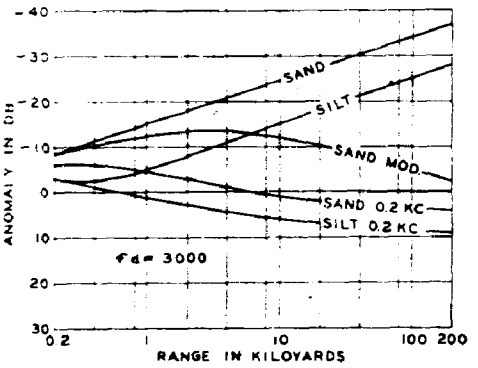

Figure 14 - Computed anomaly vs range for fd = 3000 for reflection loss curves of figures 2 and 3 and directivity of figure 13

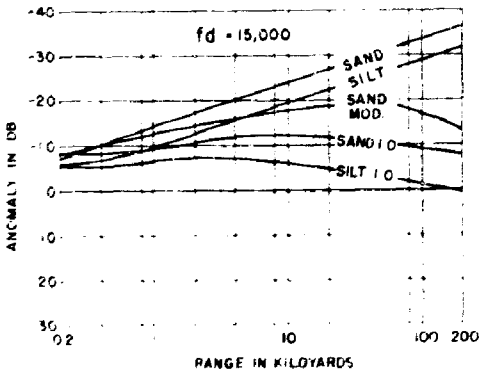

Figure 15 - Computed anomaly vs range for fd = 15,000 for reflection loss curves of figures 2 and 3 and directivity of figure 13

These figures also point out that besides the dependence on the effective doublet directivity there is a profound effect caused by the assumed bottom-reflection losses at small grazing angles. If these curves were to be approximated by a power of spreading it might be concluded from the lower curves of Fig. 14 that $N > 2$. It seems futile to speak of the power of spreading as 1, 4/3, 3/2, 5/6, 2 etc., to best describe the behavior until more information is available.

Calculations made for the slightly negative velocity profile shown in the insert of Fig. 8 are shown in Fig. 16. It is quite apparent that the lower curve will not fit the observed data but that the curve computed for sand-modified agrees somewhat. The better fit of the curve computed using sand-modified leads to the conclusion that the attenuation varied as the first power of the frequency. (This could be important, if true, in choosing an optimum frequency for the detection of buried mines.)

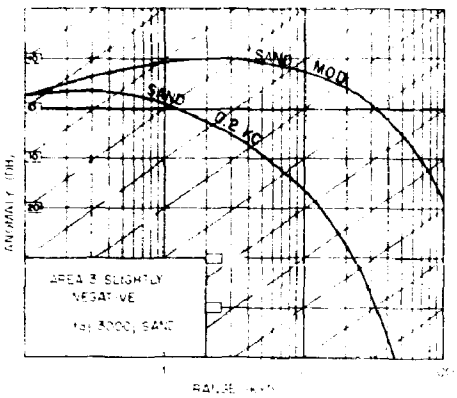

Figure 16 - Computed anomaly vs range for fd = 3000 and velocity profile shown in figure 8, directivity shown in figure 13, and sand (figure 3) with attenuation extrapolated as $f^{1/2}$ and as f.

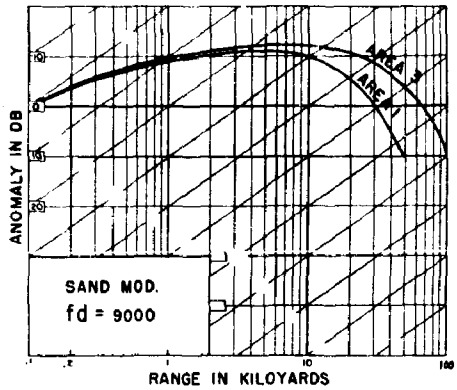

Figure 17 - Computed anomaly vs range for fd = 9000 for sand-modified, figure 3, directivity, figure 13, and velocity profiles shown in figures 6 and 8

Calculations were also made using sand-modified for the profile shown in Fig. 6, which is quite negative. The curves for both velocity profiles for fd = 9000 are shown in Fig. 17. The agreement with experimental data is reasonable, considering our lack of precise velocity knowledge of the bottoms. The dependence of computed transmission loss on the properties of the bottom certainly indicates more work on the acoustic properties of bottoms is necessary.

A similar approach was made by M. J. Daintith and C. A. Teer (4) using the simple assumption that the loss per reflection equalled $a\phi$ and neglecting any doublet directivity. A spreading with N = 1.5 was predicted for a flat bottom at long ranges. The equation developed for a flat bottom, isovelocity water, and ranges over a 1000 yards where $\sqrt{R/(\alpha_1 D)} >> 1$ is

$$L = L_o + 2.2 - 15 \log R - 5 \log \alpha_1 D - \alpha R$$

where R and D are in yards and the bottom loss constant α_1 is

$$\alpha_1 = \frac{\log r}{\phi} = \frac{a}{10}$$

where r is the ratio of reflected to incident intensity and ϕ is the grazing angle in radians. (SECRET)

Also, the theory was extended for upslope and downslope transmission. The formula for transmission upslope is

$$L = L_o + 2.2 - 15 \log R - 5 \log \alpha_1 (D_R + 0.5\ \beta R) - \alpha R$$

where D_R is the depth at the receiver and β is the bottom slope in radians. (SECRET)

The formula for transmission downslope is the same except that β has a negative value. (SECRET)

The theory was also extended to cover the case of negative and positive velocity gradients. The gain over free-field propagation (negative anomaly) for transmission in a positive gradient is

$$3 + 10 \log \left[1 + 0.826 \left(\frac{R}{\alpha_1 (D_R + 0.5\ \beta R)} \right)^{\frac{1}{2}} + \frac{R}{(D_R + \beta R)} \tan \delta \right]$$

where δ is the angle at the source for the bottom limited ray. (SECRET)

The gain over free-field propagation for transmission in a negative gradient when the amount by which the ray is bent between the surface and depth h of the source or receiver is greater than $\tan^{-1} 2h/R$ is

$$3 + 10 \log \left[0.826 \left(\frac{R}{\alpha_1 (D_R + 0.5\ \beta R)} \right)^{\frac{1}{2}} \right] + 10 \log F \left[3.04\ n' \left(\frac{\alpha_1 D_R + 0.5\ \beta R}{R} \right)^{\frac{1}{2}} \right]$$

where

$$n' = \frac{R}{2D_s} \tan \gamma$$

D_s = bottom depth at the source

γ = grazing angle for a ray leaving the source horizontally

and F is the error integral defined by

$$F(z) = \sqrt{\frac{2}{\pi}} \int_z^\infty e^{-t^2/2}\, dt. \qquad \text{(SECRET)}$$

Their computations are compared with experimental data by assuming that theoretical and experimental levels agree at some minimum range, the smallest of which was one-half-mile or 1000 yards. They found good agreement (as might be expected (1) but concluded that the gain over spherical spreading (negative anomaly) was too small at shorter ranges and too great at the large ranges. This would argue for a power of spreading greater than 1.5. (SECRET)

These theories based on rays appear to give good agreement with the data. Figures 14, 15, and 17, which are based on Figs. 2, 3, and 13, give a fair agreement with the experimental data. It is to be noted that there were no arbitrary constants but all are calculated from the best estimates of the physical properties of the bottom and the doublet directivity of the source.

The dependence on velocity profiles for the computed curves may seem at variance with the conclusion from experimental data that no significant dependence was observed. However, the dependence indicated in Fig. 16 is not large over the range of most data. Ray computations for small grazing angles are sensitive to the velocity profile. However, the doublet directivity for near-surface sources minimizes the contribution of energy arriving at small grazing angles and thus depreciates the effect of refraction. This effect, of course, dependent on the parameter fd. There is always the uncertainty of generalizing the many slightly different velocity profiles, and bottom properties over a long transmission path when computing values to compare with experimental data. Another uncertainty that warrants further attention is the accuracy of determining velocity profiles for shallow water from only temperature, salinity, and depth information. Shallow waters are often too turbid to permit taking bottom photographs, and bubbles are certainly whipped into the water at higher sea states. Sound-velocity meters have been developed to operate at frequencies from 30 kc upwards. It is quite possible that the velocity is frequency dependent and neither the present velocity meters nor computations based on salinity, temperature, and depth give the correct velocity at sonic frequencies. This could be important in long-range shallow-water computations. The assumption was made that the sound pulse was long enough for all of the energy to add up. This is usually so for most

long-range work. Of course at short ranges, sound that is direct or surface reflected will arrive before the bottom-reflected rays. This direct sound will exhibit the usual Lloyd Mirror Interference pattern (42). The bottom-reflected sound may exhibit interference phenomena (28) or may add powerwise (21). In either case the anomaly decreases (sound level rises) out to a range of $R = 10D$ and then levels off. Generally the contribution of the direct and the surface-reflected sound is quite small for $R > 10D$ because the range is usually some distance beyond the range of the last surface interference maximum.

Although the agreement is satisfactory, more information is desired. Transmission runs should be made at the same location with different velocity profiles. Some of these have been obtained by USNUSL on Cruise I-5 but the results of the analysis are not available at present. The data shown in Figs. 6, 7, 8, and 9 were from runs made in a short period of time and the effects of velocity profile and the bottom, both of which were different at different locations, could not be separated.

The calculations of anomaly can all be expressed in terms of the ratio R/D instead of R (horizontal scale on anomaly plots). Because of the reasonable agreement of theory and experiment, extrapolation of the extensive experimental propagation anomalies with the parameter R/D appears to be a logical method of estimation at the present time.

High Frequencies

The propagation characteristics for high frequencies where the sources are directional and the attenuation in the sea water limits the range have been more amenable to analysis.

The simple concept (43) that has worked reasonably well is illustrated in Fig. 18. The sound beam is a relatively narrow cone that suffers successive bottom reflections. If the range between successive bottom reflection is R_m kiloyards then the beam undergoes R_m^{-1} reflections/kyd. The beam thus loses energy at the rate of BR_m^{-1} db/kyd. B includes both specular and non-specular parts. The scattering and absorption in the water cause a minimal loss of α_o db/kyd. The attenuation coefficient is then

$$\alpha = \alpha_o + BR_m^{-1} \text{ db/kyd.} \tag{12}$$

The spreading is simple spherical spreading.

For a uniform temperature gradient, g, the value of R_m^{-1} is approximately

$$R_m^{-1} = \left(10^3 \frac{g}{D}\right)^{\frac{1}{2}} \text{ kyd}^{-1}. \tag{13}$$

A value of $\alpha_o = 3$ db/kyd was used for the 22.5 and 24 kc data.

The data for 22.5 kc (43) as well as the data for 24 kc (44) were plotted on the same graph in Fig. 19. They group about the curve

$$\alpha = 3 + 4\, R_m^{-1} \text{ db/kyd}$$

reasonably well. It is to be noted that the assumption is made that the bottom loss is independent of angle. The grazing angle certainly varies with R_m. Perhaps reworking the data further, with the assumption that the loss varies as the first power of the grazing angle, would group the data closer and also yield a value for bottom loss that would be of theoretical interest.

The values for the sand-mud bottoms gave $\alpha = 3 + 16\, R_m^{-1}$ db/kyd as the best fit.

The value for rock bottoms was $\alpha = 3 + 11\, R_m^{-1}$ db/kyd.

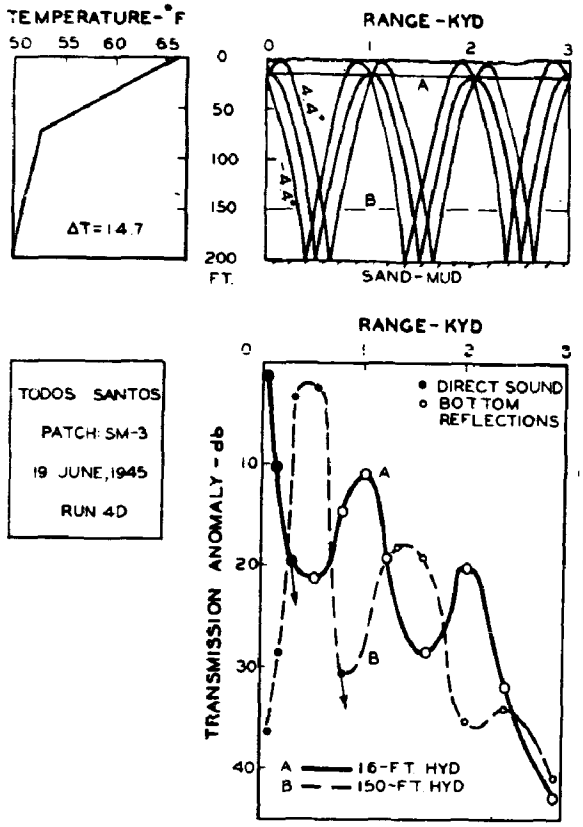

Figure 18 - Transmission with directional beam over sand-mud with strong downward refraction

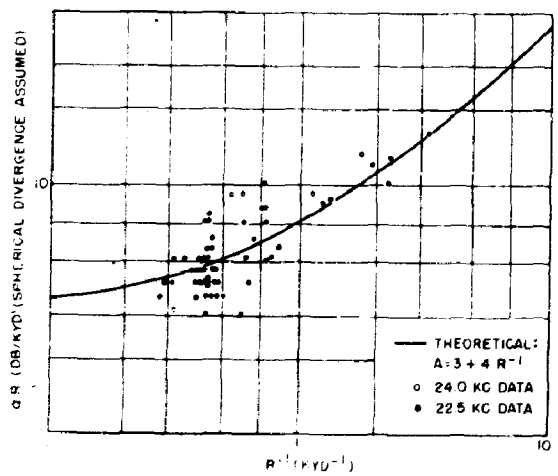

Figure 19 - Anomaly vs R_m^{-1} for 22.5 and 24-kc sound over sand bottoms

These are empirical values for 24 kc and are based on assumed spherical spreading.

Figure 20 shows some 22.5-kc data (1) obtained in 25-fathom water with the profiles shown in Fig. 21. This illustrates the effect of a very strong layering. The reception on the hydrophone at a depth of 16 feet was definitely better than the reception at 100 feet. For small gradients there does not appear to be a significant dependence on receiver depth.

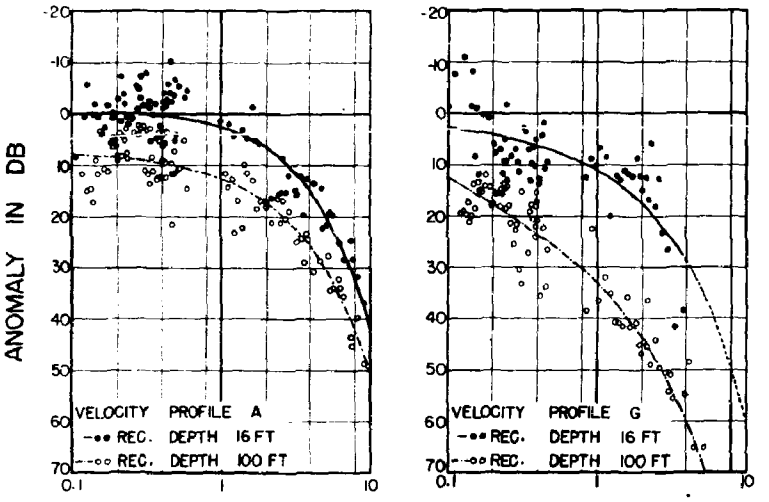

Figure 20 - Anomaly vs range for 22.5-kc sound in and near a brashy ice pack with source depth of 15 feet

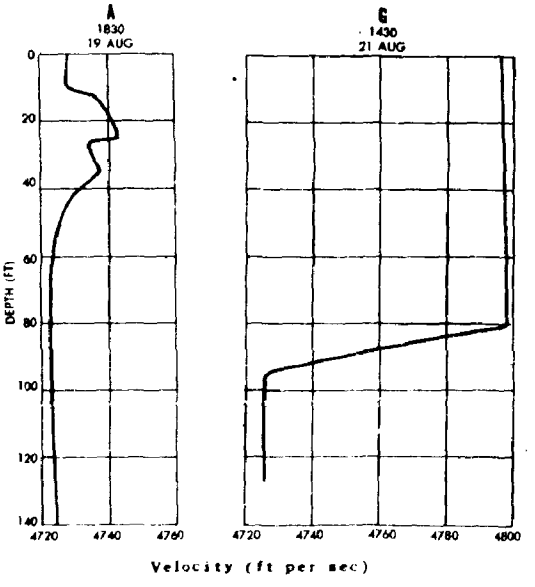

Figure 21 - Velocity profile A in a brashy ice pack and profile G just outside the pack

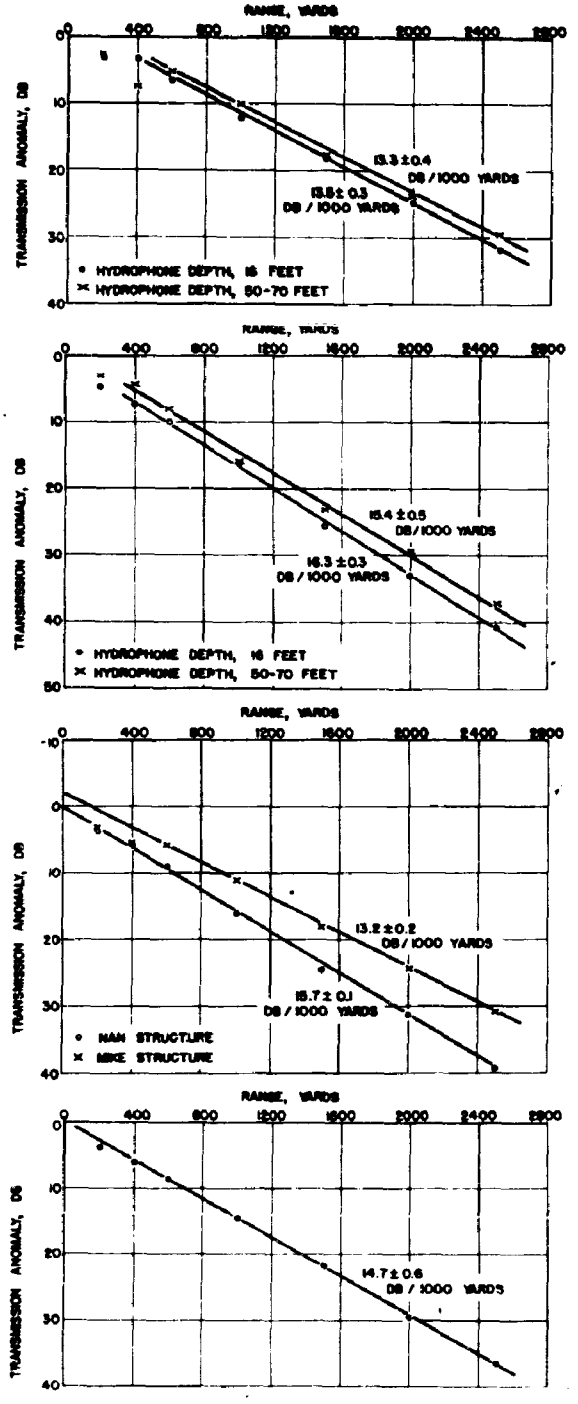

Figure 22 - Average transmission anomaly vs range for 56-kc sound over sand bottom

The work at 56 kc is summarized (45) for sand bottoms in Fig. 22. The straight lines fit the averaged data very well and since this is a linear plot of the anomaly vs range, the straight line indicates that the spreading is spherical. The attenuation values for two types of thermal conditions are given as well as the grand average of 14.7 ±0.6 db/kyd.

Summary

Master fits were made to the data from the Bering and Chukchi Seas with receiver depths and areas combined. These are presented in Fig. 23, where the transmission loss is plotted on an inclined axis. The vertical ordinate is the usual anomaly. No effort was made to adjust the curves vertically. They are as they were calculated in reference to the best obtainable "free-field" source level at 1 yard. Perhaps the differences at the lower frequencies are real and have a physical explanation but, in any event, the generalized curves represent the data fairly well. In addition, they fit data off San Diego reasonably well and also data obtained in the east, except for a shift in apparent source levels. The 1.0-kc source was at 90 feet and the others were at a depth of 15 feet. The bottoms, sandy-silt and silty-sand, were quite flat at a depth of 25 fathoms. Observed losses may be more or less than those shown, as can be seen from Figs. 6, 7, 8, and 9. For the lower frequencies the attenuation may be neglected and the anomalies generalized for other depths by using a parameter R/D. For example, for 50 fathoms the value of transmission loss for 20 kiloyards would be read, from Fig. 23, at 10 kiloyards.

It must be realized that the bottom material and the velocity profile can affect the results; the transmission loss can be greater over some bottoms and also be greater in the presence of greater downward refraction as indicated in Figs. 16 and 17. A large effect (46) was observed by the British for propagation above 200 cps. (SECRET)

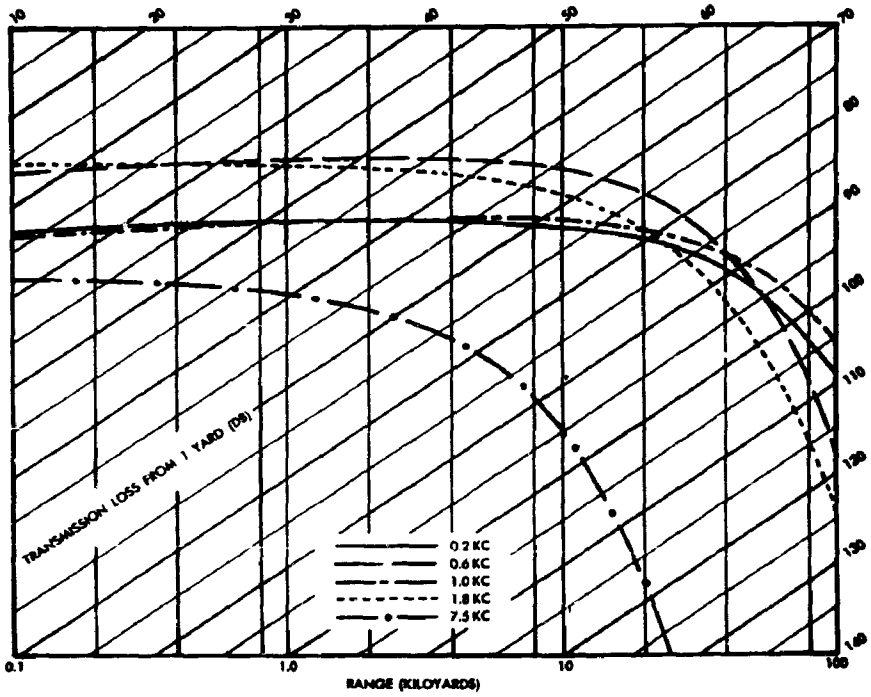

Figure 23 - Summary plot for several frequencies of sound transmission loss vs range over the shallow Bering and Chukchi Seas

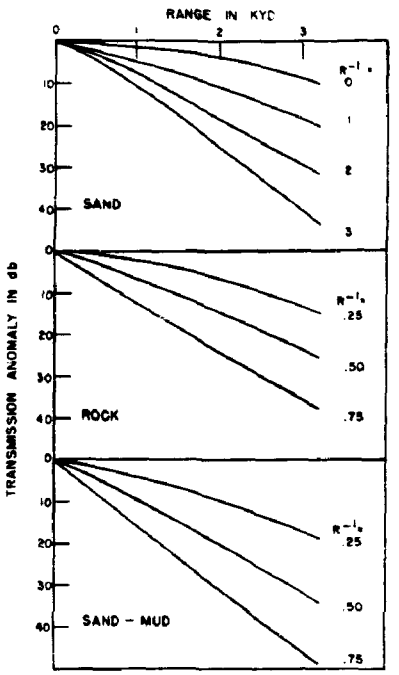

Figure 24 - Average transmission anomaly, αR, vs range curves for 24-kc sound over sand, rock, and sand-mud bottoms

The curve for 7.5 kc shows the effect of seawater attenuation. If this curve is to be extrapolated a correction should be made for this attenuation. The value extrapolated should be corrected by subtracting 0.45 times the range in kyd on Fig. 23 and adding 0.45 times the range in kyd desired. For example, for 20 kyd and 50 fathoms, read the value from Fig. 23 at 10 kyd and add 0.45 (20-10) = 4.5 db to obtain the transmission loss.

The transmission losses near 24 kc can be computed by assuming spherical spreading plus the additional loss shown in Fig. 24. These are from Ref. 44. To use these anomalies, which are the departure from simple spherical spreading, calculate R_m^{-1} from the velocity profile and read the anomaly αR from Fig. 22 at the range desired, then the level L is

$$L = L_o - 20 \log R - \alpha R \qquad (14)$$

where L_o is the free-field source level at 1 yard.

The values near 56 kc can be computed by assuming spherical spreading and an attenuation of 15 db/kyd,

$$L = L_o - 20 \log R - 0.015 R. \qquad (15)$$

The departures (residuals) from the regression lines are almost normally distributed (1) and give a practical measure of the fluctuation. The standard errors for CW sound are about 3 db for the intermediate frequencies and 5 db for frequencies above 5 kc. Examples of low-frequency-data scatter are shown in Figs. 6, 7, 8, and 9. The shaded part indicates plus and minus one standard error. Some recent data (46) indicate that 245-cps-CW-sound fluctuation decreases with range. An example of 7.5 kc with a standard error of 5 db is shown in Fig. 25. This figure illustrates the scatter to be expected from several runs under seemingly identical conditions. (SECRET)

REFERENCES

1. K. V. Mackenzie, "Long-Range Sound Transmission in the Shallow Bering and Chukchi Seas," NEL Report 640 (Confidential), November 1955.

2. G. D. Camp and C. Eckart, "Some Theoretical Studies of the Propagation of Sound in Shallow Water," UCDWR U 102, August 1943.

3. T. P. Condron and P. A. Barakos, "Analysis of Shallow-Water Sound Propagation in Frequencies from 0.1 to 8 kc," USL Report 254 (Confidential), December 1954.

4. M. J. Daintith and C. A. Teer, "An Application of Ray Theory to Sound Propagation in Coastal Water," UDE Report 152 (Secret), May 1955.

5. K. V. Mackenzie, "Long-Range Sound Transmission in Shallow Water," 12th USN Symposium, Paper in preparation (Confidential), November 1955.

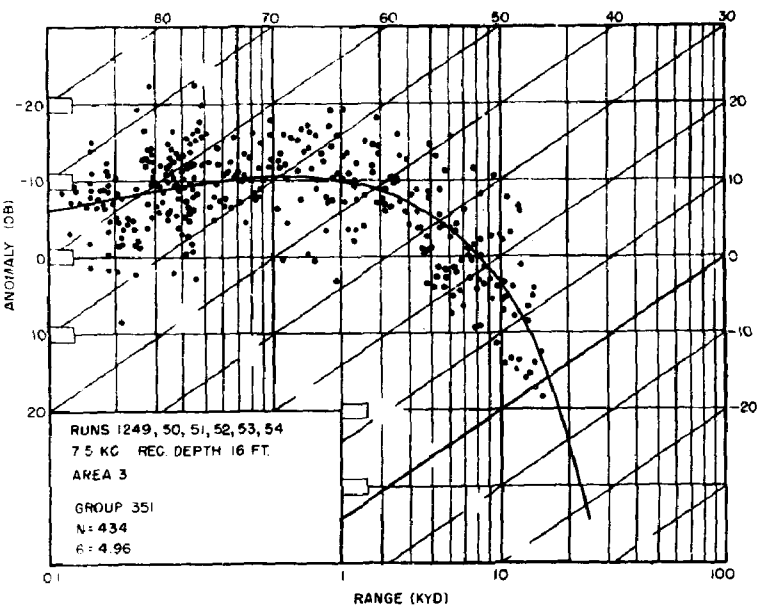

Figure 25 - Sound level and anomaly vs range for several runs under same conditions for 7.5 kc. (SECRET)

6. J. W. S. Rayleigh, "The Theory of Sound," 2d Ed., Dover, 1945.

7. "The Cooperative Research Program of Navy Electronics Laboratory and the National Research Council on Bottom Sea-Mine Countermeasures," NEL Report 272, Chap. VII (Secret), June, July and August 1951.

8. E. T. Kornhauser and W. P. Raney, "Attenuation in Shallow-Water Propagation Due to an Absorbing Bottom," J. Acoust. Soc. Amer. 27:689-692, 1955.

9. R. W. Morse, "Acoustic Propagation in Granular Media," J. Acoust. Soc. Amer., 24:696-700, 1952.

10. "Phase III First Interim Report of Contract N123s-86919 for U. S. Navy Electronics Laboratory," California Research Corporation (Confidential), June 1953.

11. Univ. of Texas Defense Research Laboratory Monthly Progress Report for February 1953.

12. E. L. Hamilton, G. Shumway, H. W. Menard, and C. J. Shipek, "Acoustic and Other Physical Properties of Shallow-Water Sediments off San Diego," J. Acoust. Soc. Amer., 28:1-5, January 1956.

13. E. L. Hamilton, "Low Sound Velocities in High Porosity Sediments," J. Acoust. Soc. Amer., 28:16-19, January 1956.

14. P. M. Morse, "Vibration and Sound," 2d Ed., McGraw-Hill Book Co., Inc. N. Y., 1948.

15. K. V. Mackenzie, "Study of Bottom Reflection Losses for Underwater Sound," NEL Internal Tech. Memo. No. 32, September 1952.

16. K. V. Mackenzie, "Short-Range Sound Transmission in the Deep Bering Sea," NEL Report 299, September 1942.

17. D. L. Davidson, K. M. Murray, and C. W. Searfoss, "Some Sound Properties of Bottom Sediments Pertinent to Small-Objects Location," USN J. Underwater Acoustics, 3(No. 2): 83-89 (Confidential), April 1953.

18. H. W. Marsh and M. Schulkin, "Sound Transmission at Frequencies Between 2 and 25 Kilocycles per Second," USL Tech. Memo. No. 1110-110-54 (Confidential), August 1954.

19. T. P. Condron, D. L. Cole, and J F. Kelly, "Comparison of Computed and Measured Intensities for Project AMOS Noisemaker Measurements," USN J. Underwater Acoustics, 5(No. 1):46-51 (Confidential), January 1955.

20. A. N. Guthrie and M. C. Rinehart, "Determination of Bottom Characteristics by Reflection," USN J. Underwater Acoustics, 5(No. 3):184-190 (Confidential), July 1955.

21. T. P. Condron and P. A. Barakos, "Investigation of Bottom Reflection Coefficients in Shallow Water over a Mud Bottom in the Frequency Range 555-6100 cps," USL Tech. Memo. No. 1110-030-55 (Confidential), September 1955.

22. Scripps Institute of Oceanography Interim Progress Report on Classified Activities April to June 1955, SIO Ref. 55-21 (Confidential), August 1955.

23. M. A. Pedersen, "A Long-Range, Low-Frequency, Underwater Sound Transmission Experiment in 3100-Fathom Water," NEL Report 618 (Confidential), July 1955.

24. R. R. Goodman, "A Method for the Determination of the Critical Angle of Reflection of Sound from the Bottom of the Ocean," Mich. Univ. Engrg. Res. Inst. Report 1936-2-T, August 1954.

25. T. E. Stringer and F. M. V. Flint, "The Sound Field about a Continuous Wave Source in Shallow Water. Pt. 1, Theoretical Prediction of the Sound Field," UCWE Informal Report No. 1573/53 (Secret), August 1953.

26. K. V. Mackenzie, "Bottom Reverberation in 2100-Fathom Water," USN J. Underwater Acoustics, 6(No. 1):24-36 (Confidential), January 1956.

27. "Principles of Underwater Sound," STR Div. 6, NDRC, Vol. 7, 1946.

28. T. McMillian, "Some Transmission Characteristics of Bottom Reflected Sound," NEL Report 14, July 1947.

29. L. Liebermann, "Reflection of Sound from Coastal Sea-Bottoms," J. Acoust. Soc. Amer., 22:305-309, 1948.

30. C. W. Horton, "The Acoustic Properties of the Ocean Bottom at Bahia Todos Santos, Lower California," Defense Research Laboratory, Univ. of Texas, Report DRL-A-94, September 1955.

31. J. M. Ide and R. F. Post, "Underwater Sound Pressures Beneath a Ship-Mounted Source as a Function of Bottom Impedance," NRL Report S-2032 (Confidential), March 1943.

32. J. M. Ide, R. F. Post, and W. J. Fry, "Propagation of Underwater Sound at Low Frequencies as a Function of the Acoustic Properties of the Bottom," NRL Report S-2113, August 1943.

33. "Military Oceanography," STR Div. 6, NDRC, Vol. 6A (Confidential), 1946.

34. F. P. Shepard, "Nomenclature Base on Sand-Silt-Clay Ratios," J. Sediment. Petrol., 24(No. 3):151-158, September 1954.

35. "Study of Bottom Materials," UCDWR Report M404, September 1946.

36. "Physics of Sound in the Sea, Part I: Transmission," STR Div. 6, NDRC, Vol. 8, 1946.

37. W. B. Snow, H. B. Hoff, and J. J. Markham, "Transmission Survey Block Island Sound," NDRC 6.1-sr 1128-1027, Report D 12/R616 CUDWR (Confidential), March 1944.

38. T. P. Condron, "Summary of Cruise I-4 Siren Data," USL TM 1110-023 (Confidential).

39. T. P. Condron, "Completion of Processing of Cruise I-4 Siren Data," USL TM 1110-044-54 (Confidential), September 1954.

40. R. W. Young, "Example of Propagation of Underwater Sound by Bottom Reflection," J. Acoust. Soc. Amer., 20:455-462, 1948.

41. R. A. Walker, "Propagation of Very-Low-Frequency Sound in Shallow Water. Transmission Measurements in the Halifax Area," December 1954, Bell Telephone Laboratories, Inc., Memo. for File (Secret), September 1955.

42. R. W. Young, "Image Interference in the Presence of Refraction," J. Acoust. Soc. Amer., 19:1-7, 1947.

43. R. W. Young and T. McMillian, "Underwater Sound Transmission at Sonic Frequencies," UCDWR No. M448, September 1946.

44. R. R. Carhart, R. W. Raitt, and L. A. Thacker, "Transmission of 24 kc Sound in Shallow Water," UCDWR No. M423, August 1946.

45. M. J. Sheehy, "Transmission of 56-kc Sound in Shallow Water over a Sand Bottom," NEL Report 15, July 1947.

46. H. R. Alexander, "Some Recent Measurements of Propagation of Low Frequency Sound at Perranporth, Cornwall," ONR, London Branch Project TM 4 (Secret), July 1955.

SECRET

SECRET

DEPARTMENT OF THE NAVY
OFFICE OF NAVAL RESEARCH
800 NORTH QUINCY STREET
ARLINGTON, VA 22217-5660

IN REPLY REFER TO
5510/1
Ser 93/057
20 Jan 98

From: Chief of Naval Research
To: Commanding Officer, Naval Research Laboratory (1221.1)

Subj: DECLASSIFICATION OF DOCUMENTS

Ref: (a) NRL ltr 5510 Ser 1221.1/S0048 of 25 Feb 97
(b) NRL memo Ser 7103/713 of 29 Jan 97
(c) ONR Report "A Summary of Underwater Radiated Noise Data, March 1966"

Encl: (1) ONR Report "A Summary of Underwater Acoustic Data, Part I" AD-030 750
(2) ONR Report "A Summary of Underwater Acoustic Data, Part II" AD-039 542
(3) ONR Report "A Summary of Underwater Acoustic Data, Part III" AD-039 543
(4) ONR Report "A Summary of Underwater Acoustic Data, Part IV" AD-039 544
(5) ONR Report "A Summary of Underwater Acoustic Data, Part V" AD-105 841
(6) ONR Report "A Summary of Underwater Acoustic Data, Part VII" AD-115 204
(7) ONR Report "A Summary of Underwater Acoustic Data, Part VIII" AD-105 842

1. In response to reference (a), the following information is provided:

Enclosure (1) was downgraded to UNCLASSIFIED by CNR, 7/29/74;
Enclosure (2) was downgraded to UNCLASSIFIED by NRL, 12/3/90;
Enclosure (3) was downgraded to UNCLASSIFIED by CNR, 7/29/74;
Enclosure (4) was downgraded to UNCLASSIFIED by CNR, 7/29/74;
Enclosure (5) was downgraded to UNCLASSIFIED by NRL, 12/3/90;
Enclosure (6) was downgraded to UNCLASSIFIED by CNR, 7/29/74; and
Enclosure (7) was downgraded to UNCLASSIFIED by CNR, 7/29/74.

Enclosures (1) through (7) have been appropriately stamped with declassification information and, based on the recommendation contained in reference (b), Distribution Statement A has been assigned.

2. To my knowledge, reference (c) AD-396737 has not been previously reviewed for declassification. Based on our discussions in April 1997, I am still holding it for Dr. Hurdle's comments.

3. Questions may be directed to the undersigned on (703) 696-4619.

Completed
18 Apr 2000
B.W.

PEGGY LAMBERT
By direction